FORSCHUNGSZENTRUM ROSSENDORF FZR

FZR-195
October 1997

U. Grundmann, U. Rohde

Verification of the Code DYN3D/R with the Help of International Benchmarks

Herausgeber:
FORSCHUNGSZENTRUM ROSSENDORF
Postfach 51 01 19
D-01314 Dresden
Telefon (03 51) 26 00
Telefax (03 51) 2 69 04 61

Als Manuskript gedruckt

Verification of the Code DYN3D/R with the Help of International Benchmarks

U. Grundmann, U. Rohde

Research Center Rossendorf, Inc.
Institute for Safety Research
P.O. Box 510119
D-01314 Dresden

Abstract

Different benchmarks for reactors with quadratic fuel assemblies were calculated with the code DYN3D/R. In this report comparisons with the results of the reference solutions are carried out. The results of DYN3D/R and the reference calculation for the eigenvalue k_{eff} and the power distribution are shown for the steady-state 3-dimensional IAEA-Benchmark. The results of NEACRP-Benchmarks on control rod ejections in a standard PWR were compared with the reference solutions published by the NEA Data Bank. For assessing the accuracy of DYN3D/R results in comparison to other codes the deviations to the reference solutions are considered. Detailed comparisons with the published reference solutions of the NEA-NSC Benchmarks on uncontrolled withdrawal of control rods are made. The influence of the axial nodalization is also investigated. All in all, a good agreement of the DYN3D/R results with the reference solutions can be seen for the considered benchmark problems.

Kurzfassung

Verschiedene Benchmarks für Reaktoren mit quadratischen Brennelementen wurden mit dem Code DYN3D/R berechnet. In diesem Bericht erfolgen Vergleiche mit den Ergebnissen der Referenzlösungen. Die Ergebnisse von DYN3D/R und der Referenzrechnung für Eigenwert k_{eff} und Leistungsverteilung des stationären 3-dimensionalen IAEA-Benchmarks werden dargestellt. Die Ergebnisse der NEACRP-Benchmarks für die Auswürfe von Steuerstäben in einem typischen DWR werden mit den von der NEA Data Bank veröffentlichten Referenzlösungen verglichen. Zur Einschätzung der Genauigkeit der DYN3D/R Resultate im Vergleich zu anderen Rechenprogrammen werden die Abweichungen zu den Referenzlösungen betrachtet. Detaillierte Vergleiche mit den Referenzlösungen erfolgen für die NEA-NSC Benchmarks zum unkontrollierten Ausfahren von Steuerstäben. Dabei wird der Einfluß der axialen Nodalisierung untersucht. Insgesamt wird eine gute Übereinstimmung der DYN3D/R Resultate mit den Referenzlösungen für die betrachteten Benchmarkprobleme festgestellt.

Content

1 Introduction

The code DYN3D/M2 has been developed for steady state and transient analysis of reactor cores with rectangular fuel assemblies [1]. The code was verified with the help of benchmark solutions and code comparisons. The neutron kinetic part was validated by the kinetic experiments at the zero power reactor LR-0. Now the code is in use in several institutions for safety analyses of VVER-type reactors. The validation of the code was completed by comparisons of calculational results with measured data from various steady-state and transient experiments.

Recently, DYN3D has been extended by a neutronic part for the solution of the 2-group neutron diffusion equation by a nodal method for the Cartesian geometry (version DYN3D/R [2]). The verification of this code version was performed by solution of different international benchmark tasks. The verification of DYN3D/R with the help of the 3-dimensional IAEA benchmark is described in chapter 2. The results of the code for the NEACRP rod ejection benchmarks in comparison to the refence solution and other codes is presented in chapter 3. In chapter 4, the comparisons of DYN3D/R results with the reference solutions for the NEA-NSC benchmarks on withdrawal of control rods at hot zero power of a standard PWR are shown.

2 Three-Dimensional IAEA Benchmark

Calculations for the well known steady-state 3D IAEA Benchmark contained in the "ANL Benchmark Problem Book" [3] were carried out with the code DYN3D/R. The IAEA Benchmark describes a PWR with typical cross sections for the fuel assemblies and partly inserted control rods. Eigenvalue and assembly powers compared with the reference values [3] are shown in Fig. 2.1. The maximum deviation of assembly powers is 1.4 % in assembly no. 35 at the boundary to the reflector.

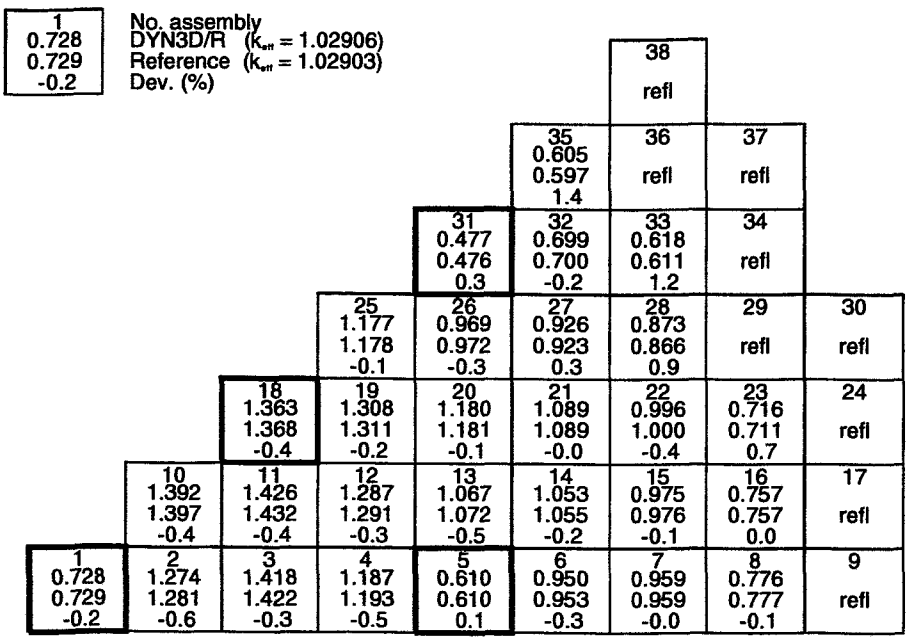

Fig. 2.1: Normalized assembly powers of DYN3D/R for the 3D IAEA Benchmark compared with the reference solution

3 Results of NEACRP Benchmarks on Control Rod Ejections

Assessing the different codes developed for transient analysis of reactor cores mathematical benchmarks were defined [4]. The PWR problems were calculated for testing the results of DYN3D/R by comparison with the published reference solutions [5]. The problems A1, A2, B1, B2, C1 and C2 consist in rod ejections of central or peripheral rods at hot zero power (HZP) and full power (FP). Fig. 3.1 shows the map of the reactor.

Short characterization of the 6 cases:

A1: Ejection of the central rod at HZP (assembly 111 in Fig. 3.1)
A2: Ejection of the central rod at FP (assembly 111 in Fig. 3.1)

B1: Ejection of a peripheral rod in octant geometry at HZP (assemblies 20, 105,115 and 202 in Fig. 3.1)
B2: Ejection of a peripheral rod in octant geometry at FP (assemblies 20, 105,115 and 202 in Fig. 3.1)

C1: Ejection of one peripheral rod at HZP (assembly 115 in Fig. 3.1)
C2: Ejection of one peripheral rod at FP (assembly 115 in Fig. 3.1)

The reactor core consists of 157 fuel elements and reflector elements with a side length of 21.606 cm (see fig. 3.1). The core including the axial reflector is divided into 18 layers of different height given in the specifications of the problems [4]. The 16 core layers height values were given by 7.7, 11.5, 15.0, 30.0, (10 layers) 12.8 (2 layers) and 8 cm (from bottom to top). The bottom and top reflectors are described by layers of 30 cm. The radial mesh is given by one node per assembly in each axial layer. The most codes used this specified mesh, but some calculations were performed with finer meshes. The nominal power of the reactor is 2775 MW. The ejection time of rods a is 0.1 s in all cases.

The figures 3.2 - 3.9 show the results for nuclear power, core averaged Doppler temperature and the core centerline temperature obtained with DYN3D/R and compared with the reference solution. The reference solution was generated by the PANTHER code using 4 nodes per assembly in radial direction. Some comparisons are shown in the tables 3.1 - 3.9 . There are the reference values and the deviations of different codes from reference values. The comparisons show a good agreement of the DYN3D/R results with the reference solution. DYN3D/R deviations are less than the deviations from the reference solutions obtained by the most other codes. However, the deviations in maximum fuel centerline temperatures of DYN3D/R from the reference values are higher than they should be expected according the small deviations in reactor power. This can be caused by the special nodal method for the solution of thermal conductions equation used in DYN3D/R which ensures high accuracy even with a few radial nodes in fuel. The fuel centerline temperature is extrapolated from the temperature of the inner node in DYN3D. In some codes the temperature value for the inner node is probably interpreted as fuel centerline temperature.

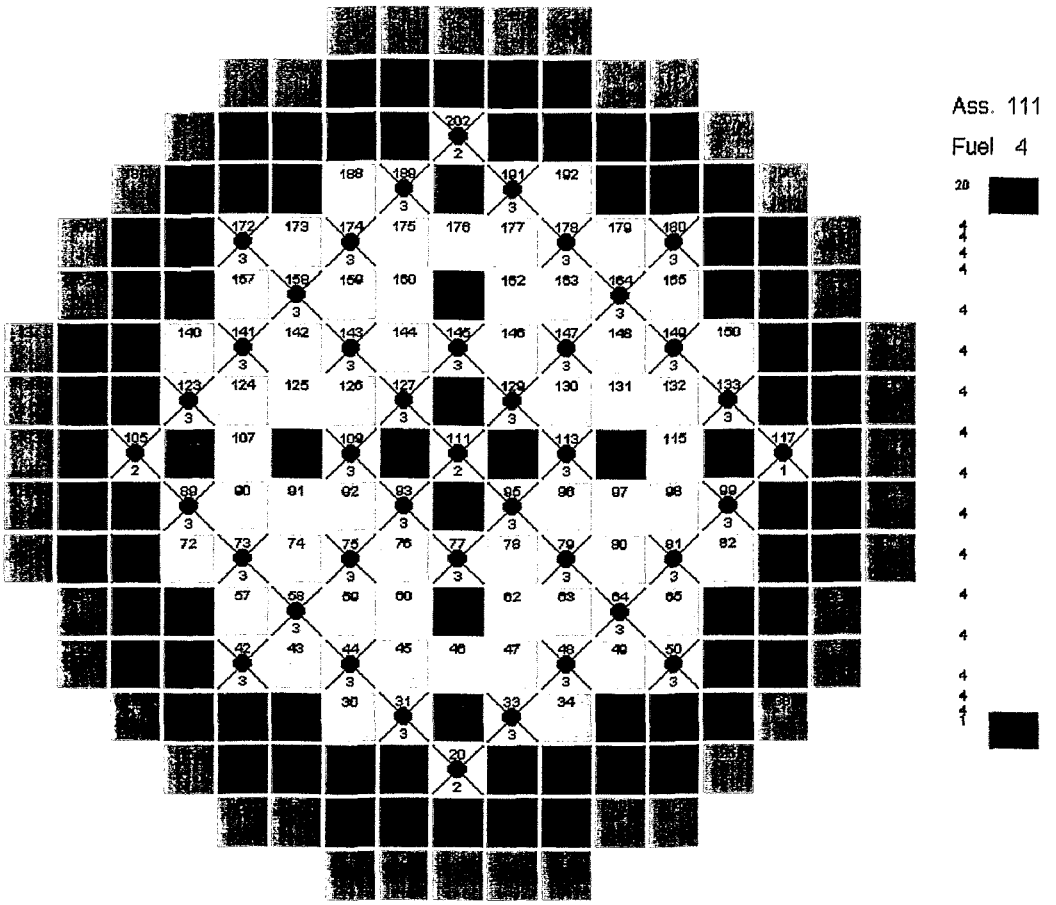

Fig. 3.1: Map of the standard PWR

Case A1: Ejection of the Central Rod at HZP

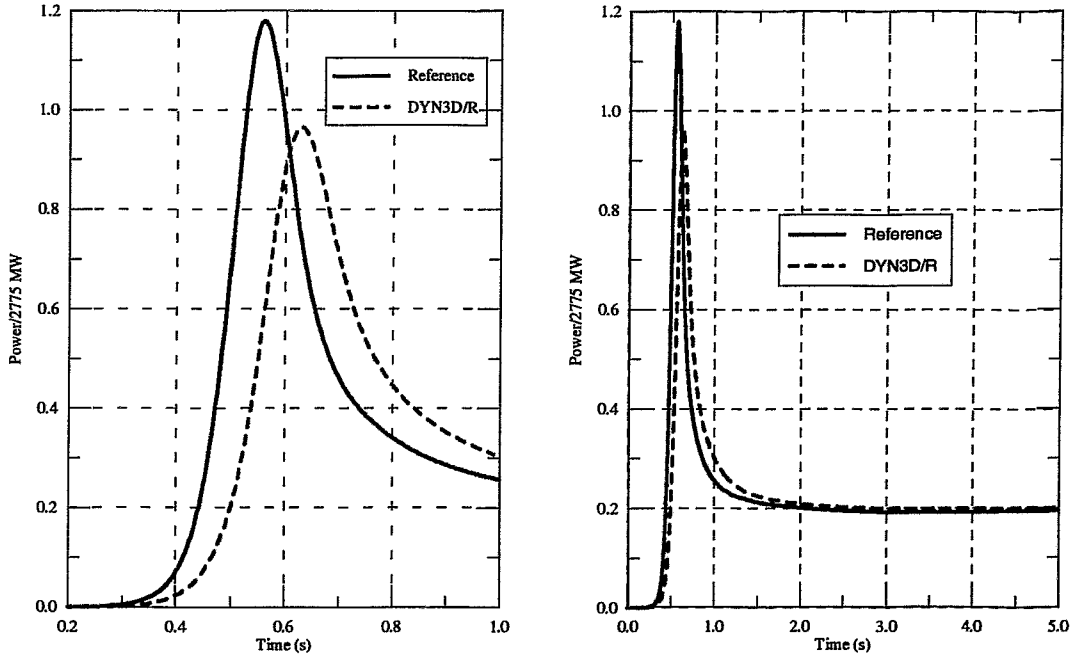

Fig. 3.2: Comparison of the DYN3D/R results for fission power with the reference solution

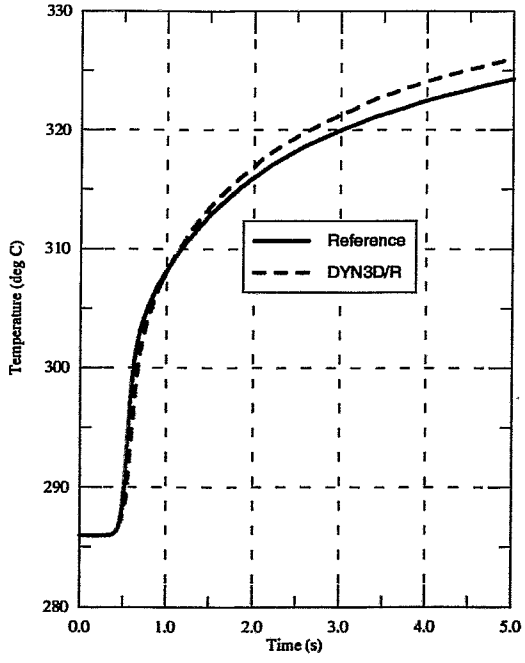

Fig. 3.A1.3: Core Averaged Doppler Temperature

Core averaged Doppler temperature

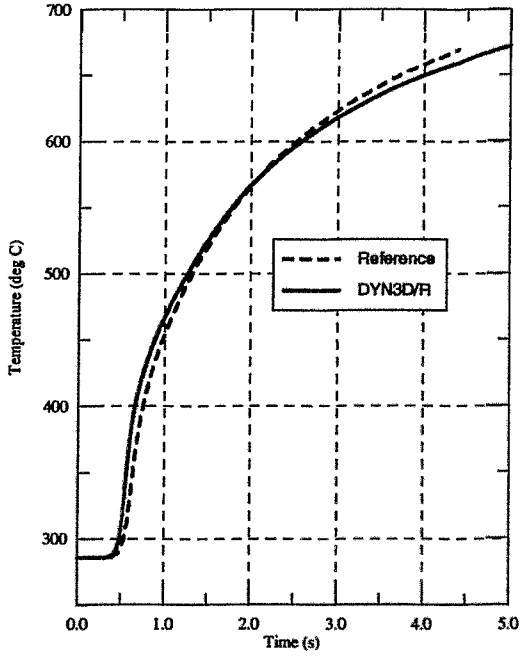

Fig. 3.A1.4: Maximum Fuel Centerline Temperature

Fuel centerline temperature

Fig. 3.3: Comparison of the DYN3D/R results for core averaged Doppler temperature and fuel centerline temperature with the reference solutions

Case A2: Ejection of the Central Rod at FP

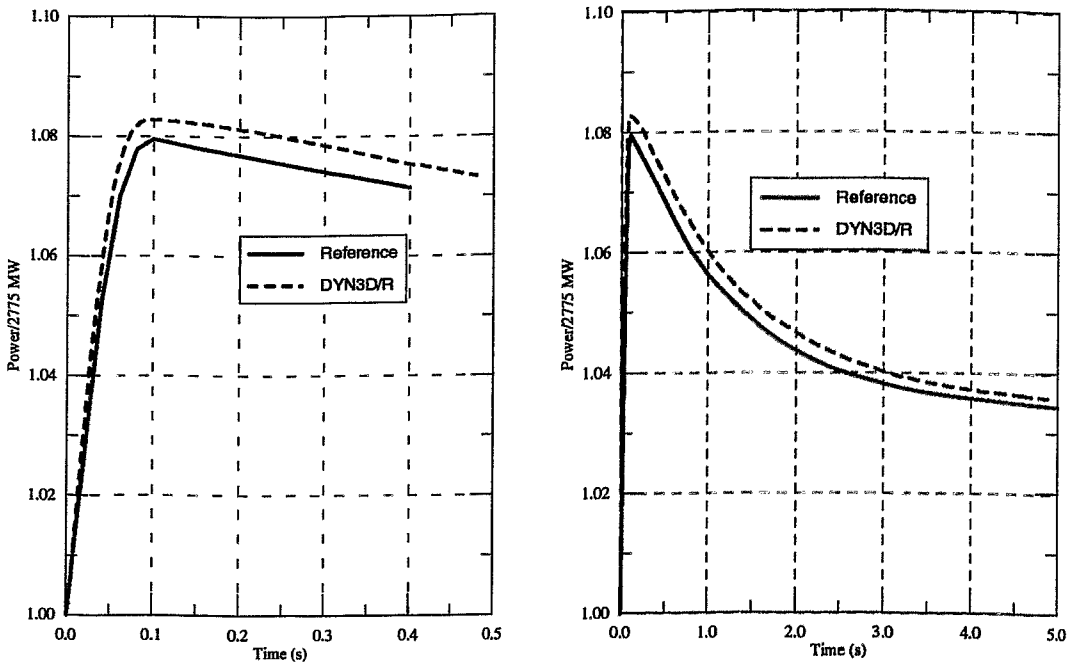

Fig. 3.4: Comparison of the DYN3D/R results for fission power with the reference solution

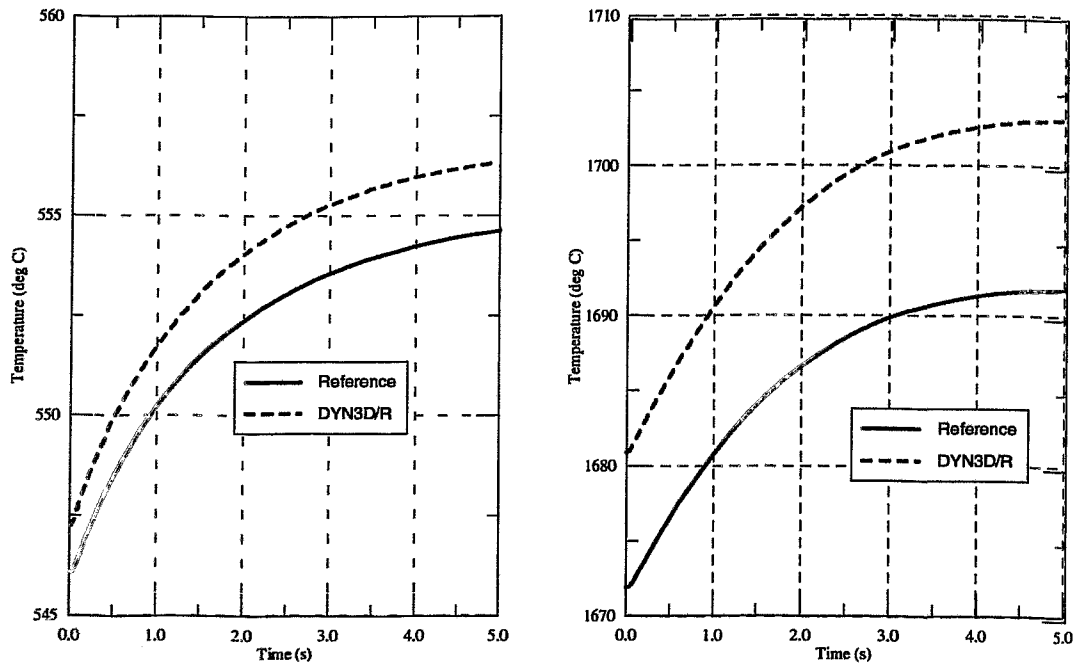

Core averaged Doppler temperature Fuel centerline temperature

Fig. 3.5: Comparison of the DYN3D/R results for core averaged Doppler temperature and fuel centerline temperature with the reference solutions

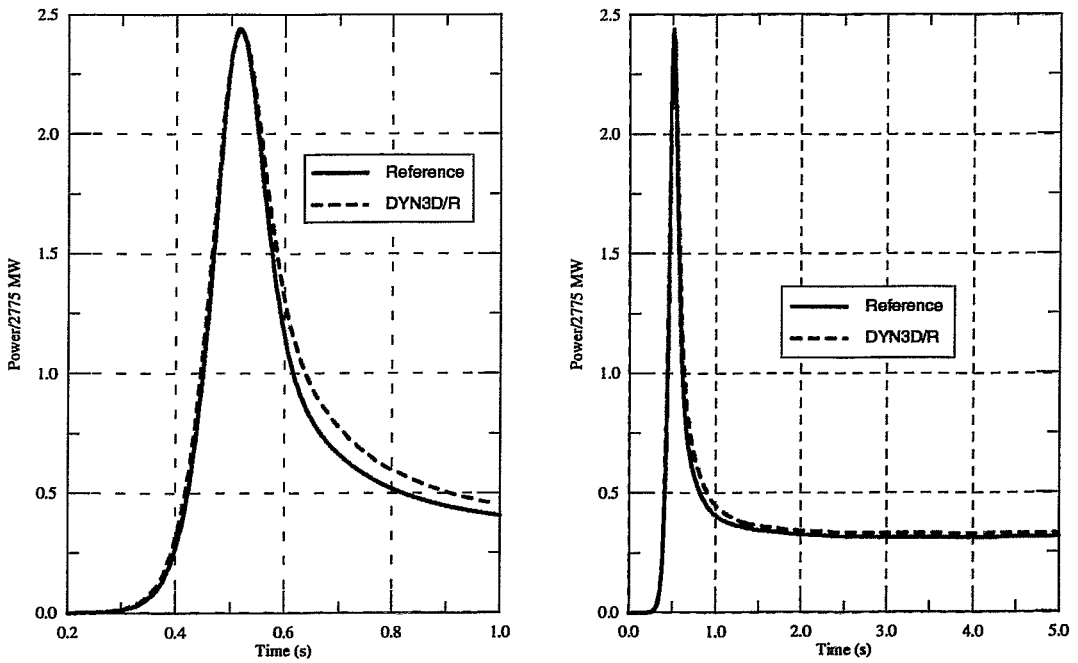

Fig. 3.6: Comparison of the DYN3D/R results for fission power with the reference solution

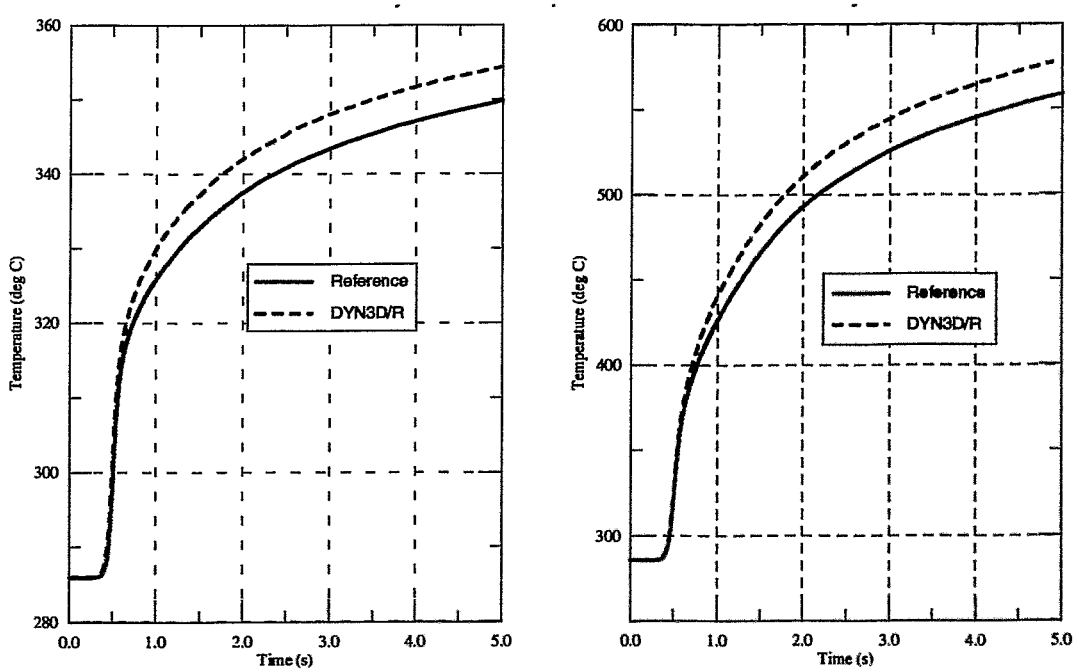

Core averaged Doppler temperature

Fuel centerline temperature

Fig. 3.7: Comparison of the DYN3D/R results for core averaged Doppler temperature and fuel centerline temperature with the reference solutions

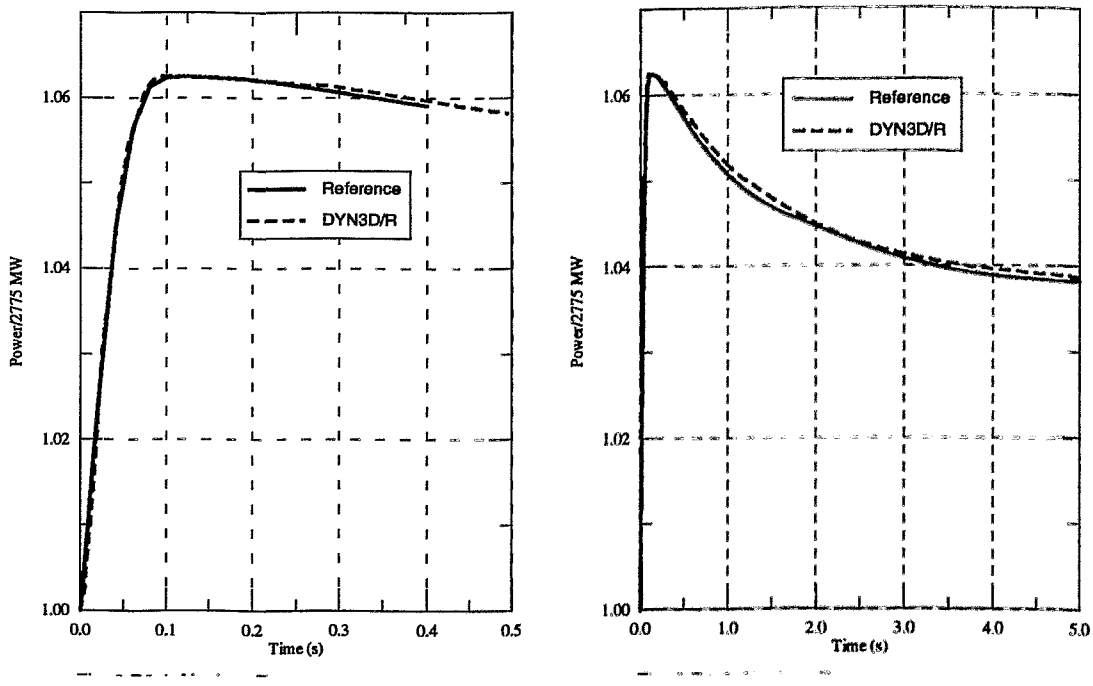

Fig. 3.8: Comparison of the DYN3D/R results for fission power with the reference solution

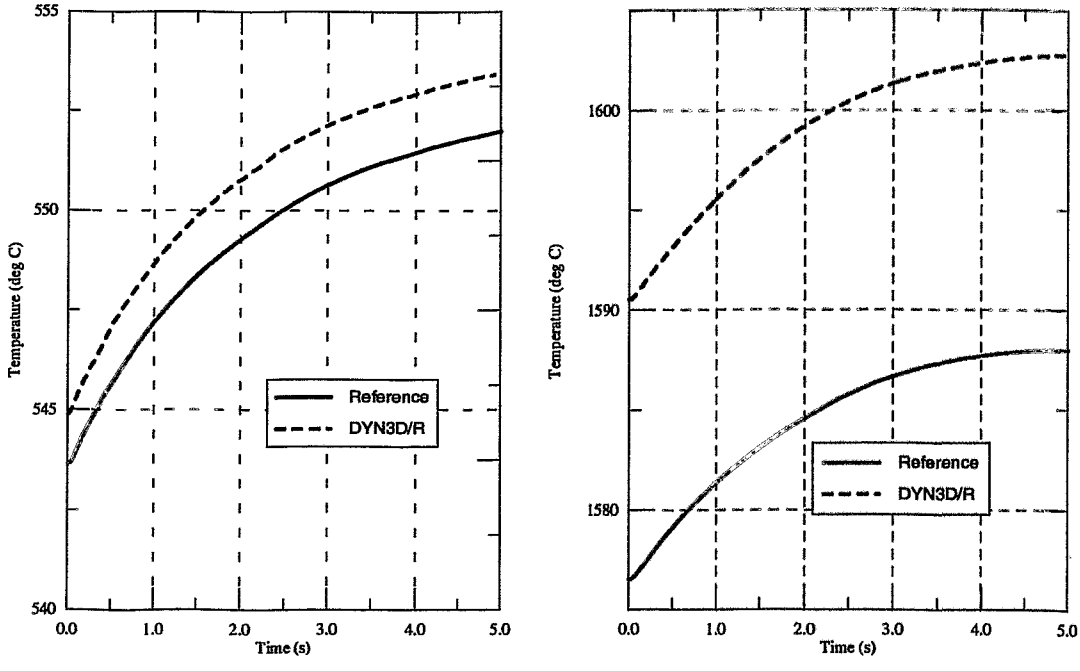

Core averaged Doppler temperature

Fuel centerline temperature

Fig. 3.9: Comparison of the DYN3D/R results for core averaged Doppler temperature and fuel centerline temperature with the reference solutions

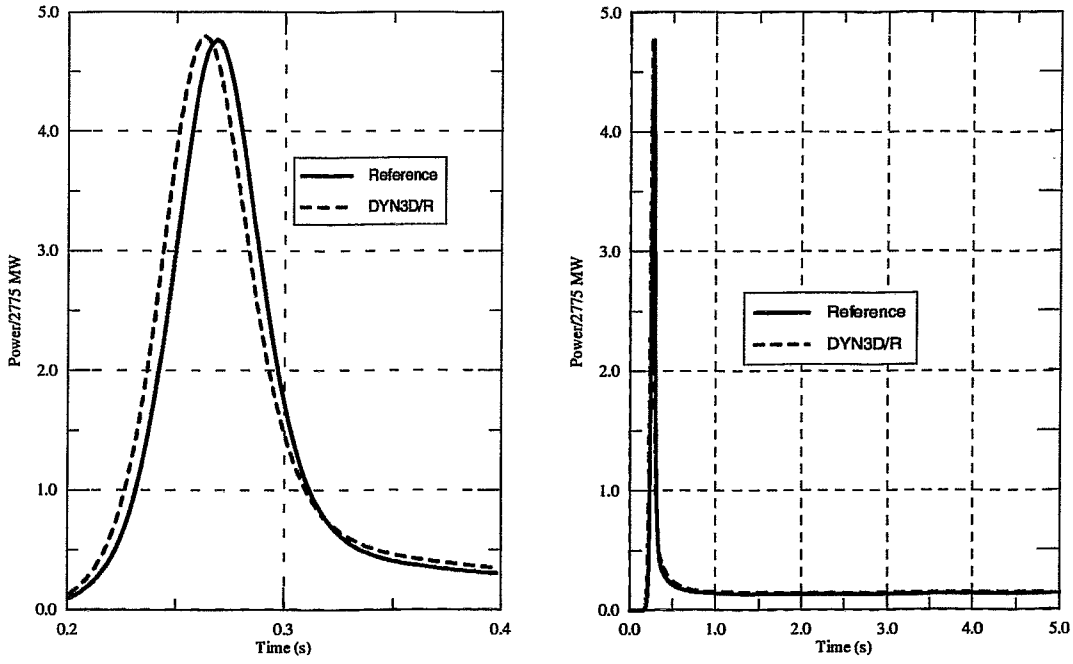

Fig. 3.10: Comparison of the DYN3D/R results for fission power with the reference solution

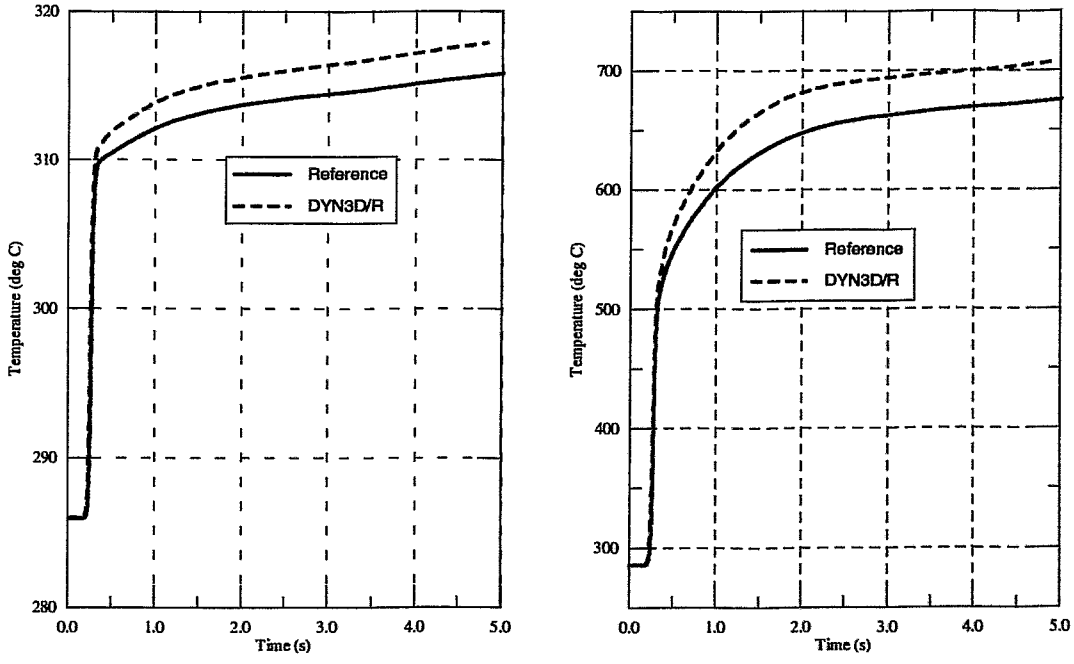

Core averaged Doppler temperature

Fuel centerline temperature

Fig. 3.11: Comparison of the DYN3D/R results for core averaged Doppler temperature and fuel centerline temperature with the reference solutions

Case C2: Ejection of the Peripheral Rod at FP

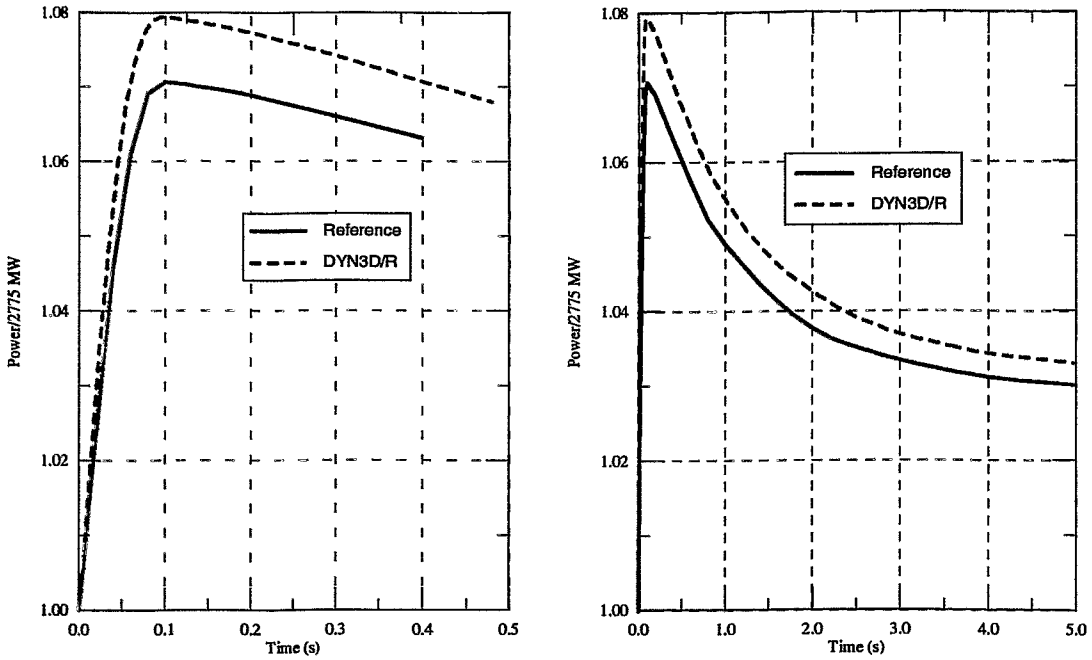

Fig. 3.12: Comparison of the DYN3D/R results for fission power with the reference solution

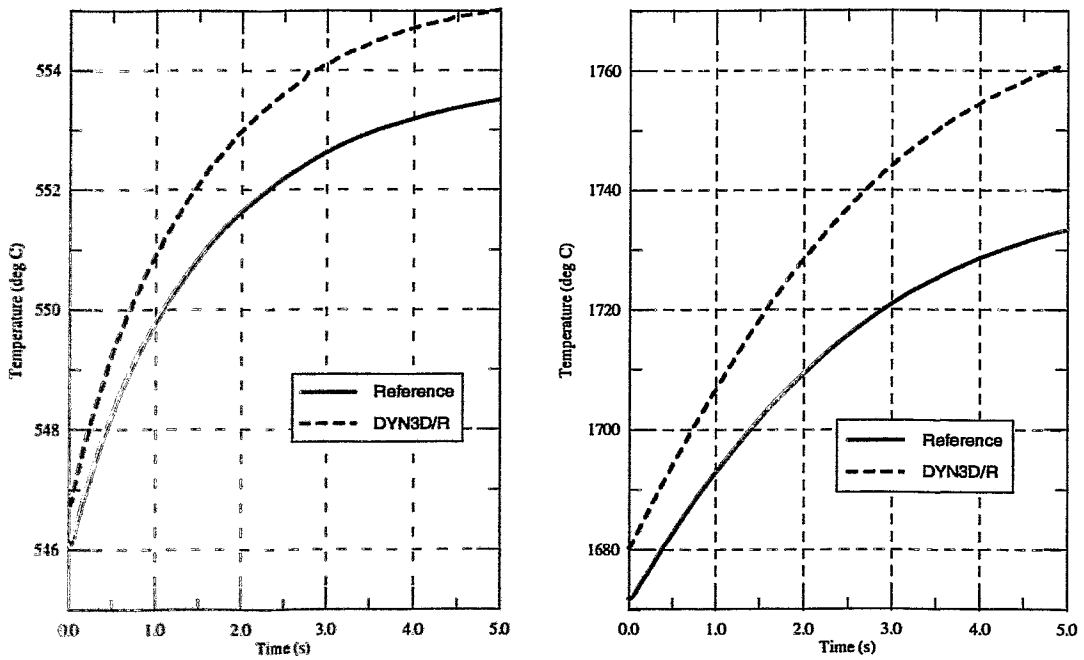

Core averaged Doppler temperature

Fuel centerline temperature

Fig. 3.13: Comparison of the DYN3D/R results for core averaged Doppler temperature and fuel centerline temperature with the reference solutions

Table 3.1: PWR CORE TRANSIENT BENCHMARKS
Reference Value of Critical Boron Concentration and Deviations (%)

Case	A1	A2	B1	B2	C1	C2
Reference (ppm)	567.70	1160.60	1254.60	1189.40	1135.30	1160.60
OKAPI(s)	-1.215	0.974	-0.375	0.572	-0.484	0.974
OKAPI(a)	-1.215	0.974	-0.375	0.572	-0.484	0.974
BOREAS/TRAB	23.71	-0,250	0.486	- 0.681	1.964	-0.250
CESAR	3.576	-2.292	0.988	- 2.22	1.295	-2.292
PANBOX	-0.511	0.172	-0.072	0.00	-0.167	0.181
QUABOX/CUBBOX	0.458	0.327	1.124	0.336	1.092	0.310
QUANDRY- EN			0.510		0.502	
THYDE-NEU				5.936		
PRORIA	-41.695	3.739			-0.467	4.170
LWRSIM	3.329	1.086	0.319	0.832	0.573	1.086
SIMTRAN	0.194	0.207	0.279	0.193	0.317	0.207
ARROTTA					0.326	5.032
PANTHER	0.740	0.698	0.558	0.504	0.590	0.698
DYN3DR	0.856	0.263	0.138	0.236	0.020	0.252

Table 3.2: PWR CORE TRANSIENT BENCHMARKS
Steady State Solution: Reference Value of Nodal Power Peaking Factor and Deviations (%)

Case	A1	A2	B1	B2	C1	C2
Reference (abs.)	2.874	2.221	1.932	2.109	2.187	2.221
OKAPI(s)	0.244	1.486	-0.259	0.711	-0.137	1.486
OKAPI(a)	0.244	1.486	-0.259	0.711	-0.137	1.486
BOREAS/TRAB	17.606	0.855	4.555	-0.427	2.423	0.855
CESAR	8.559	-1.846	8.178	-2.323	13.397	-1.846
PANBOX	-0.974	-0.630	-0.259	-0.759	-0.137	-0.675
QUABOX/CUBBOX	-1.113	-0.540	0.155	-0.142	0.503	-0.495
QUANDRY- EN			-0.104		-0.137	
LWRSIM	4.175	1.891	3.621	0.806	3.978	1.891
ARROTTA					-1.920	7.249
PANTHER	-0.974	-0.225	-0.311	-0.284	-0.183	-0.225
DYN3DR	-0.574	0.090	0.430	0.474	-0.274	0.135

Table 3.3: PWR CORE TRANSIENT BENCHMARKS
Reference Value of Reactivity Release and Deviations (%)

Case	A1	A2	B1	B2	C1	C2
Reference (pcm)	822.00	90.00	831.00	99.00	958.0	78.00
CESAR	-4.015	-4.444	-2.407	8.081	-1.983	2.564
PANBOX	-1.460	-1.111	-0.963	2.020	-0.731	2.564
SIMTRAN	-1.460	0.000	0.000	2.020	0.313	3.846
PANTHER	-1.825	-3.333	0.120	1.010	0.731	1.282
DYN3DR	-1.749	-1.754	0.564	-2.92	-0.063	4.782

Table 3.4: PWR CORE TRANSIENT BENCHMARKS
Time of Power Maximum (Reference) and Deviations (%)

Case	A1	A2	B1	B2	C1	C2
Reference (s)	0.560	0.100	0.520	0.120	0.270	0.100
OKAPI(s)	5.357	-20.000	-3.846	-16.667	-11.111	0.000
OKAPI(a)	3.571		-7.692		-11.111	
BOREAS/TRAB	12.500	110.000	-5.769	241.667	3.704	110.0
CESAR	37.500	0.000	17.308	-16.667	11.111	0.000
COCCINELLE					18.519	-20.0
PANBOX	7.143	0.000	0.000	-8.333	0.000	0.000
QUABOX/CUBBOX	5.357	-10.000	-19.231	-33.333	11.111	-10.0
QUANDRY- EN			-3.846		-3.704	
REFLA/TRAC	-73.214					
THYDE-NEU				575.000		
PRORIA	221.490	0.000				0.000
SIMTRAN	14.286	0.000	0.000	-8.333	0.000	0.000
ARROTTA					-3.704	-20.0
PANTHER	16.071	0.000	0.000	0.000	-3.704	20.0
DYN3DR	11.340	0.000	-0.960	-12.500	-1.852	-2.500

Table 3.5: PWR CORE TRANSIENT BENCHMARKS
Reference of Power Maximum (% of P/2775 MW) and Deviations (%)

Case	A1	A2	B1	B2	C1	C2
Reference (%)	117.900	108.000	244.100	106.300	477.300	107.100
OKAPI(s)	-35.199	-0.370	2.417	-3.104	-36.141	-0.654
OKAPI(a)	-0.339		20.401		30.170	
BOREAS/TRAB	25.106	-0.185	3.154	-0.188	164.215	-0.093
CESAR	-46.141	1.019	-30.602	0.659	-31.636	1.401
COCCINELLE					-41.400	-0.093
PANBOX	-12.383	0.000	-1.680	0.282	-1.152	0.280
QUABOX/CUBBOX	12.299	0.833	125.604	1.035	130.254	1.774
QUANDRY- EN			0.901		10.245	
THYDE-NEU				-0.188		
PRORIA	-73.028	0.278				0.187
SIMTRAN	-28.329	0.278	-5.326	0.282	-7.668	0.560
ARROTTA					3.394	0.934
PANTHER	-23.749	-0.278	8.193	0.094	16.740	0.093
DYN3DR	-20.322	0.268	3.978	-0.039	-0.071	-1.666

Table 3.6: LWR CORE TRANSIENT BENCHMARKS
PWR: Reference of Final Power (% of P/2775 MW) and Deviations (%)

Case	A1	A2	B1	B2	C1	C2
Reference (%)	19.600	103.500	32.000	103.800	14.600	103.000
OKAPI(s)	-1.020	-0.676	-4.688	-1.927 -1	7.534	-0.485
OKAPI(a)	25.000		1.250		47.260	
BOREAS/TRAB	70.408	0.773	12.500	0.674	191.096	0.874
CESAR	-13.265	-0.097	-12.187	0.000	-13.014	0.000
COCCINELLE					1.370	0.097
PANBOX	0.510	0.097	1.563	0.289	2.740	0.194
QUABOX/CUBBOX	-0.510	0.676	3.750	0.771	4.110	1.068
QUANDRY- EN			-23.438		-17.123	
THYDE-NEU				0.963		
PRORIA	26.020	0.193				0.583
SIMTRAN	6.122	0.097	4.688	0.193	6.164	0.194
ARROTTA					19.178	0.000
PANTHER	-0.510	-0.097	1.563	0.096	2.740	0.097
DYN3DR	2.791	0.095	4.653	0.070	5.932	0.303

Table 3.7: PWR CORE TRANSIENT BENCHMARKS
Reference of Final Core Averaged Doppler Temperature and Deviations in (%)

Case	A1	A2	B1	B2	C1	C2
Reference (°C)	324.300	554.600	349.900	552.000	315.900	553.500
OKAPI(s)	-0.278	-0.252	-0.343	-0.707	0.380	-0.199
OKAPI(a)	3.238		0.800		4.653	
BOREAS/TRAB	10.207	3.642	4.201	4.638	21.937	3.668
CESAR	-0.648	-7.339	-0.657	6.902	-0.443	7.371
COCCINELLE					0.222	0.452
PANBOX	0.463	1.100	0.915	1.159	0.538	1.102
QUABOX/CUBBOX			2.686	2.428		
QUANDRY- EN			0.714		0.823	
THYDE-NEU				9.601		
PRORIA	2.744	2.669				3.847
SIMTRAN	1.079	2.164	1.600	2.174	0.950	2.186
ARROTTA					-2.501	-23.035
PANTHER	-0.123	-0.072	0.372	-0.018	0.348	-0.018
DYN3DR	0.469	0.315	1.294	0.264	0.681	0.275

Table 3.8: LWR CORE TRANSIENT BENCHMARK
Reference of Maximum Fuel Centerline Temperature and Deviations (%)

Case	A1	A2	B1	B2	C1	C2
Reference (°C)	673.30	1691.80	559.80	1588.10	676.10	1733.50
OKAPI(s)	-2.866	-0.307	-1.304	-0.441	-0.666	-2.798
OKAPI(a)	19.768		2.697		33.279	
CESAR	-6.728	0.254	-5.359	-0.252	-2.721	-0.329
COCCINELLE					1.834	3.340
PANBOX	0.965	0.106	1.536	-0.025	2.588	0.317
REFLA/TRAC	-0.624		0.714			
THYDE-NEU				-0.617		
SIMTRAN	3.802	1.170	3.019	0.686	5.118	1.546
PANTHER	-1.233	-0.136	0.875	-0.164	3.062	-0.012
DYN3DR	1.604	0.669	3.530	0.929	4.788	1.603

Table 3.9: LWR CORE TRANSIENT BENCHMARKS
Reference of Final Coolant Outlet Temperature and Deviations (%)

Case	A1	A2	B1	B2	C1	C2
Reference (^{o}C)	293.100	324.600	297.600	324.700	291.500	324.500
OKAPI(s)	-0.102	-0.031	-0.134	-0.154	0.069	0.000
OKAPI(a)	0.580		0.101		0.892	
BOREAS/TRAB	1.638	0.154	0.470	0.123	3.636	0.154
CESAR	-0.307	-0.031	-0.437	-0.031	-0.206	-0.031
COCCINELLE						
PANBOX	0.034	0.154	0.101	0.154	0.069	0.154
QUABOX/CUBBOX	-0.034	0.092	0.101	0.154	-0.034	0.062
QUANDRY- EN			-1.647		-0.755	
THYDE-NEU				0.400		
REFLA/TRAC	2.900					
PRORIA	0.068	1.078				-1.079
SIMTRAN	0.068	-0.031	0.101	-0.031	0.069	-0.031
ARROTTA					0.343	0.000
PANTHER	-0.034	0.031	0.067	0.031	0.069	0.031
DYN3DR	0.060	-0.117	0.239	0.176	0.129	0.200

4 Calculations of the NEA-NSC Benchmarks on Uncontrolled Withdrawal of Control Rods

Transients consisting of uncontrolled withdrawal of control rods at HZP were defined for the reference PWR considered in the previous benchmarks [4,5]. Fig. 4.1 shows the core map with the different fuel types and the locations of assemblies with control rods. The positions of the control rod banks A, B, C, D and the shut down bank S are shown. Different banks are withdrawn from different initial positions in the considered problems. It is assumed that the control rods withdraw with the velocity of 72 steps/min. The control rods are moved from bottom to top of core in 228 steps. The rods begin to drop 0.6 s after the fission power has reached 35% of nominal power (2775 MW). The rods move down with the constant velocity of 228 steps in 2.2 s. The moderator inlet conditions as flow, pressure, temperature and boron concentration are constant during the transient. The initial power is 10^{-13} of nominal power. Neutron physical constants and thermophysical properties of fuel and clad were prescribed. Own correlations of the heat transfer from cladding to coolant and of the water properties have to be used.

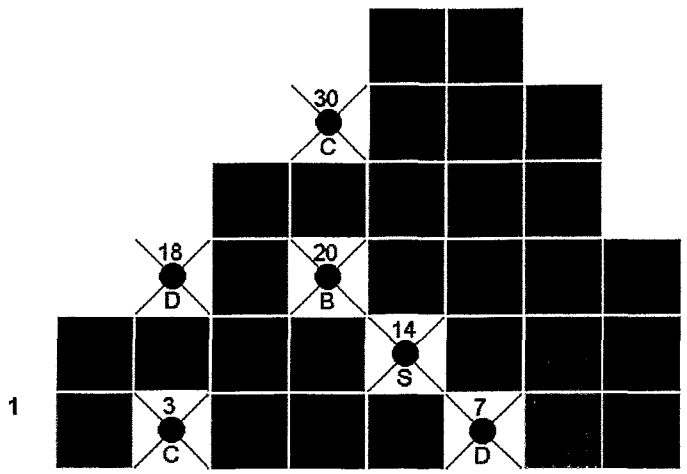

Fig. 4.1: Configuration of the core with positions of control rods and the axial division of fuel assembly number 11.

In the following comparisons of the DYN3/R results with the reference solution are shown. The reference solution was generated by Nuclear Electric with the help of the PANTHER code. A finer mesh of 3x3 nodes per assembly and 48 axial layers were used. The time steps has been reduced until the convergence of the results [7,8].

The three problems A, B and D are considered:

Case A: bank D withdrawal
other banks A, B, C, S are fully withdrawn until scram.

Case B: bank B and C withdrawal
bank A and D remains fully inserted
other bank S is fully withdrawn until scram.

Case D: peripheral banks A and B withdrawal
bank C and D remains fully inserted
other bank S is fully withdrawn until scram.

The case C is different from B only by a constant heat transfer coefficient between cladding and water of 30000 W/(m^2K). The results are not considered here, because the reference results showed only small differences to case B .

As in the benchmarks of chapter 3 the calculations with DYN3D/R for the comparisons with the reference solutions were performed with one node per assembly and the 16 axial layers in the core given by layer thickness of 7.7, 11.5, 15.0, 30.0, (10 layers) 12.8 (2 layers) and 8 cm (from bottom to top). The bottom and top reflectors are described by layers of 30 cm.

The comparisons of DYN3D/R results with the reference solution were performed for

- State state results:

critical boron concentration	(result B1)
radially averaged axial power distribution	(result B2)
axially averaged radial power distribution	(result B3)
radial power distribution at axial layer number 6	(result B4)
radial power distribution at axial layer number 13	(result B5)
envelope axial power distribution Fq(z)	(result B6)

- Transient core averaged results:

fission power relative to nominal	(result C1)
coolant heating	(result C2)
coolant outlet temperature	(result C3)
fuel Doppler temperature	(result C4)

- Transient hot pellet results (DYN3D/R: results of the hottest node):

fission power to nominal	(result D1)
coolant heating	(result D2)

coolant temperature at the outlet of the hot channel	(result D3)
heat exchange coefficient between cladding and moderator	(result D4)
fuel enthalpy	(result D5)
fuel centerline temperature	(result D6)
cladding outer surface temperature	(result D7)

- Snapshots at time of power maximum:

fission power	(result E1)
radially averaged axial power distribution	(result E2)
axially averaged radial power distribution	(result E3)
radial power distribution at axial layer number 6	(result E4)
radial power distribution at axial layer number 13	(result E5)
envelope axial power distribution Fq(z)	(result E6)

The fuel centerline temperature is calculated in DYN3D/R by an extrapolation of the average temperature of the inner node of the fuel pin to the inner boundary. It can explain the small deviations to the reference solution. The fuel enthalpy were calculated by using the single enthalpies of the radial nodes of the fuel pin.

Special calculations for investigating the influence of the number of the core layers carried out with the total number of 20 axial layers are described in chapter 4.2.5 and chapter 4.3.5.

4.1 Case A - Withdrawal of Bank D

4.1.1 Initial Steady State

The critical boron concentration of case A calculated by DYN3D is 1267.38 ppm. The deviation to the reference value of 1262.71 ppm is 4.67 ppm (result B1).

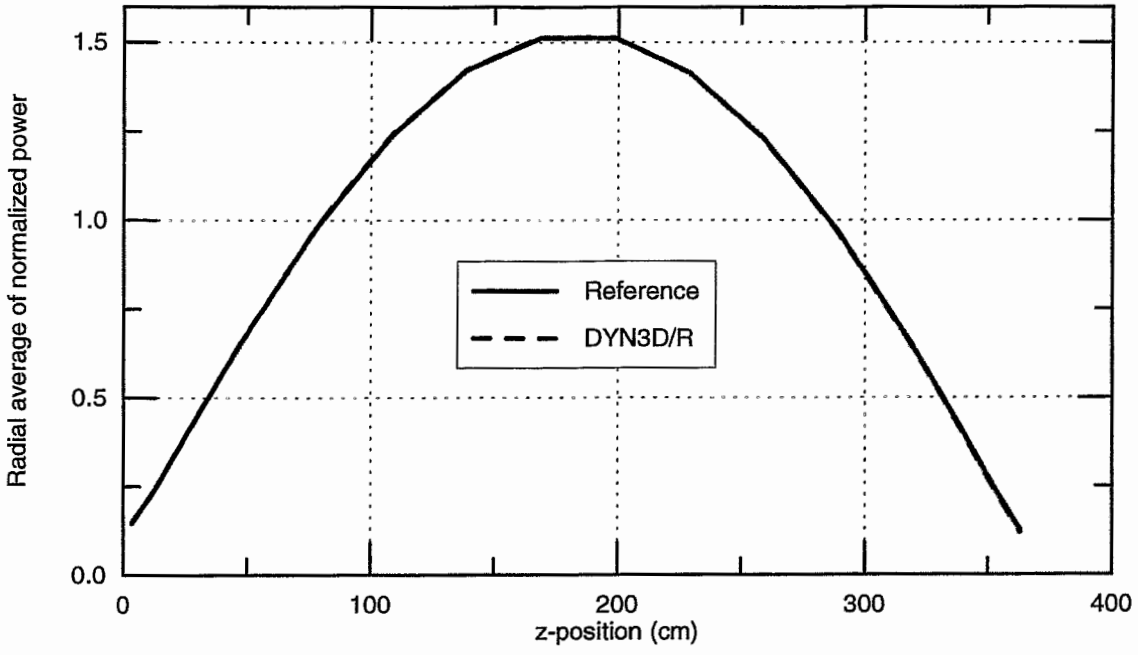

Fig. 4.1.1: Radially averaged axial power distribution (result B2)

8 0.529 0.531 0.57	Assembly no. (DYN3D/R) Reference DYN3D/R Dev. (%)				34 -	35 -		
				30 1.084 1.103 1.76	31 0.850 0.855 0.61	32 -	33 -	
			25 1.168 1.166 -0.15	26 1.178 1.186 0.67	27 1.171 1.189 1.53	28 0.751 0.752 0.14	29 -	
		18 0.576 0.573 -0.50	19 1.051 1.049 -0.27	20 1.236 1.232 -0.30	21 1.145 1.153 0.61	22 1.017 1.021 0.41	23 -	24 -
	10 1.060 1.046 -1.34	11 0.991 0.982 -0.91	12 1.145 1.136 -0.82	13 1.226 1.224 -0.15	14 1.137 1.134 -0.23	15 0.863 0.870 0.80	16 0.476 0.476 0.04	17 -
1 1.101 1.083 -1.66	2 1.045 1.035 -0.98	3 1.119 1.105 -1.25	4 1.124 1.118 -0.54	5 1.242 1.233 -0.72	6 1.087 1.083 -0.36	7 0.466 0.469 0.56	8 0.529 0.531 0.57	9 -

Fig. 4.1.2: Axially averaged radial power distribution (result B3)

8 0.656 0.661 0.75	Assembly no. (DYN3D/R) Reference DYN3D/R Dev. (%)				34 -	35 -		
				30 1.346 1.372 1.94	31 1.055 1.064 0.79	32 -	33 -	
			25 1.449 1.449 -0.01	26 1.463 1.475 0.82	27 1.454 1.478 1.69	28 0.932 0.935 0.32	29 -	
		18 0.713 0.710 -0.40	19 1.304 1.302 -0.15	20 1.534 1.532 -0.15	21 1.422 1.433 0.76	22 1.262 1.270 0.61	23 -	24 -
	10 1.315 1.299 -1.22	11 1.230 1.220 -0.80	12 1.422 1.412 -0.71	13 1.521 1.521 -0.02	14 1.412 1.411 -0.07	15 1.071 1.082 0.95	16 0.591 0.592 0.23	17 -
1 1.366 1.346 -1.52	2 1.296 1.285 -0.86	3 1.389 1.373 -1.13	4 1.395 1.389 -0.43	5 1.542 1.533 -0.60	6 1.349 1.346 -0.23	7 0.578 0.582 0.69	8 0.656 0.661 0.75	9 -

Fig. 4.1.3: Radial power distribution at axial layer number 6 (result B4)

8 0.345 0.346 0.21	Assembly no. (DYN3D/R) Reference DYN3D/R Dev. (%)				34 -	35 -		
				30 0.708 0.718 1.40	31 0.555 0.556 0.24	32 -	33 -	
			25 0.762 0.759 -0.49	26 0.769 0.772 0.31	27 0.764 0.773 1.15	28 0.490 0.489 -0.22	29 -	
		18 0.375 0.372 -0.82	19 0.686 0.682 -0.60	20 0.807 0.802 -0.63	21 0.748 0.749 0.25	22 0.664 0.664 0.07	23 -	24 -
	10 0.692 0.681 -1.65	11 0.647 0.639 -1.22	12 0.748 0.739 -1.14	13 0.800 0.796 -0.48	14 0.742 0.738 -0.56	15 0.563 0.566 0.43	16 0.311 0.310 -0.34	17 -
1 0.719 0.705 -1.98	2 0.682 0.673 -1.31	3 0.731 0.719 -1.57	4 0.734 0.728 -0.86	5 0.811 0.803 -1.04	6 0.709 0.704 -0.69	7 0.304 0.305 0.21	8 0.345 0.346 0.21	9 -

Fig. 4.1.4: Radial power distribution at axial layer number 13 (result B5)

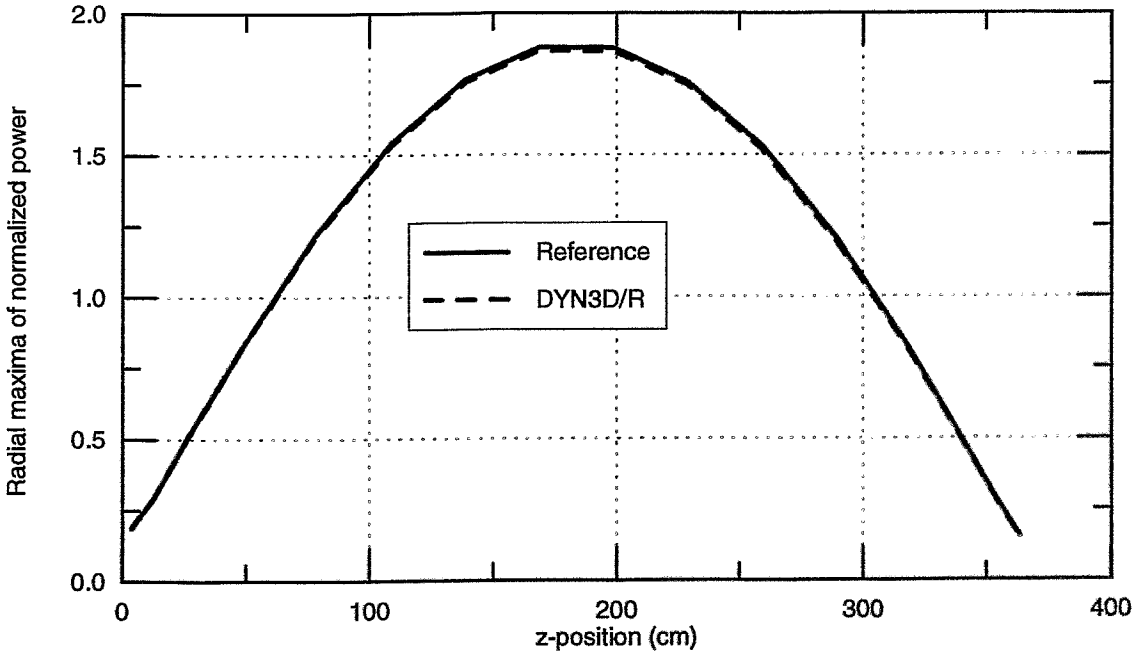

Fig. 4.1.5: Envelope axial power distribution Fq(z) (result B6)

4.1.2 Transient Core Averaged Results

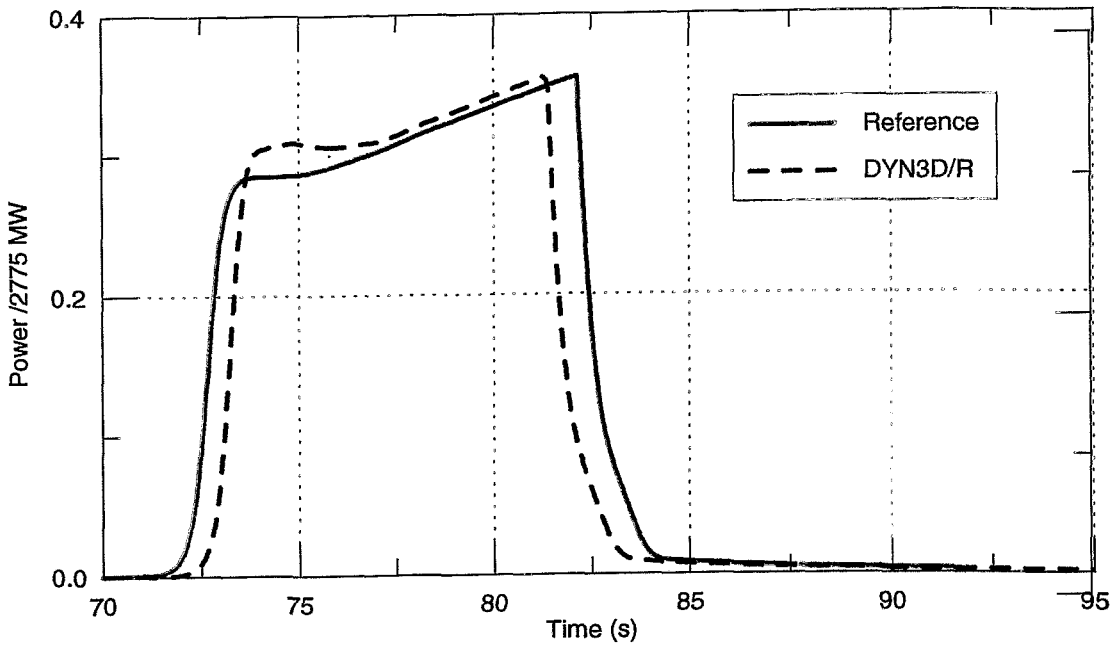

Fig. 4.1.6: Fission power of hot pellet to nominal average value (result C1)

The next figure shows the results of codes taking part at the benchmark calculations.

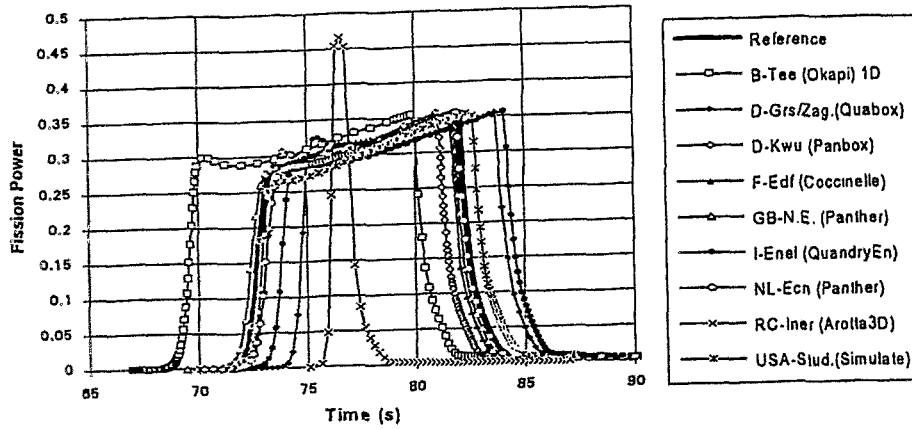

Fig. 4.1.7: Fission power to nominal value (result C1) for different codes [8].

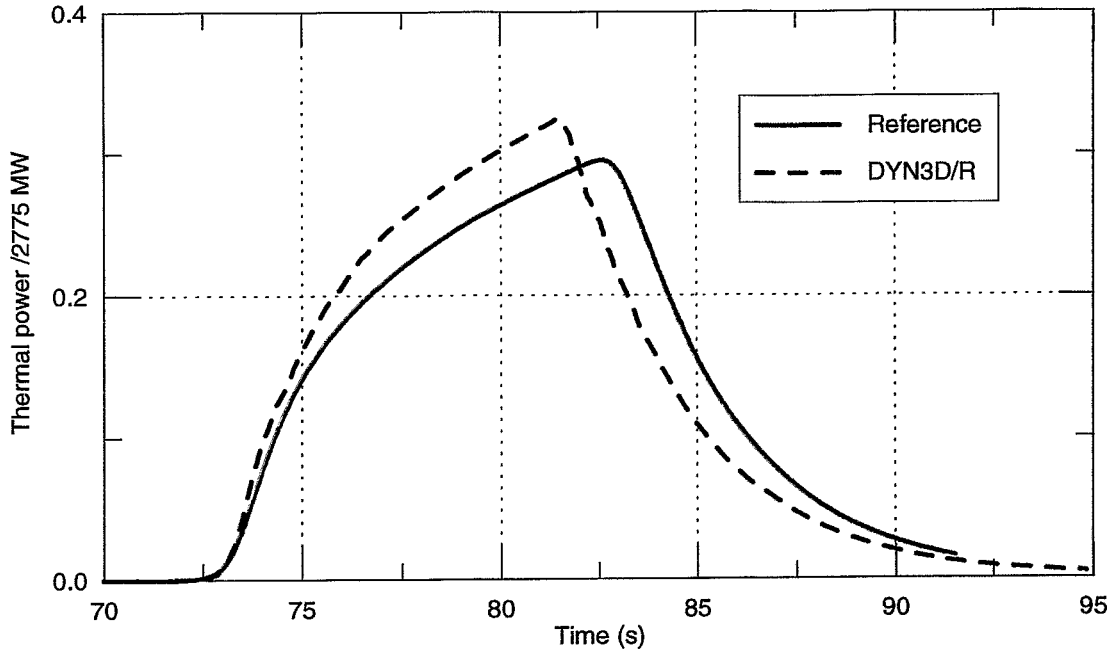

Fig. 4.1.8: Coolant heating to nominal value (result C2)

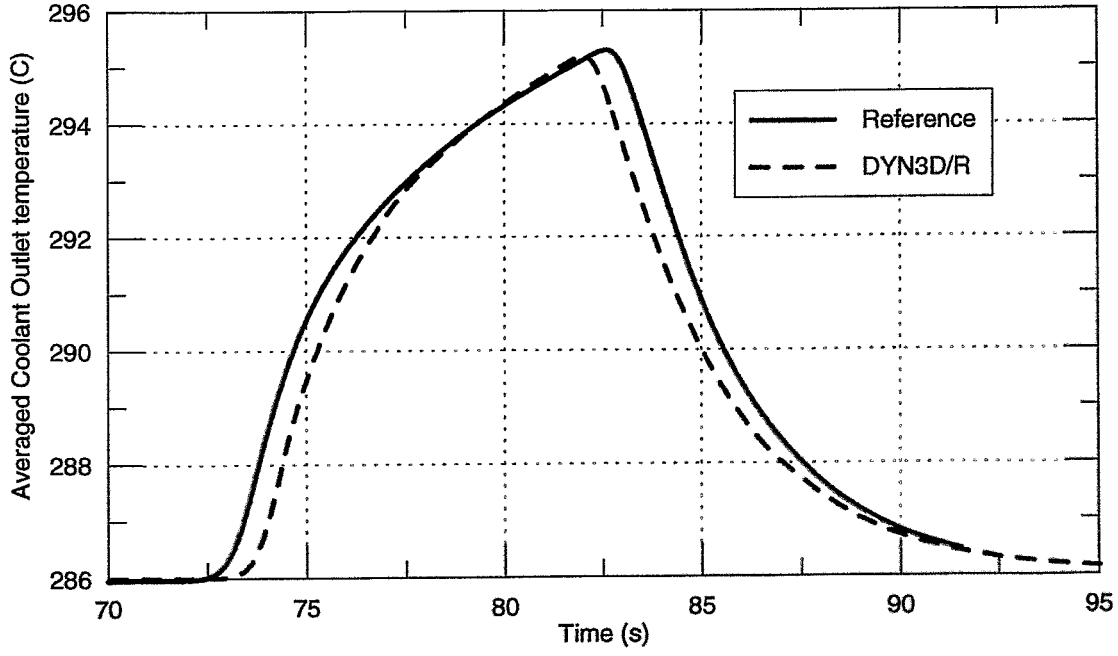

Fig. 4.1.9: Coolant outlet temperature (result C3)

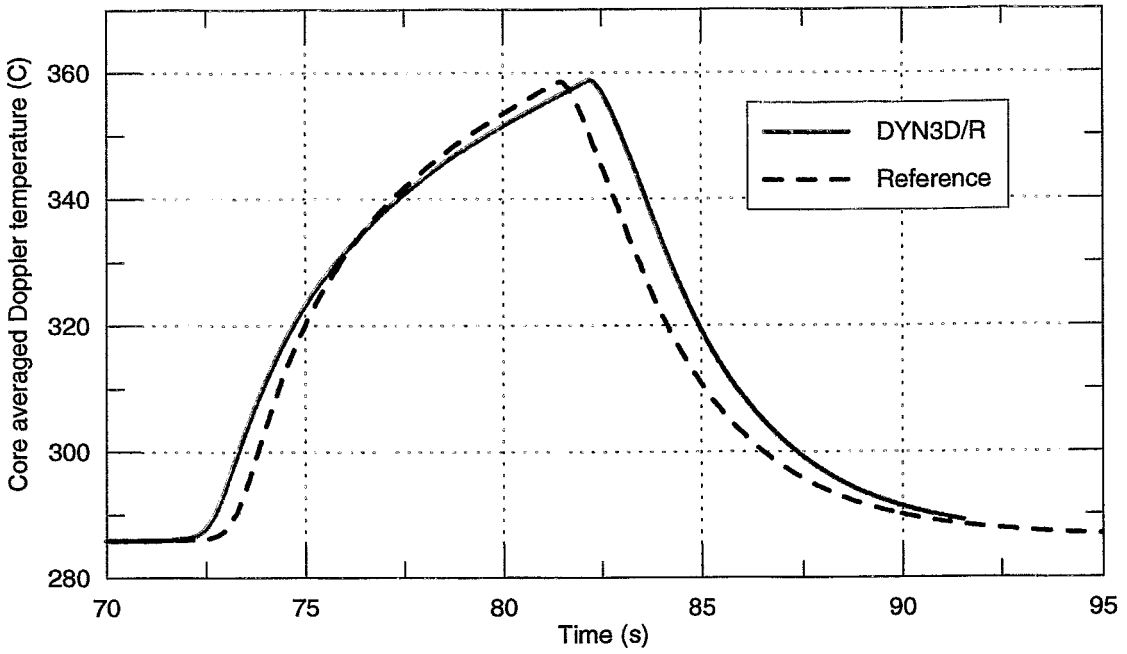

Fig. 4.1.10: Fuel Doppler temperature (result C4)

The Doppler temperatures of other codes for the benchmark are shown below.

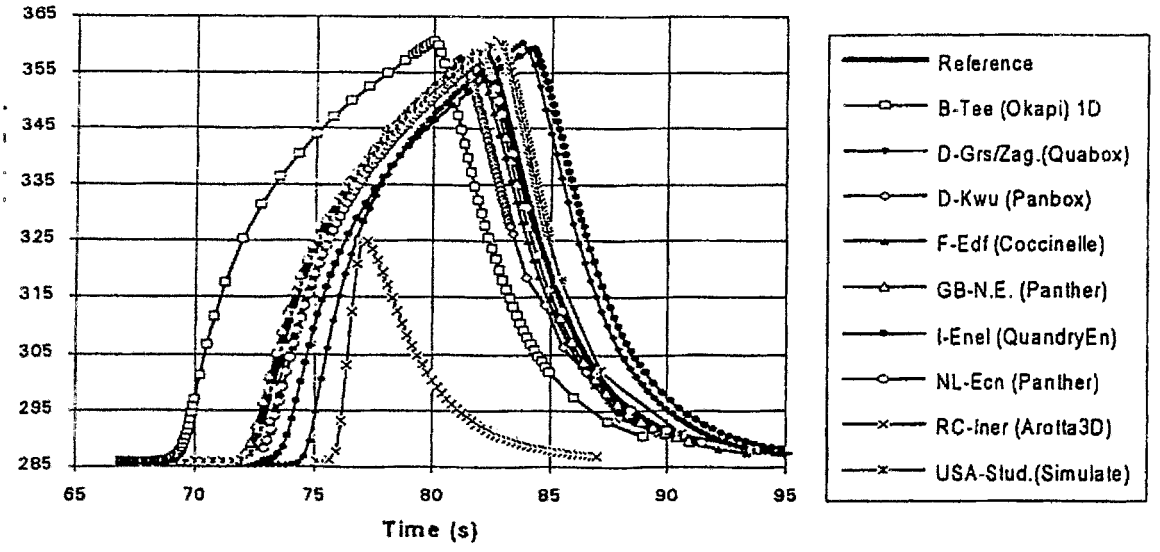

Fig. 4.1.11: Fuel Doppler temperature (result C4) for different codes [8].

4.1.3 Transient Hot Pellet Results

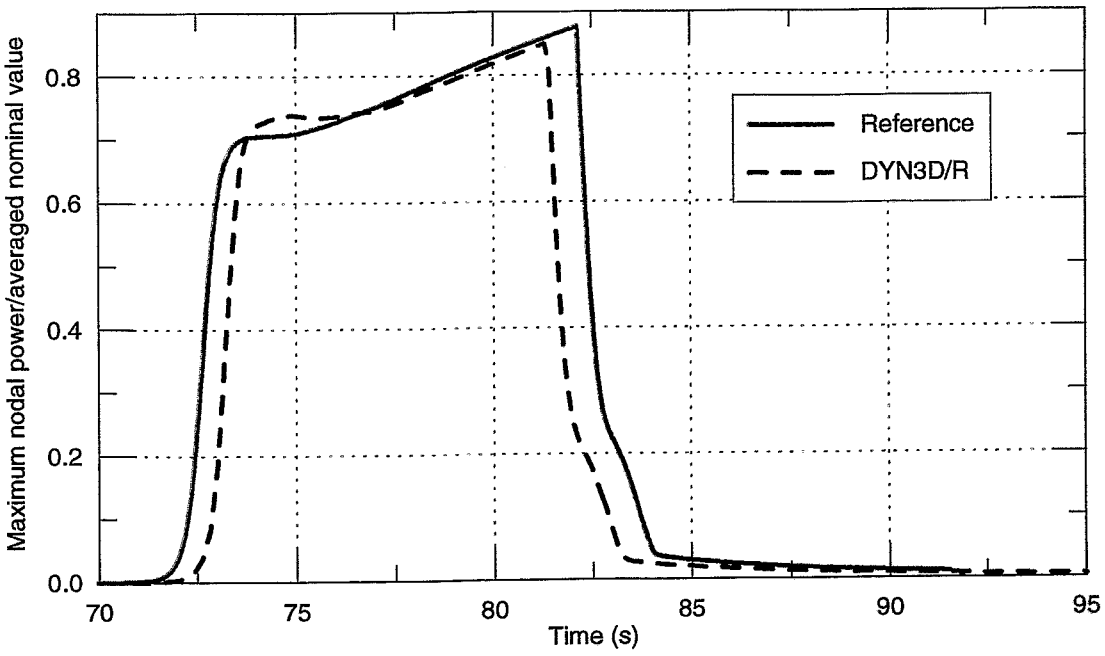

Fig. 4.1.12: Fission power to nominal average value (result D1)

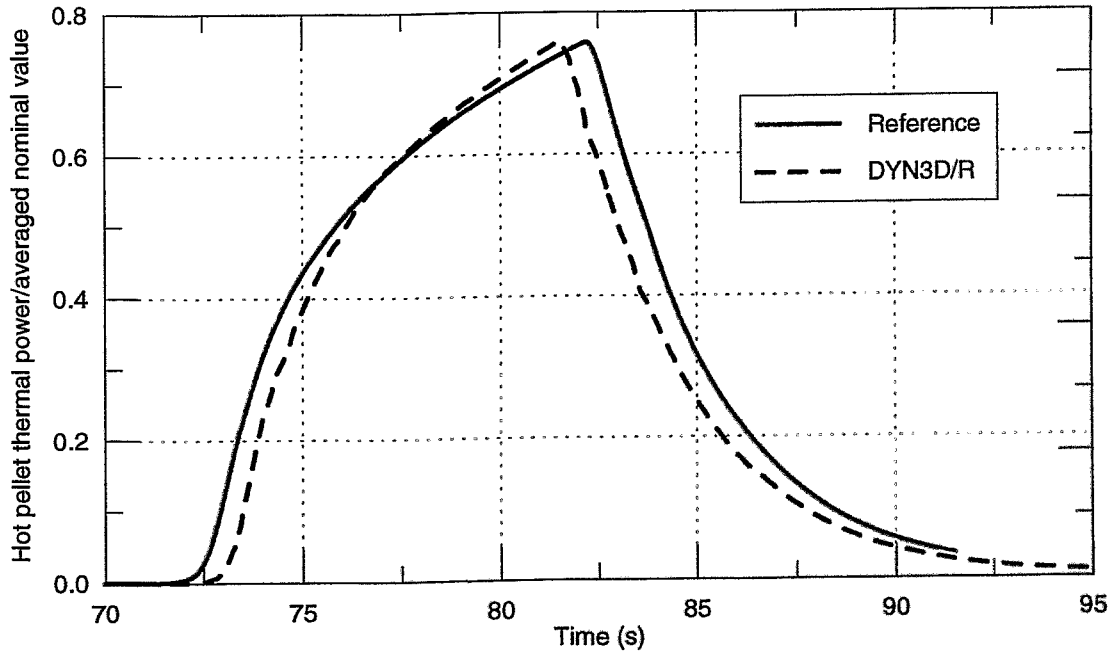

Fig. 4.1.13: Coolant heating of hot pellet to nominal average value (result D2)

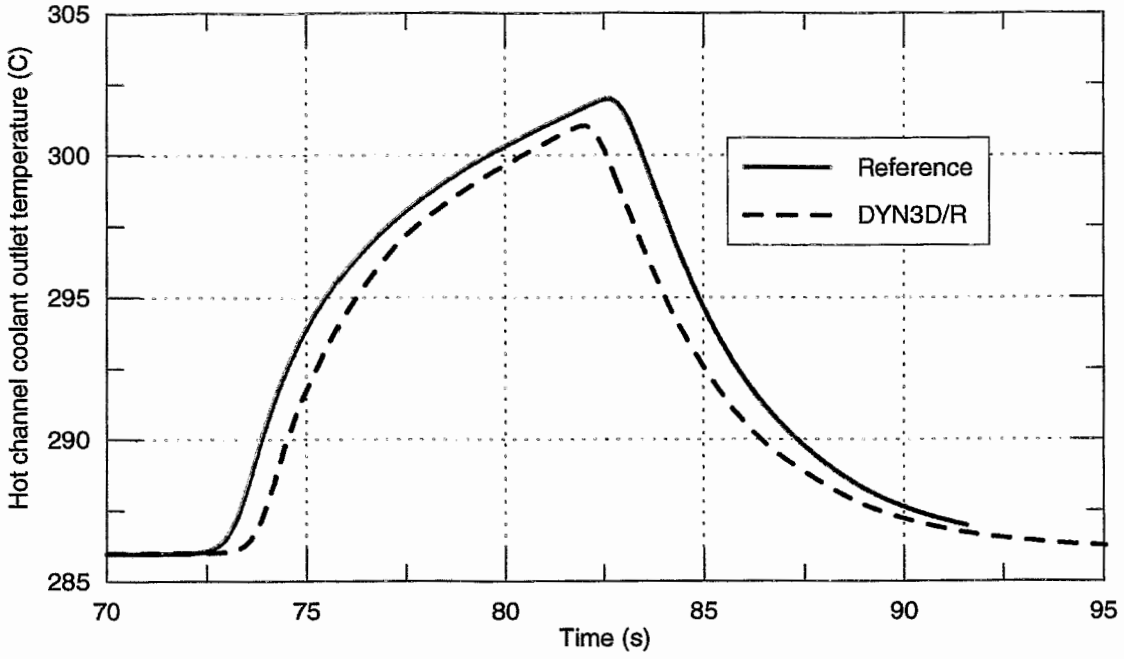

Fig. 4.1.14: Coolant temperature at the outlet of hot channel (result D3)

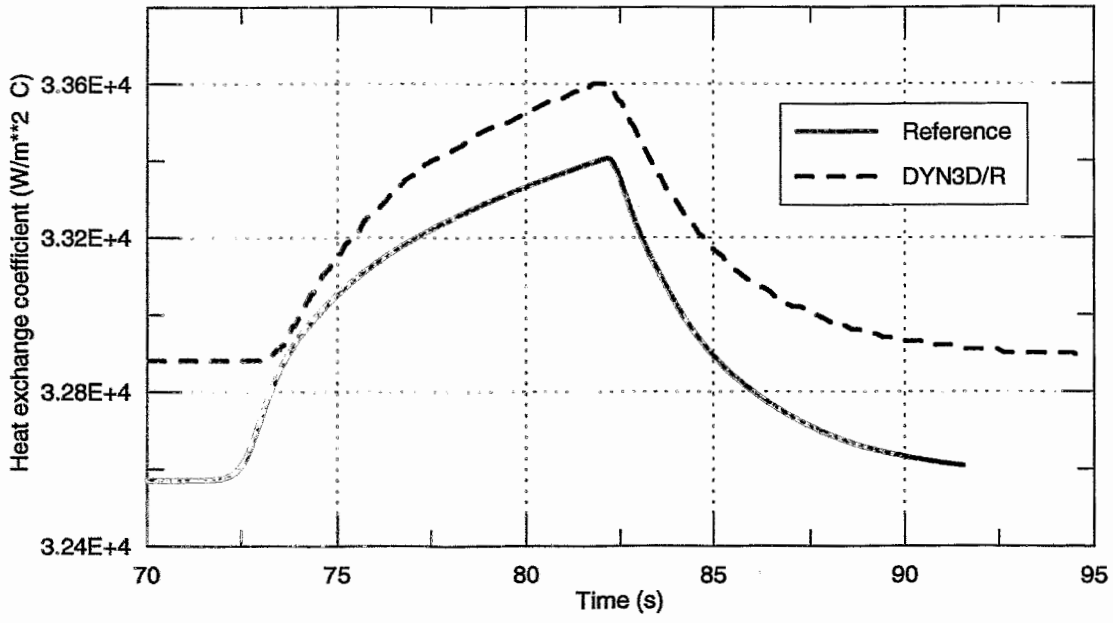

Fig. 4.1.15: Heat exchange coefficient between cladding and coolant of the hot pellet (result D4)

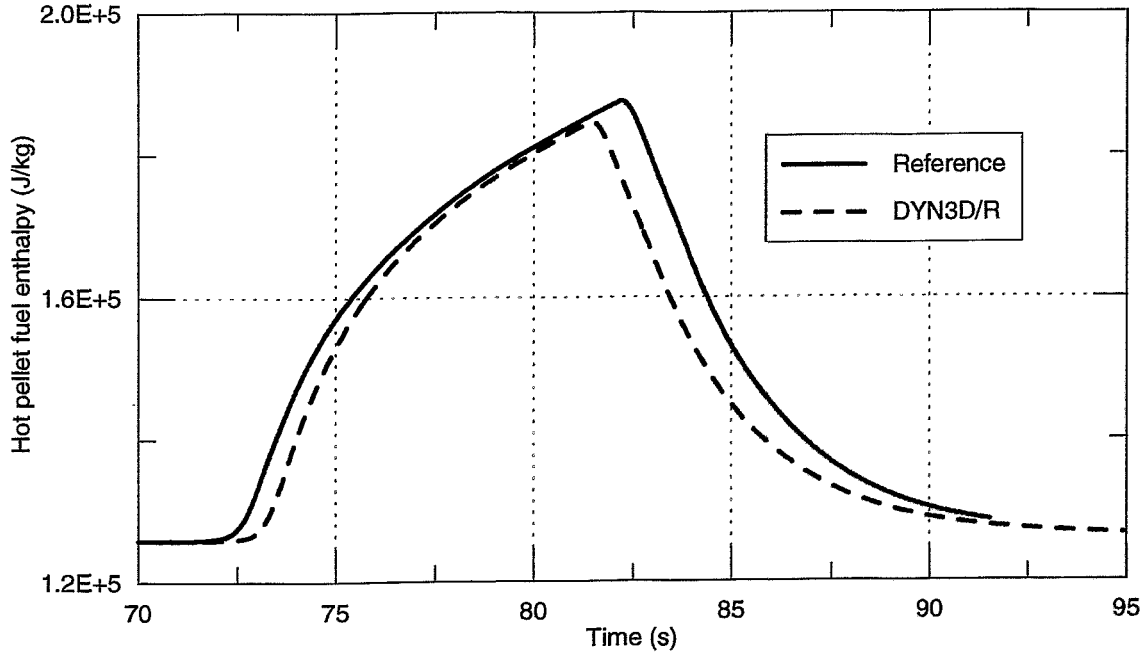

Fig. 4.1.16: Fuel enthalpy of the hot pellet (result D5)

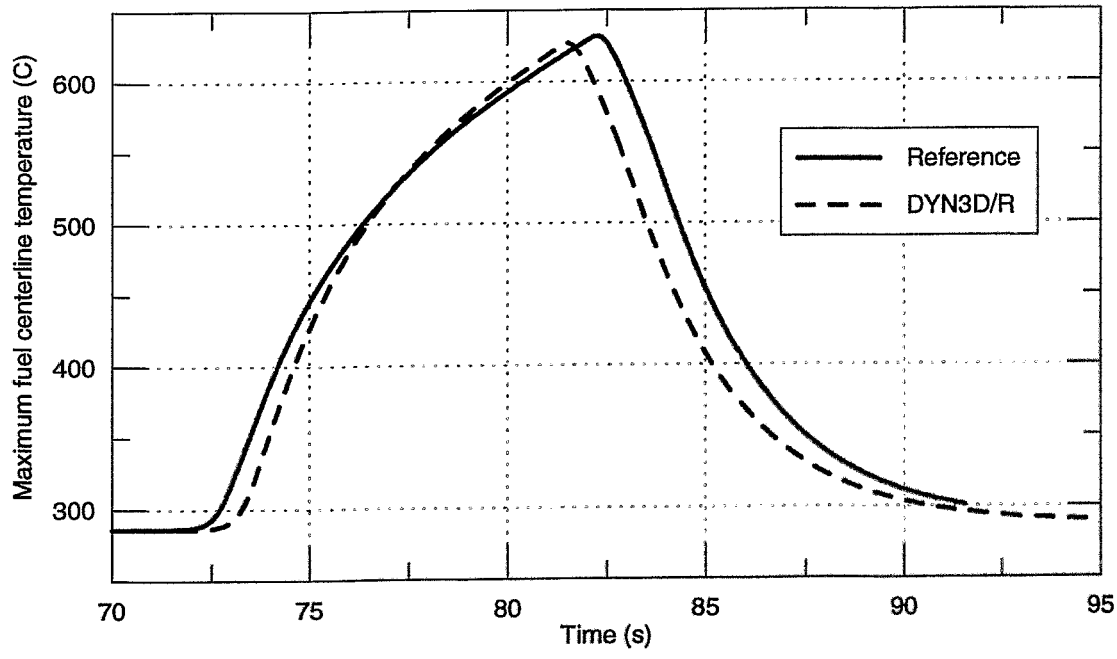

Fig. 4.1.17: Fuel temperature at hot pellet centerline (result D6)

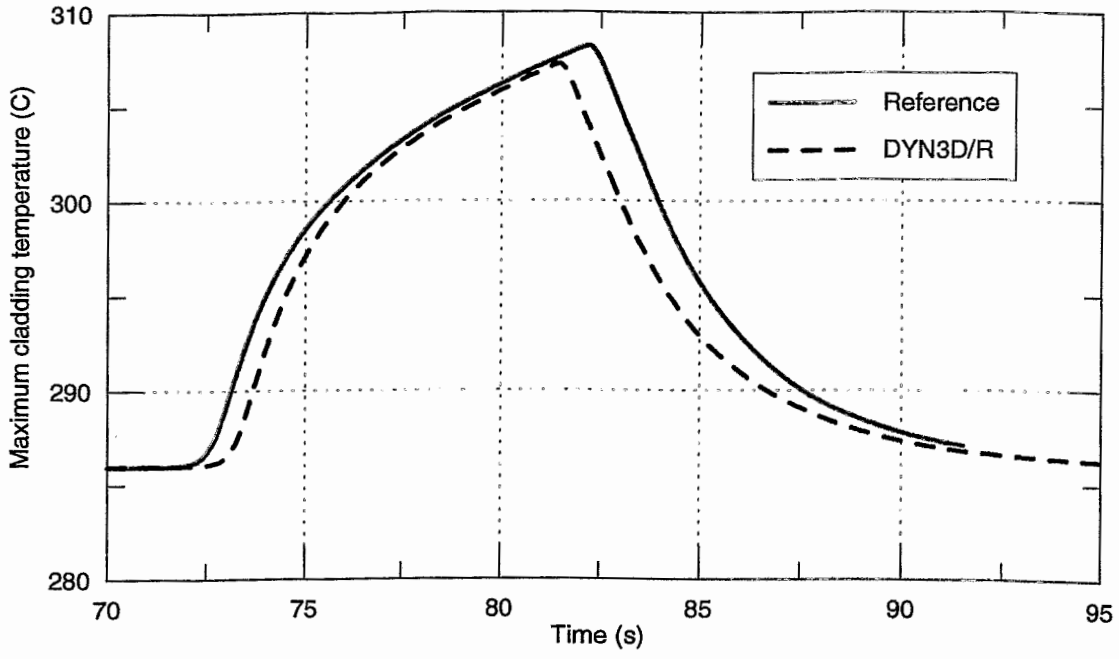

Fig. 4.1.18: Cladding outer surface temperature at the hot pellet (result D7)

4.1.4 Snapshots at Time of Power Maximum

The power maximum calculated by DYN3D/R is at the time t_{max} = 81.6 s. The value of fission power relativ to the nominal power is 0.3552. The deviation to the reference value of 0.3556 is - 0.0004 (result E1).

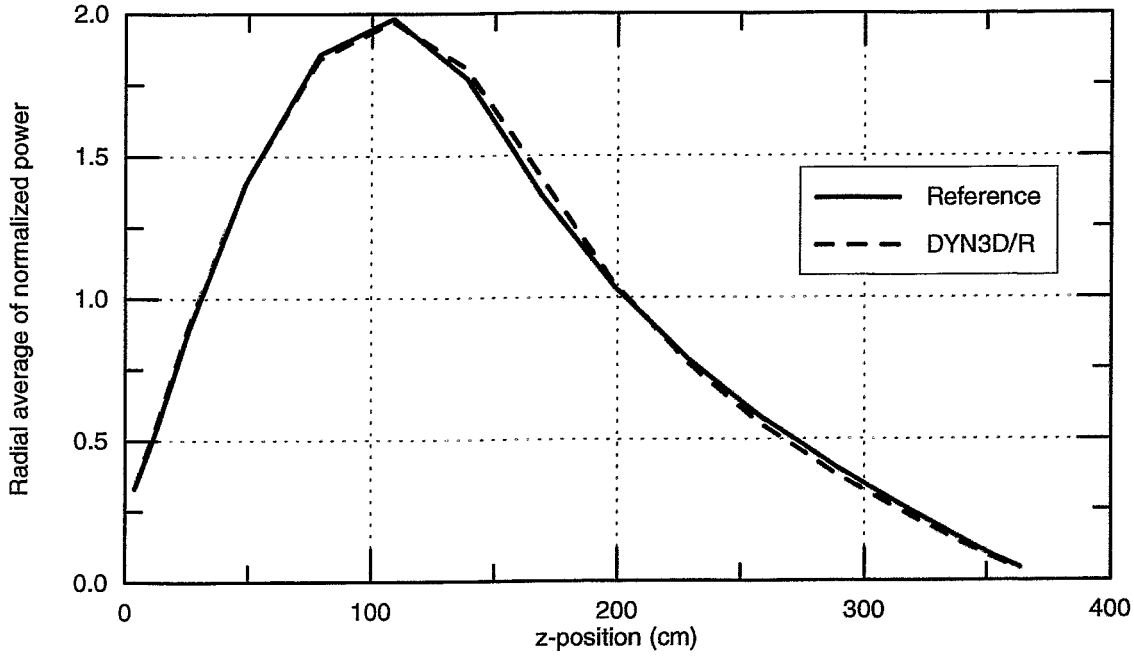

Fig. 4.1.20: Radially averaged axial power distribution (result E2)

8 0.725 0.757 4.41	Assembly no. (DYN3D/R) Reference DYN3D/R Dev. (%)				34 -	35 -	
				30 0.931 0.934 0.29	31 0.722 0.717 -0.70	32 -	33 -
			25 1.115 1.106 -0.81	26 1.051 1.045 -0.59	27 1.022 1.023 0.01	28 0.664 0.658 -0.88	29 -
		18 0.934 0.962 2.99	19 1.099 1.100 0.08	20 1.150 1.136 -1.22	21 1.056 1.053 -0.33	22 0.963 0.961 -0.16	23 -	24 -
	10 1.105 1.094 -0.96	11 1.088 1.089 0.03	12 1.154 1.143 -1.00	13 1.177 1.168 -0.79	14 1.136 1.132 -0.35	15 0.976 0.999 2.33	16 0.577 0.594 2.85	17 -
1 1.094 1.076 -1.56	2 1.054 1.045 -0.83	3 1.134 1.120 -1.22	4 1.106 1.097 -0.86	5 1.205 1.189 -1.27	6 1.166 1.172 0.46	7 0.829 0.874 5.38	8 0.725 0.757 4.41	9 -

Fig. 4.1.21: Axially averaged radial power distribution (result E3)

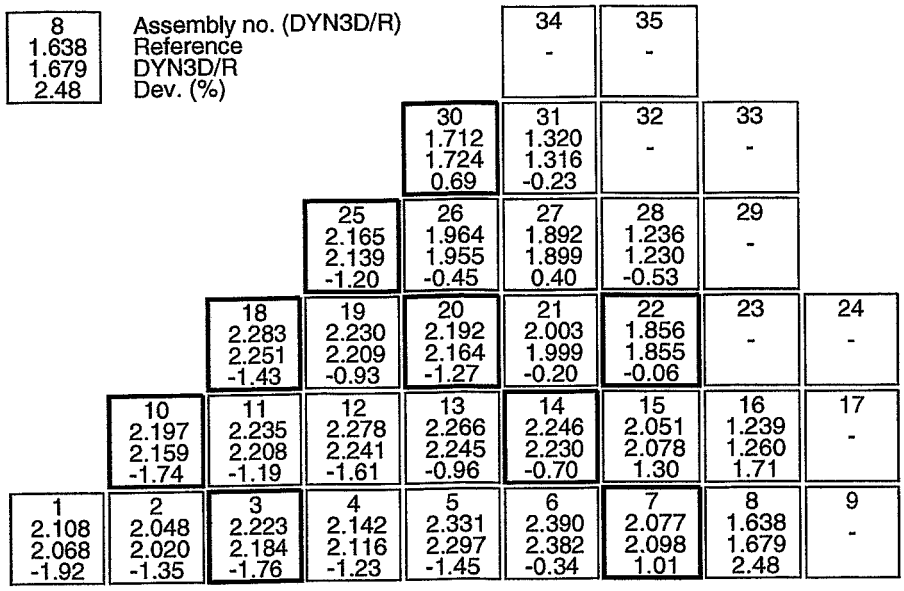

Fig. 4.1.22: Radial power distribution at axial layer number 6 (result E4)

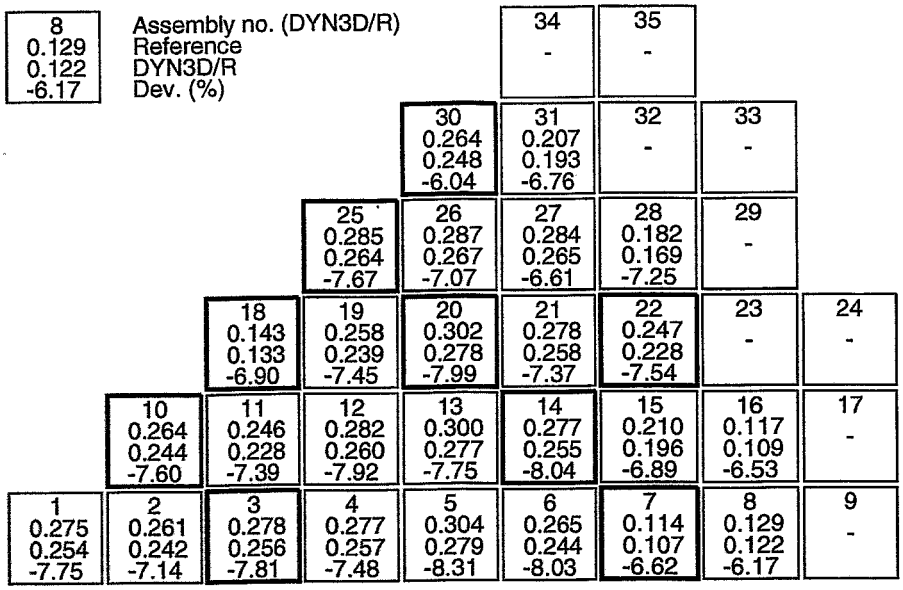

Fig. 4.1.23: Radial power distribution at axial layer number 13 (result E5)

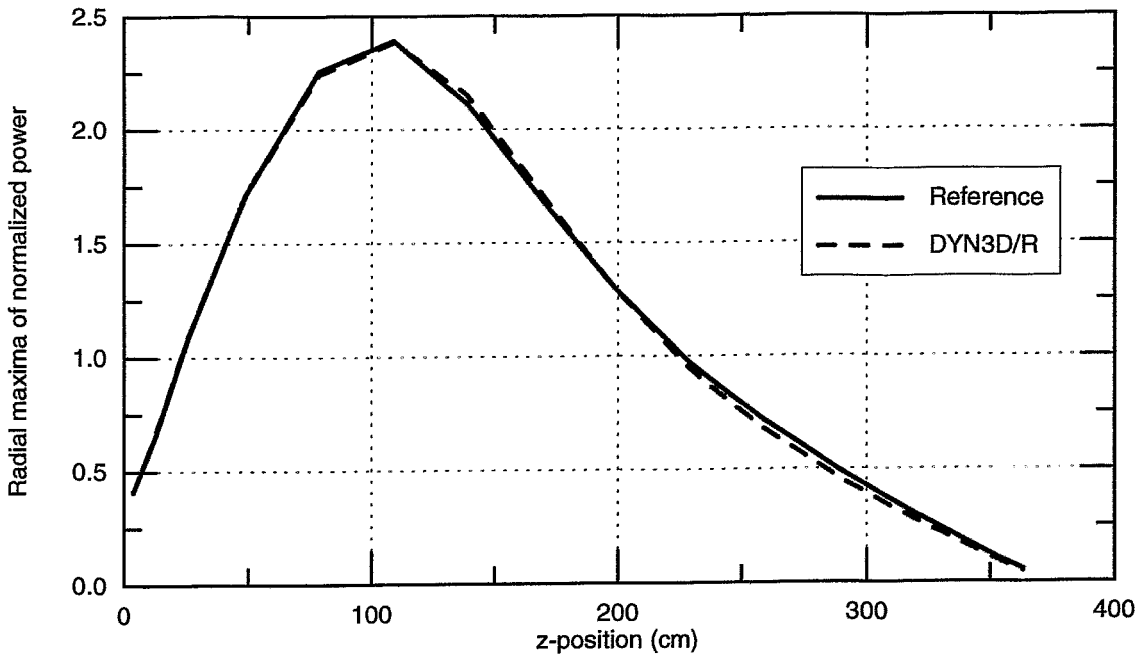

Fig. 4.1.24: Envelope axial power distribution Fq(z) (result E6)

4.2 Case B - Withdrawal of Bank B and C

4.2.1 Initial Steady State

The critical boron concentration of case B calculated by DYN3D is 796.18 ppm. The deviation to the reference value of 793.58 ppm is 0.32% (result B1).

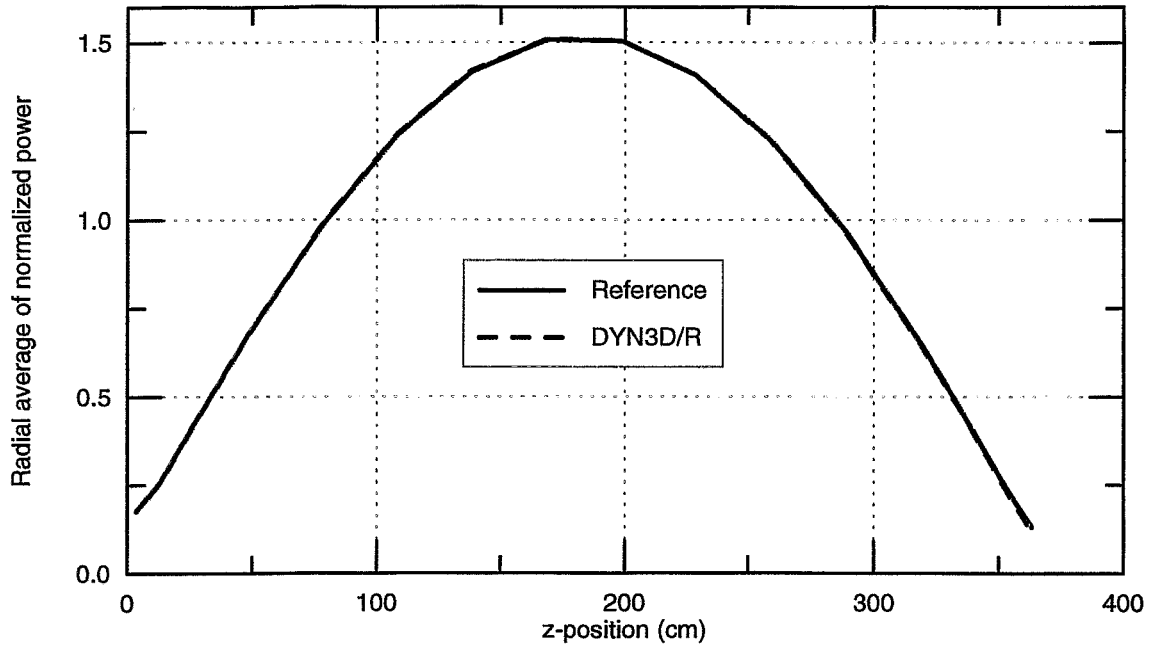

Fig. 4.2.1: Radially averaged axial power distribution (result B2)

8 0.806 0.811 0.69	Assembly no. (DYN3D/R) Reference DYN3D/R Dev. (%)				34 -	35 -		
				30 0.398 0.406 1.93	31 0.507 0.511 0.72	32 -	33 -	
			25 1.016 1.015 -0.07	26 0.775 0.778 0.42	27 0.817 0.832 1.92	28 0.503 0.503 -0.02	29 -	
		18 0.735 0.734 -0.13	19 1.077 1.074 -0.28	20 0.665 0.666 0.09	21 0.916 0.915 -0.00	22 0.505 0.506 0.15	23 -	24 -
	10 1.523 1.514 -0.62	11 1.251 1.244 -0.58	12 1.511 1.505 -0.34	13 1.532 1.531 -0.10	14 1.451 1.451 -0.02	15 1.001 1.005 0.38	16 0.641 0.640 -0.03	17 -
1 1.798 1.780 -1.00	2 1.461 1.455 -0.38	3 0.835 0.832 -0.40	4 1.490 1.487 -0.21	5 1.912 1.903 -0.47	6 1.645 1.645 -0.04	7 0.677 0.680 0.48	8 0.806 0.811 0.69	9 -

Fig. 4.2.2: Axially averaged radial power distribution (result B3)

8 1.001 1.011 0.91	Assembly no. (DYN3D/R) Reference DYN3D/R Dev. (%)				34 -	35 -		
				30 0.494 0.504 2.10	31 0.630 0.636 0.90	32 -	33 -	
			25 1.262 1.263 0.08	26 0.961 0.967 0.55	27 1.014 1.035 2.09	28 0.625 0.626 0.19	29 -	
		18 0.911 0.911 -0.02	19 1.337 1.335 -0.15	20 0.825 0.827 0.23	21 1.137 1.138 0.16	22 0.627 0.629 0.32	23 -	24 -
	10 1.893 1.883 -0.48	11 1.553 1.546 -0.45	12 1.877 1.873 -0.21	13 1.903 1.904 0.04	14 1.804 1.806 0.16	15 1.243 1.250 0.55	16 0.796 0.798 0.18	17 -
1 2.234 2.216 -0.84	2 1.814 1.809 -0.25	3 1.035 1.032 -0.28	4 1.850 1.849 -0.08	5 2.377 2.369 -0.32	6 2.045 2.047 0.11	7 0.840 0.845 0.65	8 1.001 1.011 0.91	9 -

Fig. 4.2.3: Radial power distribution at axial layer number 6 (result B4)

8 0.525 0.526 0.28	Assembly no. (DYN3D/R) Reference DYN3D/R Dev. (%)			34 -	35 -			
			30 0.259 0.263 1.55	31 0.330 0.331 0.33	32 -	33 -		
		25 0.661 0.659 -0.42	26 0.504 0.504 0.03	27 0.532 0.540 1.52	28 0.328 0.326 -0.38	29 -		
		18 0.477 0.475 -0.49	19 0.701 0.696 -0.65	20 0.432 0.431 -0.29	21 0.596 0.593 -0.39	22 0.328 0.328 -0.24	23 -	24 -
	10 0.992 0.982 -1.00	11 0.814 0.806 -0.95	12 0.984 0.977 -0.71	13 0.997 0.992 -0.48	14 0.945 0.941 -0.40	15 0.651 0.651 -0.02	16 0.417 0.415 -0.42	17 -
1 1.171 1.155 -1.39	2 0.951 0.943 -0.79	3 0.543 0.538 -0.78	4 0.970 0.964 -0.58	5 1.245 1.235 -0.85	6 1.071 1.066 -0.43	7 0.440 0.440 0.07	8 0.525 0.526 0.28	9 -

Fig. 4.2.4: Radial power distribution at axial layer number 13 (result B5)

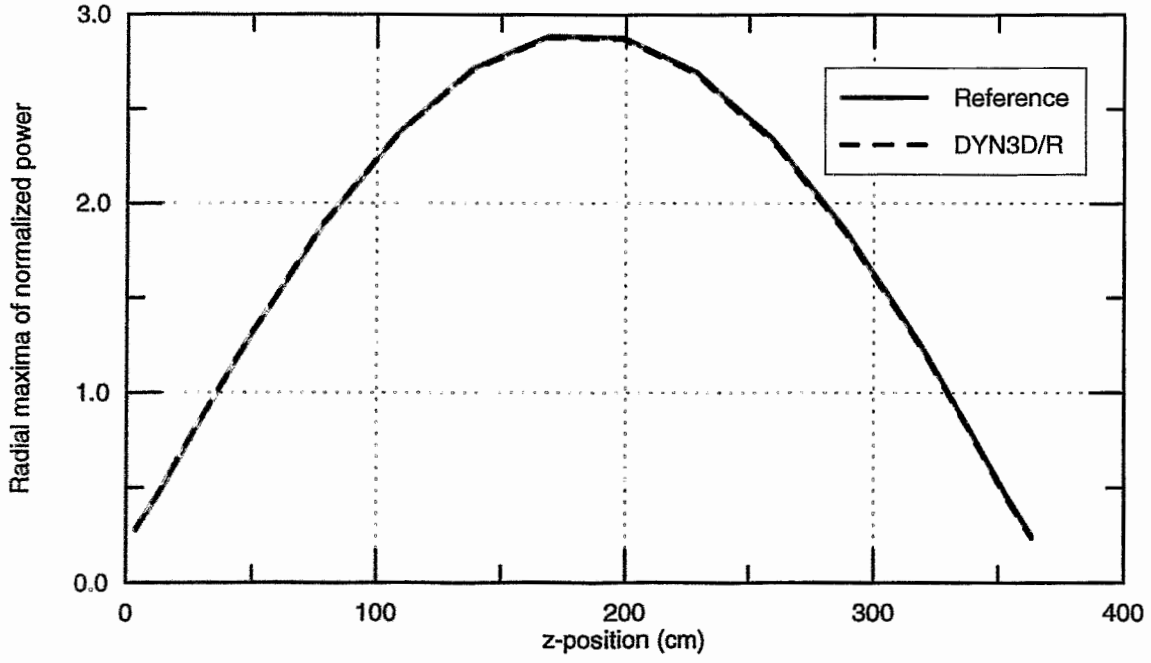

Fig. 4.2.5: Envelope axial power distribution Fq(z) (result B6)

The next figure shows the envelopes of the different codes published in [8].

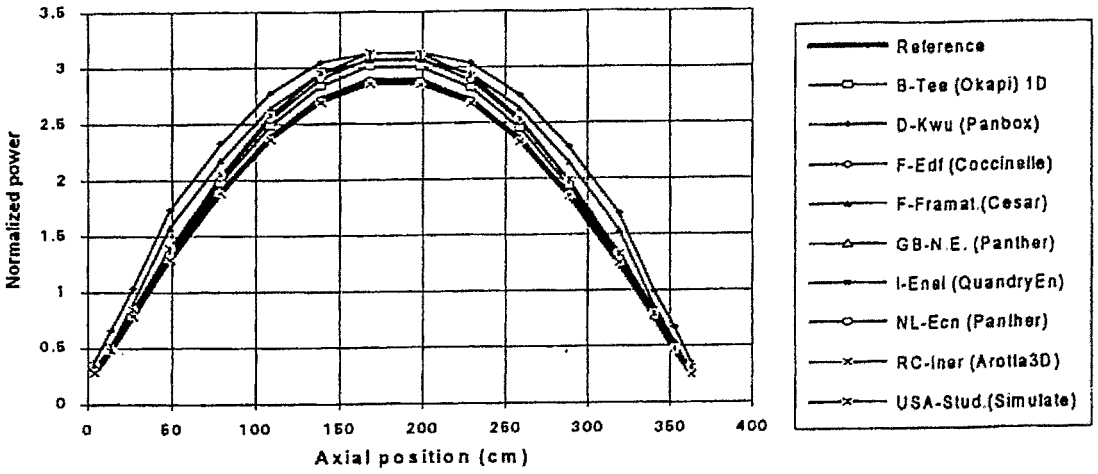

Fig. 4.2.6: Envelope axial power distribution Fq(z) (result B6) for the codes taking part in the benchmark calculations **[8]**.

4.2.2 Transient Core Averaged Results

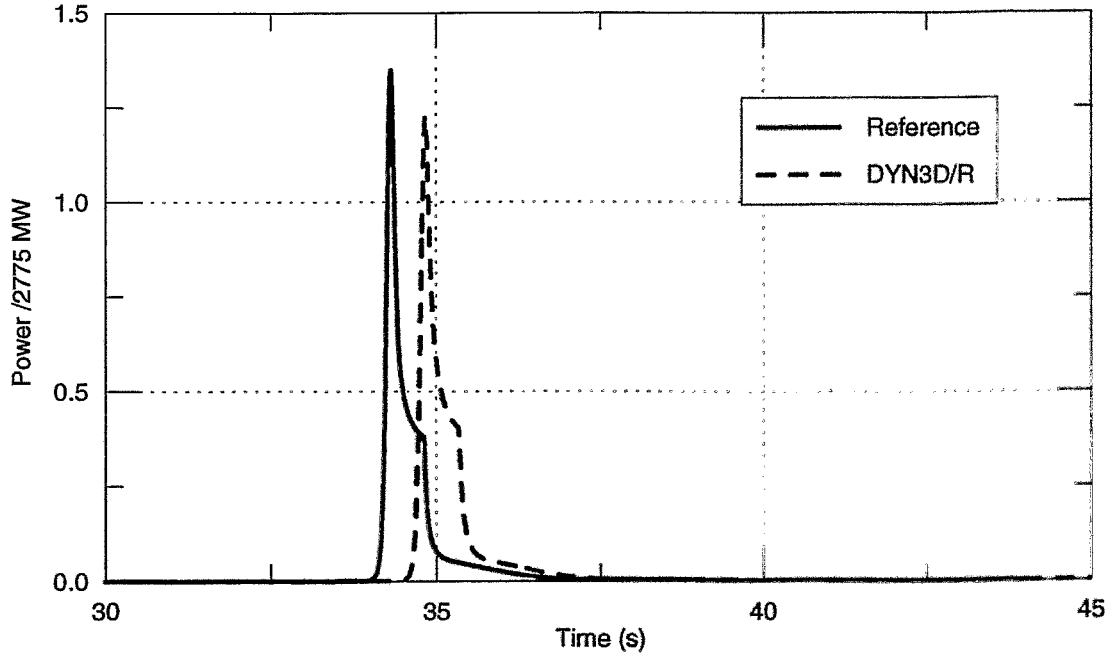

Fig. 4.2.7: Fission power to nominal value (result C1)

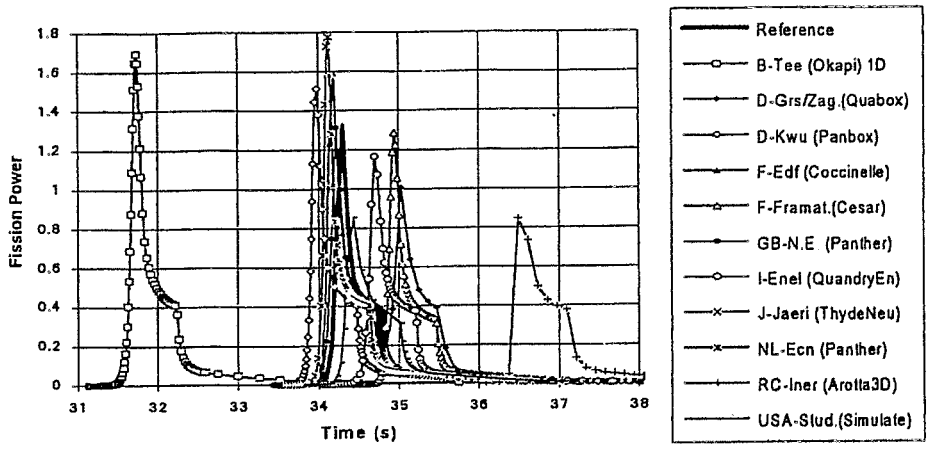

Fig. 4.2.8: Fission power to nominal value (result C1) for the codes taking part in the benchmark calculations **[8]**.

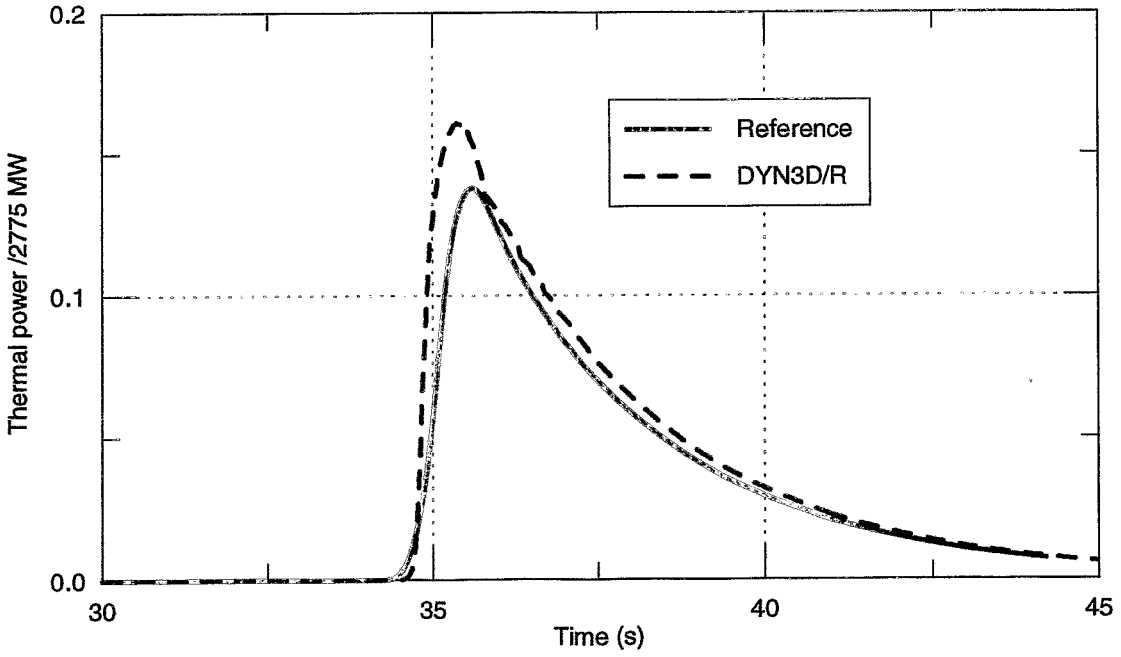

Fig. 4.2.9: Coolant heating to nominal value (result C2)

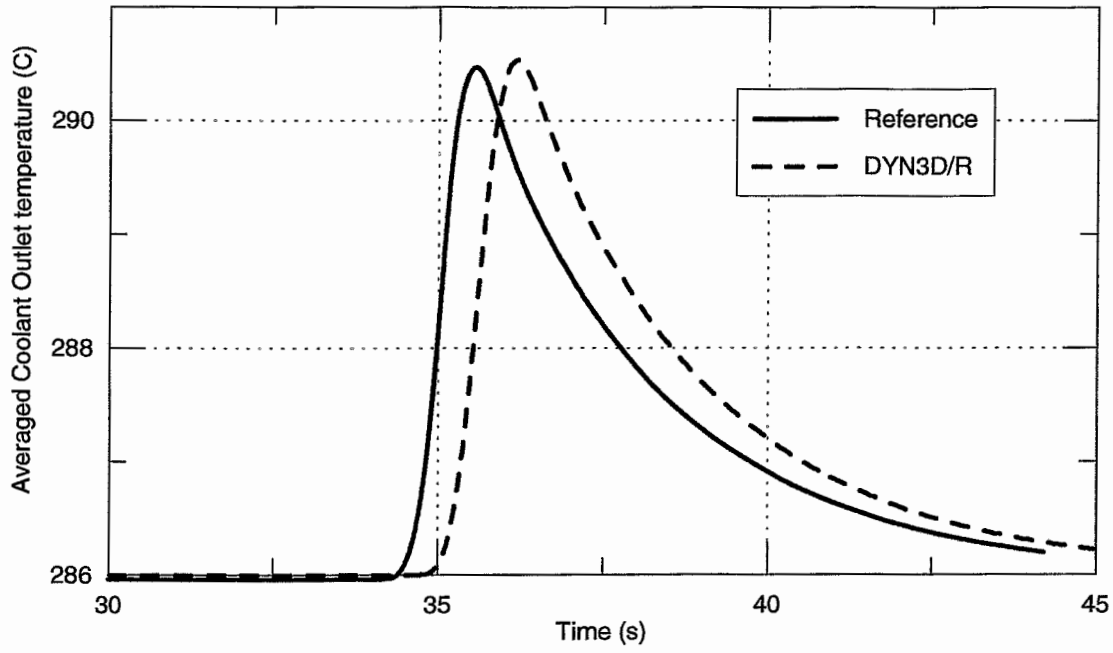

Fig. 4.2.10: Coolant outlet temperature (result C3)

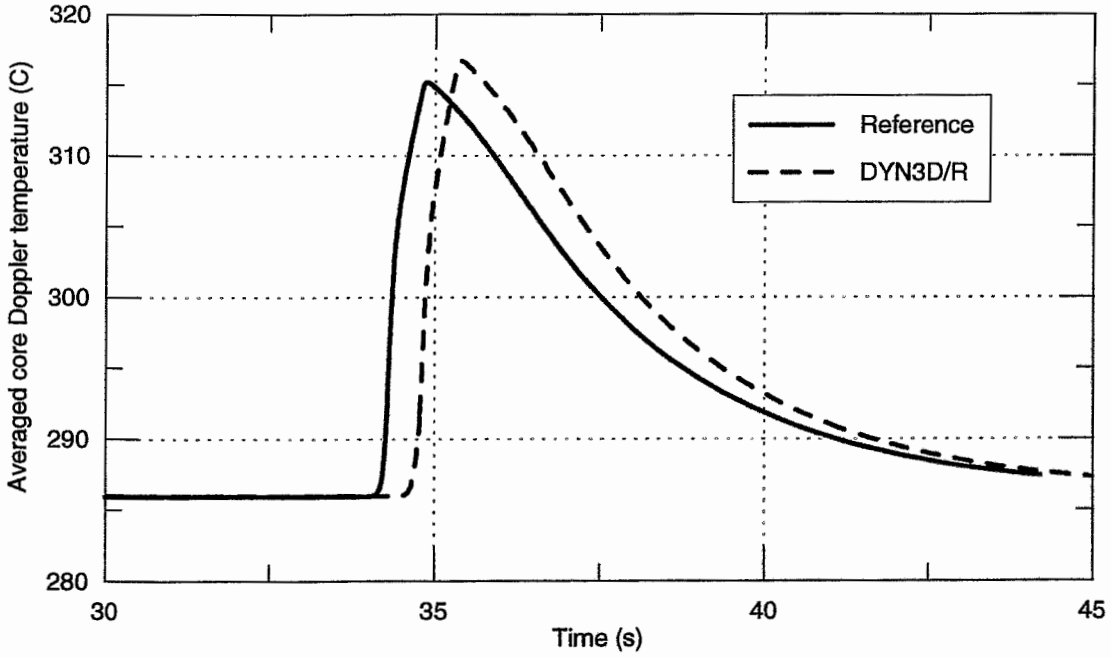

Fig. 4.2.11: Fuel Doppler temperature (result C4)

4.2.3 Transient Hot Pellet Results

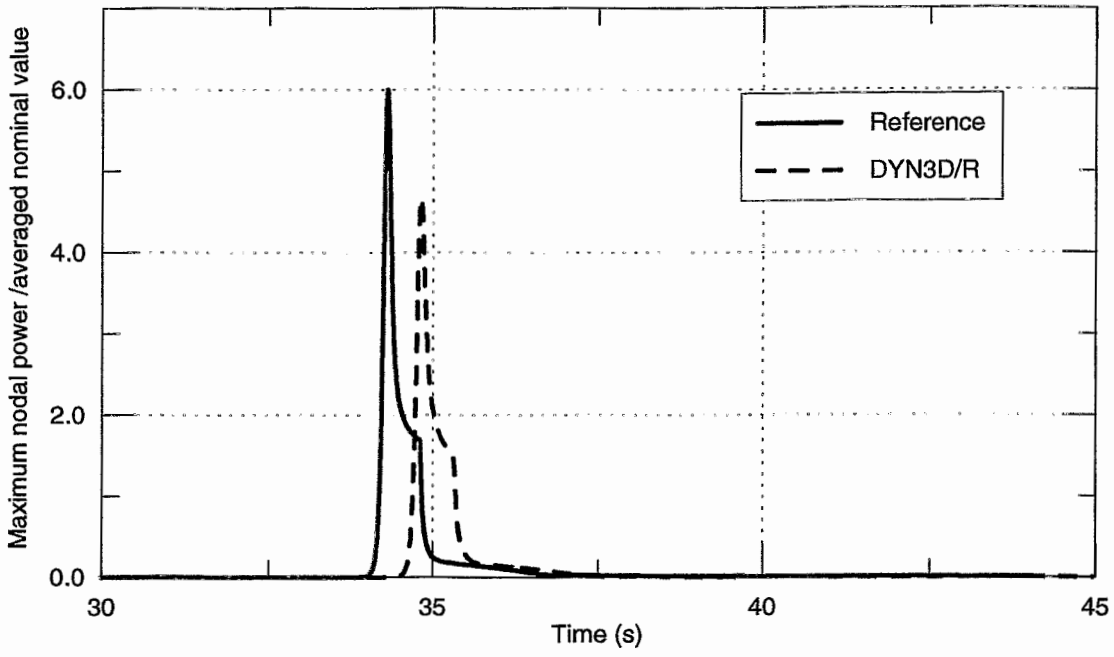

Fig. 4.2.12: Fission power of hot pellet to nominal average value (result D1)

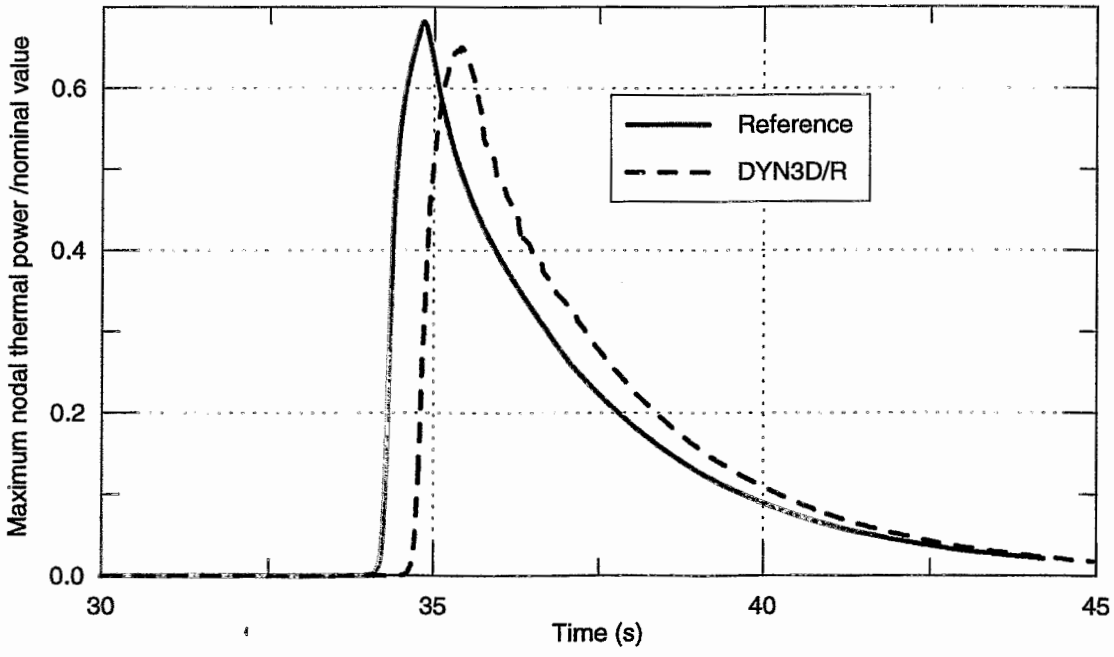

Fig. 4.2.13: Coolant heating of hot pellet to nominal average value (result D2)

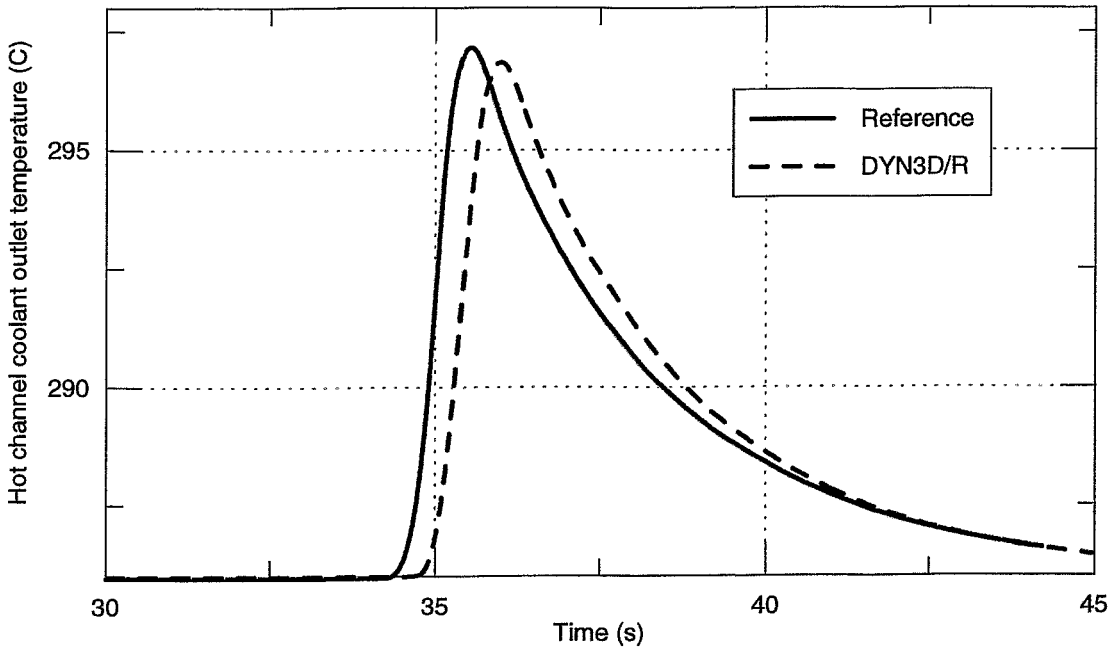

Fig. 4.2.14: Coolant temperature at the outlet of the hot channel (result D3)

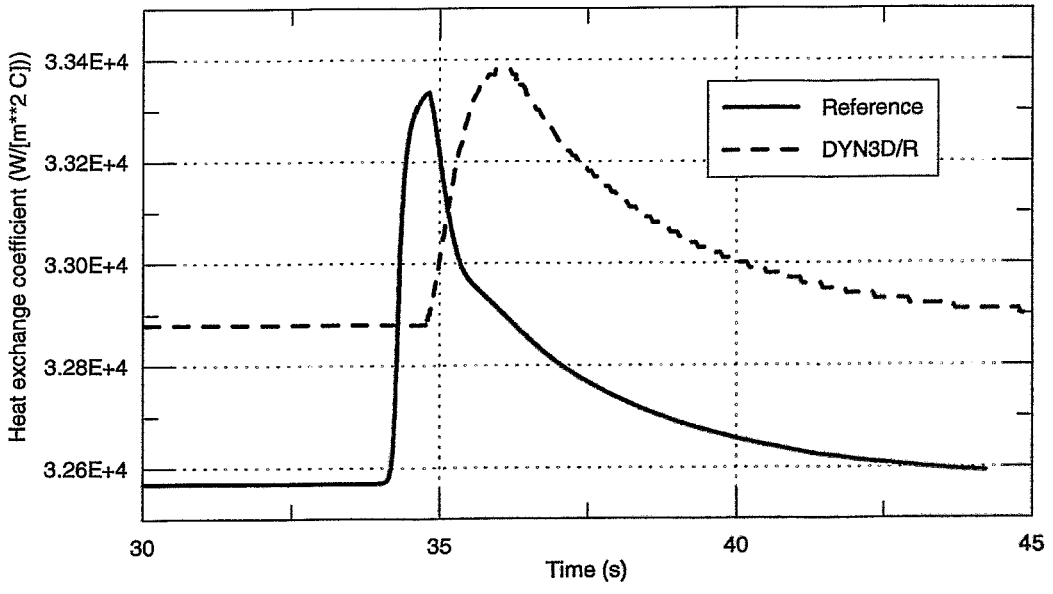

Fig. 4.2.15: Heat exchange coefficient between cladding and coolant of the hot pellet (result D4)

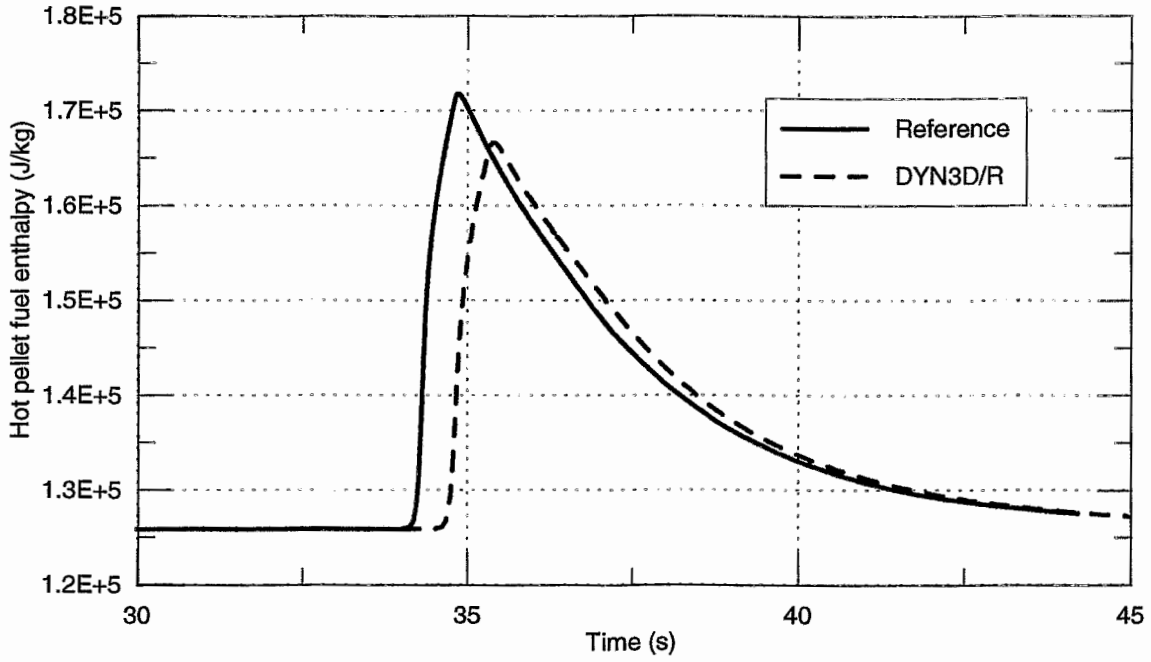

Fig. 4.2.16: Fuel enthalpy of the hot pellet (result D5)

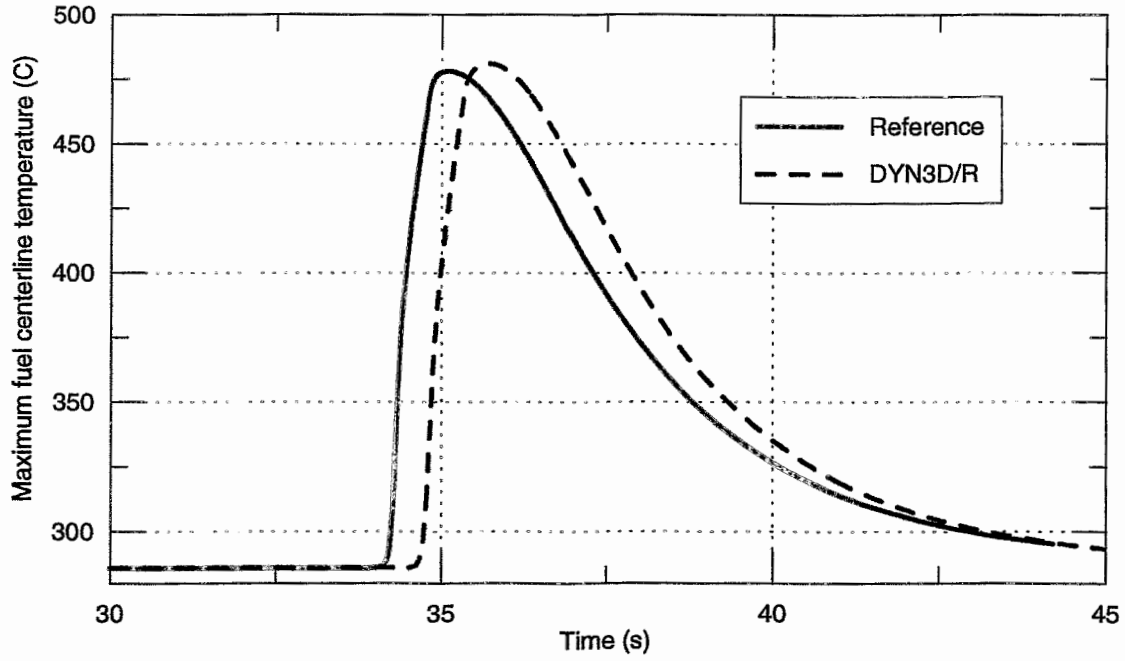

Fig. 4.2.17: Fuel temperature at the hot pellet centerline (result D6)

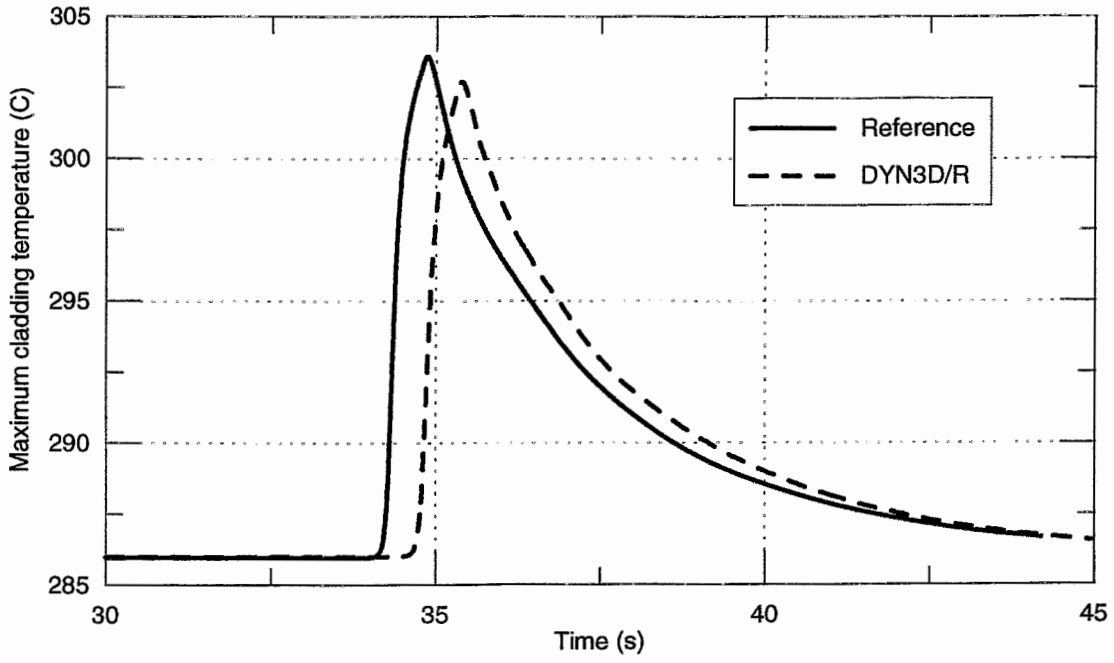

Fig. 4.2.18: Cladding outer surface temperature at the hot pellet (result D7)

4.2.4 Snapshots at Time of Power Maximum

The power maximum calculated by DYN3D/R is at the time t_{max} = 34.827 s. The value of fission power relativ to the nominal power is 1.2255. The deviation to the reference value 1.3480 is - 0.1225 (result E1).

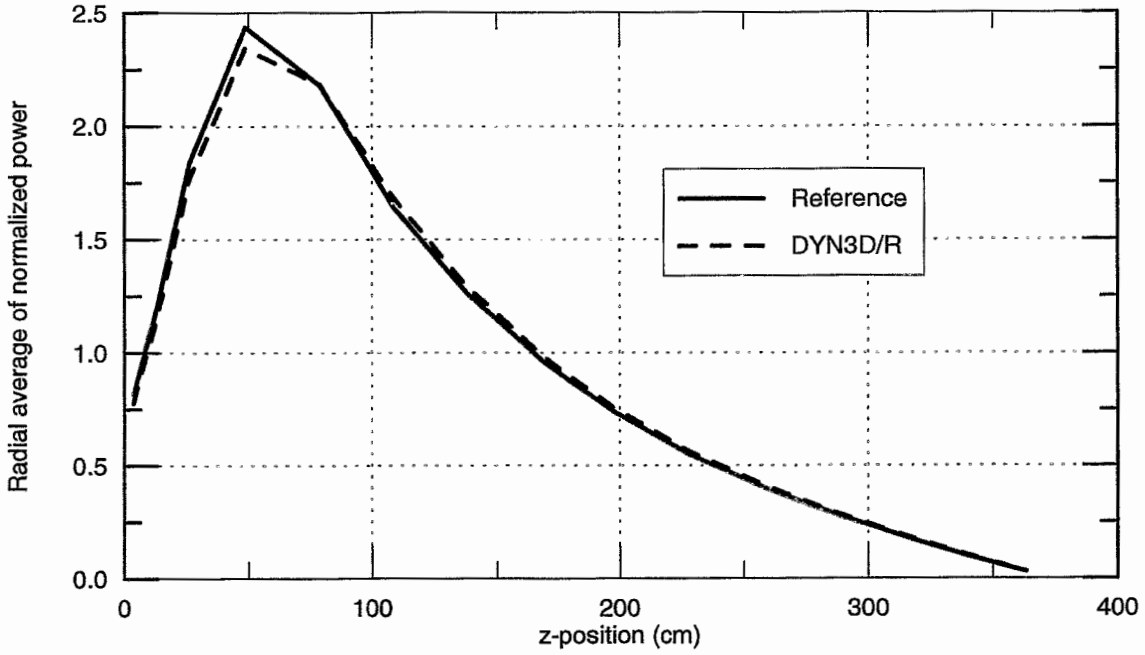

Fig. 4.2.19: Radially averaged axial power distribution (result E2)

8 0.625 0.631 1.03	Assembly no. (DYN3D/R) Reference DYN3D/R Dev. (%)				34 -	35 -		
				30 0.649 0.655 0.92	31 0.619 0.622 0.44	32 -	33 -	
			25 1.132 1.130 -0.18	26 0.939 0.941 0.23	27 0.890 0.905 1.74	28 0.498 0.498 0.08	29 -	
		18 0.741 0.740 -0.15	19 1.139 1.136 -0.26	20 0.904 0.897 -0.75	21 0.918 0.918 0.06	22 0.458 0.460 0.37	23 -	24 -
	10 1.537 1.526 -0.69	11 1.293 1.285 -0.61	12 1.477 1.472 -0.34	13 1.451 1.453 0.11	14 1.281 1.284 0.23	15 0.833 0.838 0.65	16 0.503 0.504 0.25	17 -
1 1.751 1.735 -0.94	2 1.494 1.487 -0.43	3 1.110 1.095 -1.33	4 1.458 1.456 -0.13	5 1.704 1.700 -0.20	6 1.404 1.409 0.29	7 0.553 0.558 0.85	8 0.625 0.631 1.03	9 -

Fig. 4.2.20: Axially averaged radial power distribution (result E3)

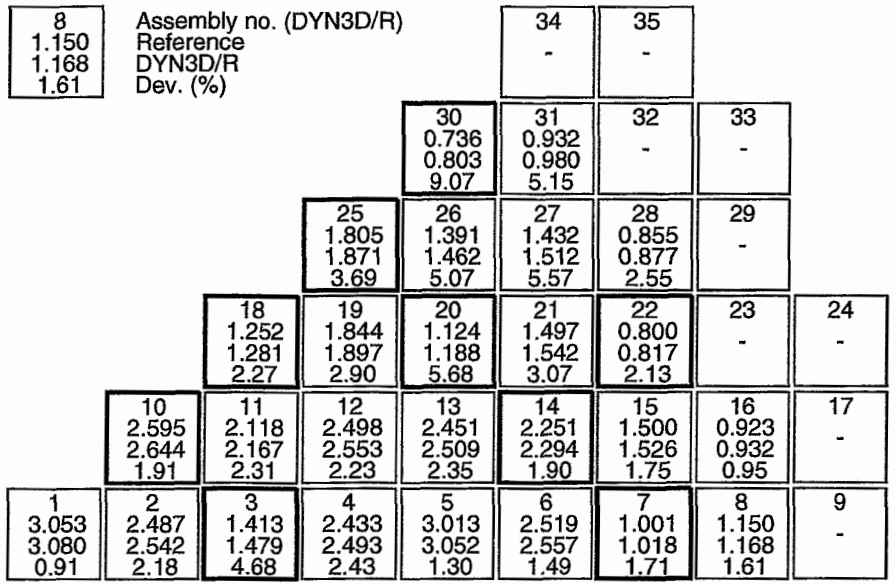

Fig. 4.2.21: Radial power distribution at axial layer number 6 (result E4)

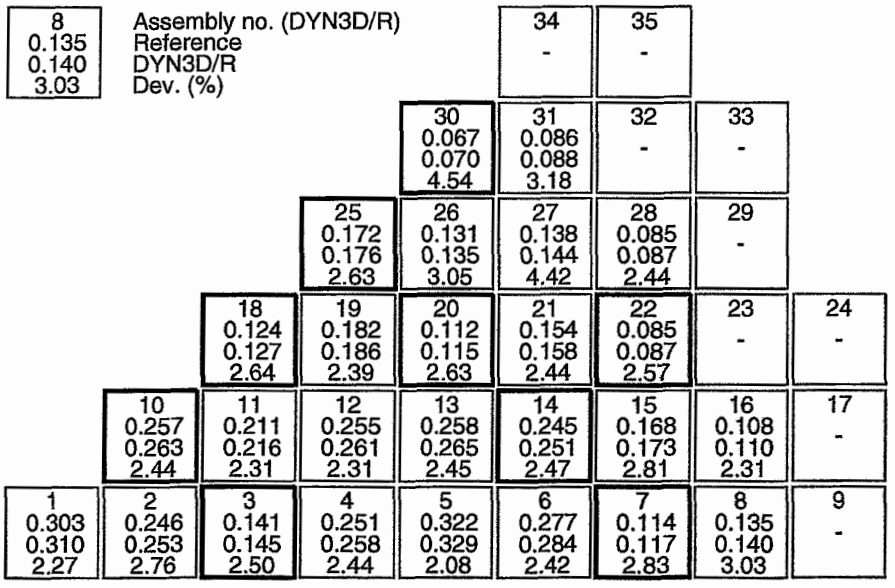

Fig. 4.2.22: Radial power distribution at axial layer number 13 (result E5)

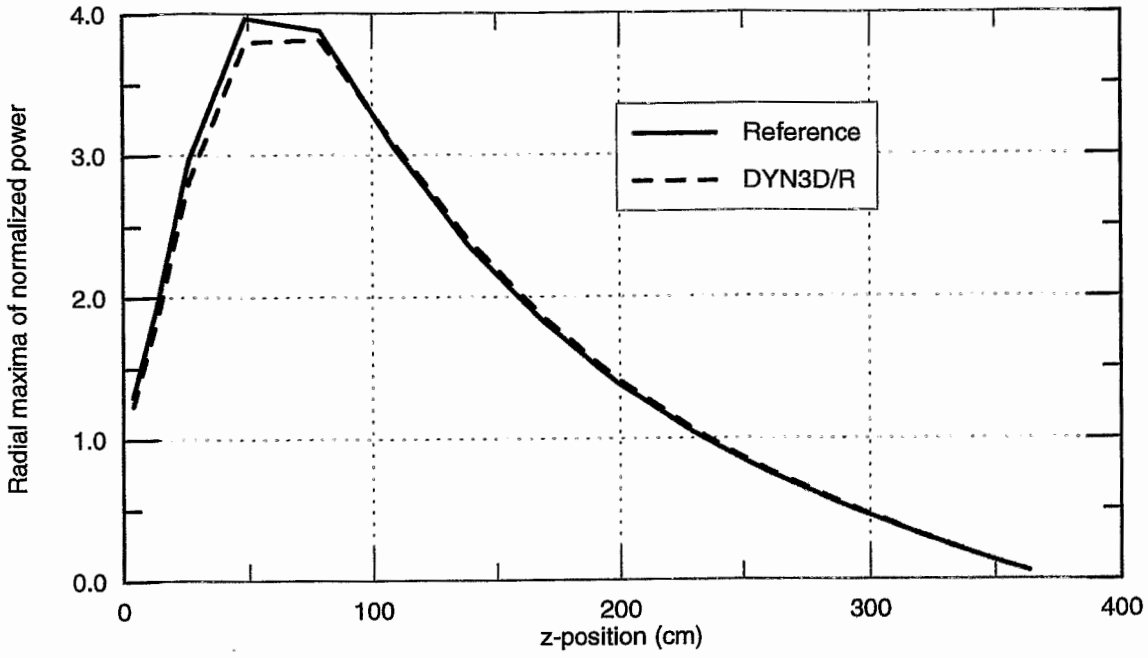

Fig. 4.2.23: Envelope axial power distribution Fq(z) (result E6)

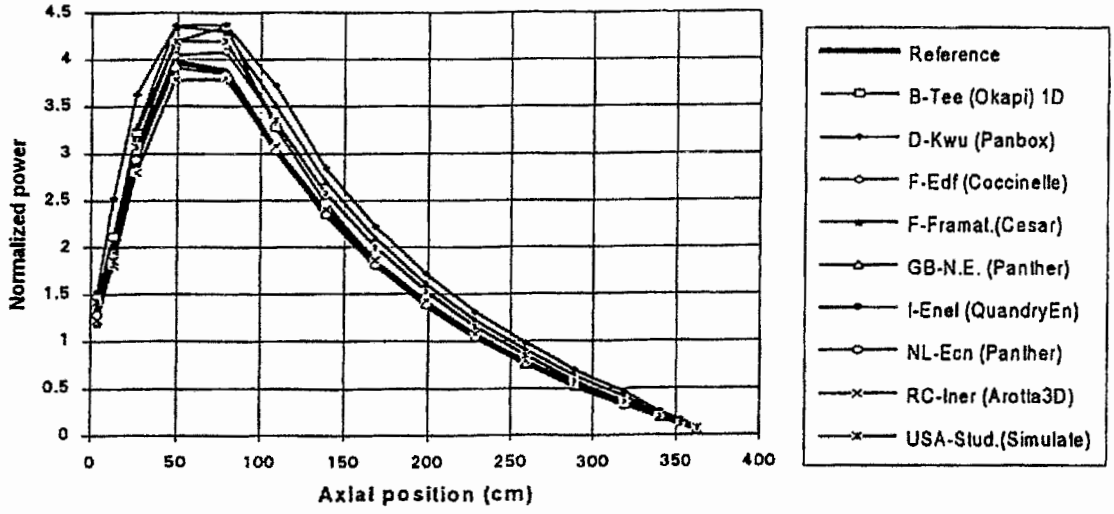

Fig. 4.2.24: Envelope axial power distribution Fq(z) (result E6) for the results of codes taking part in the benchmark calculations [8].

4.2.5 Calculation with Different Axial Nodalization

If we look at fig. 4.2.7 we see a shift of power peak calculated by DYN3D/R in comparison to the peak of reference solution. If we look to the comparisons in fig. 4.2.8 such a shift exists also in other results. The power peak occurs at the time when the reactor becomes supercritical. Therefore the localisation of power peak at the time axis is very sensitive to the reactivity gain. Small differences of reactivity during the withdrawal of control rods are caused by the axial nodalization and the different methods used to overcome the cusping effects. The effect has been investigated by performing DYN3D/R calculations with 20 axial nodes. In that case, the 18 core layers are given by thickness of 7.7, 11.5, 15.0 (5 layers), 30.0, (8 layers) 12.8 (2 layers) and 8 cm (from bottom to top). The bottom and top reflectors are described by layers of 30 cm thickness. The finer mesh of 15 cm instead of 30 cm is used at the axial positions of withdrawn control rods where the reactor becomes supercritical.

The influence of the different meshes is demonstrated in fig. 4.2.25 where we see the curves of the fission power for the reference and the results of the two different DYN3D/R calculations. The power peak of the calculation with 20 axial nodes is close to the reference. It is valid for the other results also. Fig. 4.2.26 shows the comparisons for the hot pellet fule enthalpy. The radial power distributions at the moment of power maximum are also influenced. We see on fig 4.2.27 - 4.2.29 better agreement with reference solutions than in fig. 4.2.20 - 4.2.22 which show radial power distributions in the moment of power maximum.

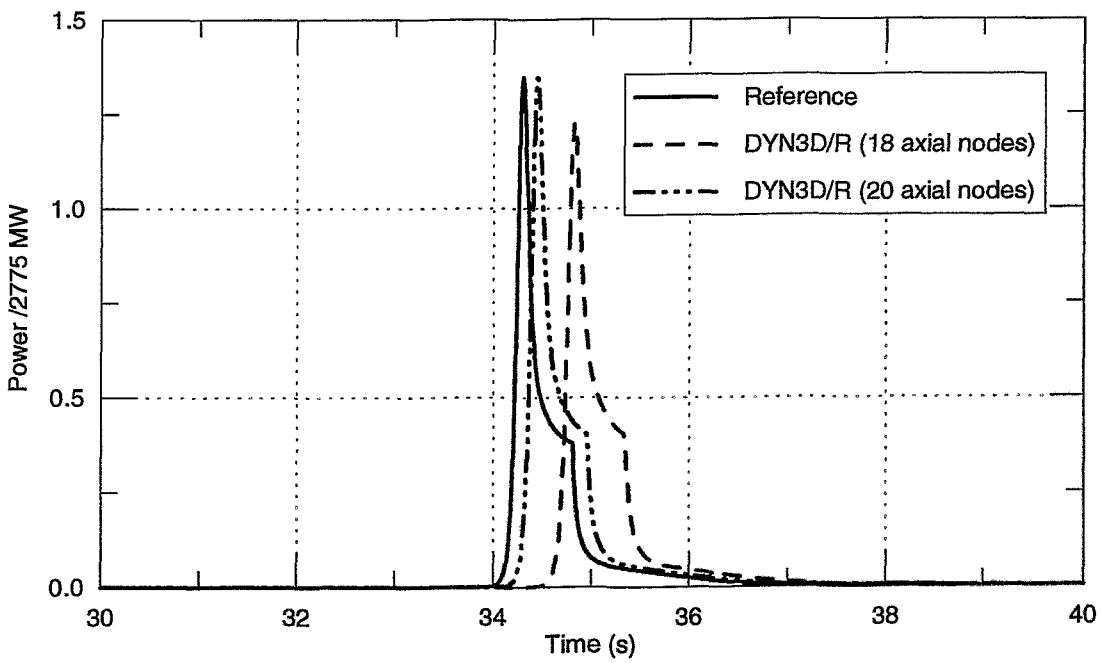

Fig. 4.2.25: Fission power to nominal value (result C1). Comparison of different DYN3D/R calculations with reference

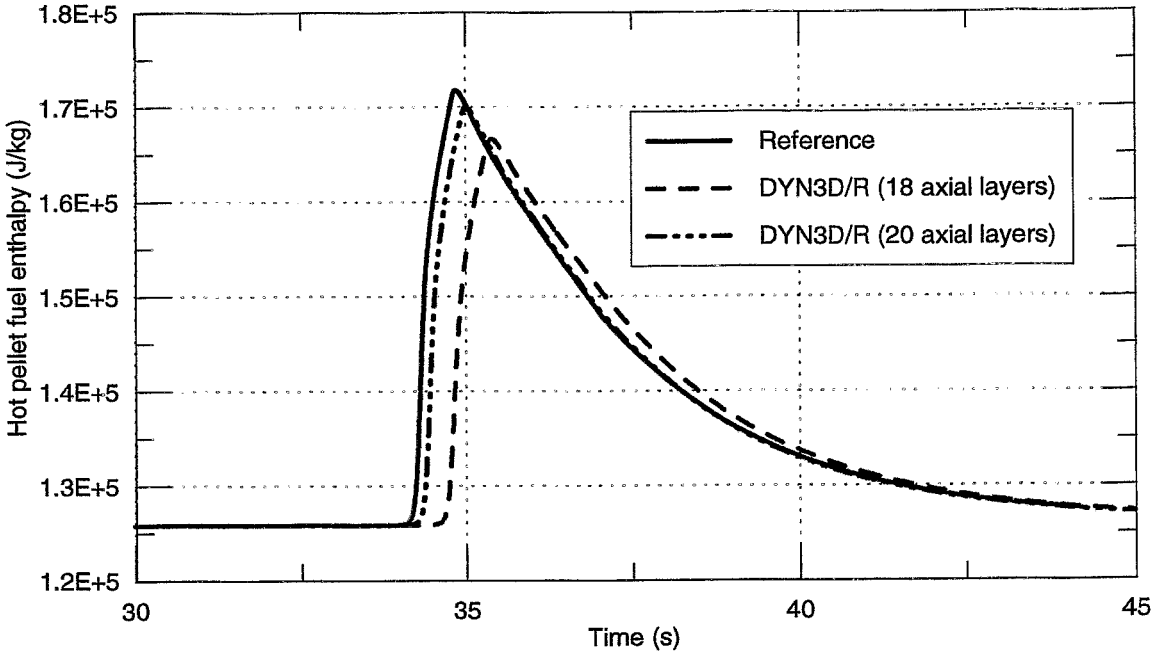

Fig. 4.2.26: Fuel enthalpy of the hot pellet (result D5). Comparison of the different DYN3/R calculations

8 0.625 0.629 0.59	Assembly no. (DYN3D/R) Reference DYN3D/R Dev. (%)				34 -	35 -		
				30 0.649 0.660 1.74	31 0.619 0.623 0.74	32 -	33 -	
			25 1.132 1.131 -0.03	26 0.939 0.944 0.53	27 0.890 0.907 1.87	28 0.498 0.498 0.04	29 -	
		18 0.741 0.740 -0.17	19 1.139 1.137 -0.19	20 0.904 0.902 -0.19	21 0.918 0.919 0.08	22 0.458 0.459 0.21	23 -	24 -
	10 1.537 1.526 -0.74	11 1.293 1.285 -0.59	12 1.477 1.472 -0.40	13 1.451 1.451 0.00	14 1.281 1.281 0.00	15 0.833 0.835 0.32	16 0.503 0.502 -0.16	17 -
1 1.751 1.733 -1.05	2 1.494 1.487 -0.44	3 1.110 1.100 -0.83	4 1.458 1.456 -0.19	5 1.704 1.696 -0.43	6 1.404 1.405 0.00	7 0.553 0.556 0.51	8 0.625 0.629 0.59	9 -

Fig. 4.2.27: Axially averaged radial power distribution (result E3). Comparison of DYN3D/R calculation using 20 axial nodes with the reference values.

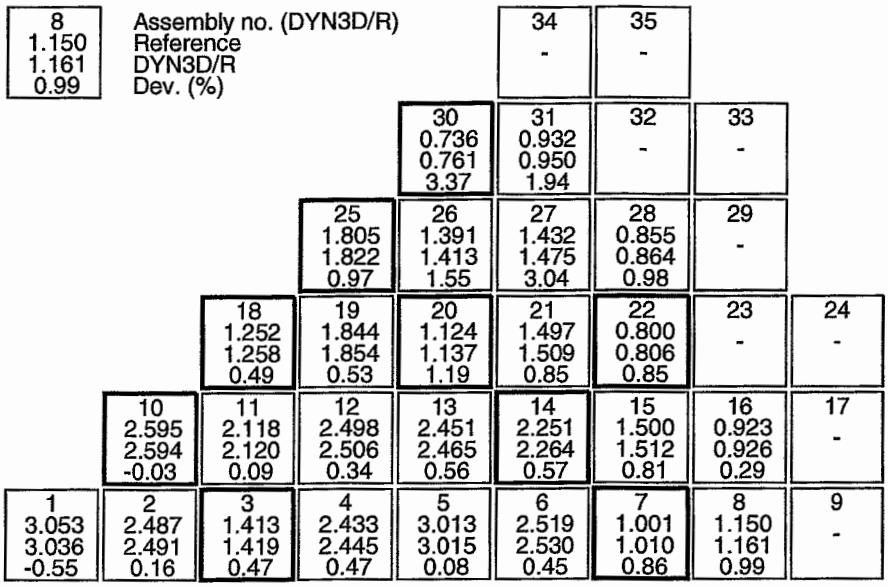

Fig. 4.2.28: Radial power distribution at axial layer number 6 (result E4). Comparison of DYN3D/R calculation using 20 axial nodes with the reference values

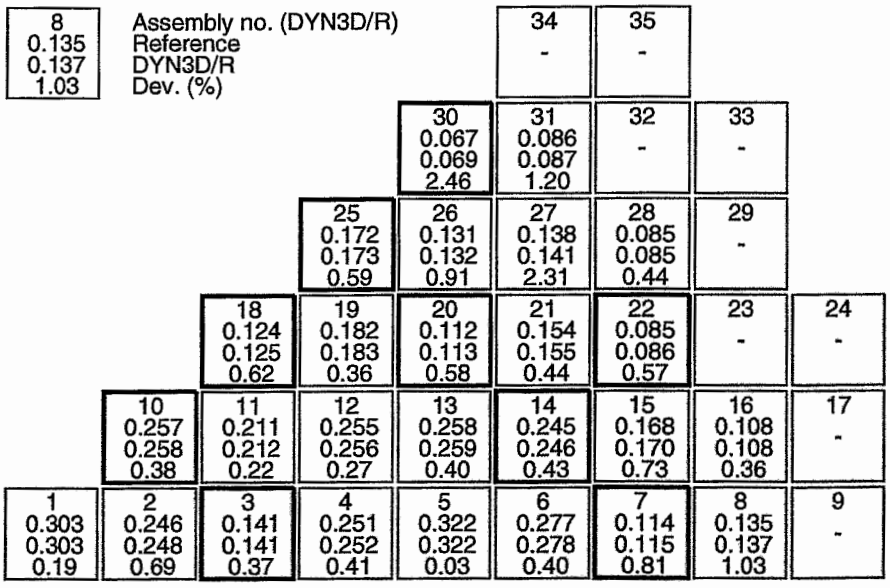

Fig. 4.2.29: Radial power distribution at axial layer number 13 (result E5). Comparison of DYN3D/R calculation using 20 axial nodes with the reference values.

4.3 Case D - Withdrawal of Bank A and B

4.3.1 Initial Steady State

The critical boron concentration of case D calculated by DYN3D is 796.11 ppm. The deviation to the reference value of 793.58 ppm is 2.53 ppm (result B1).

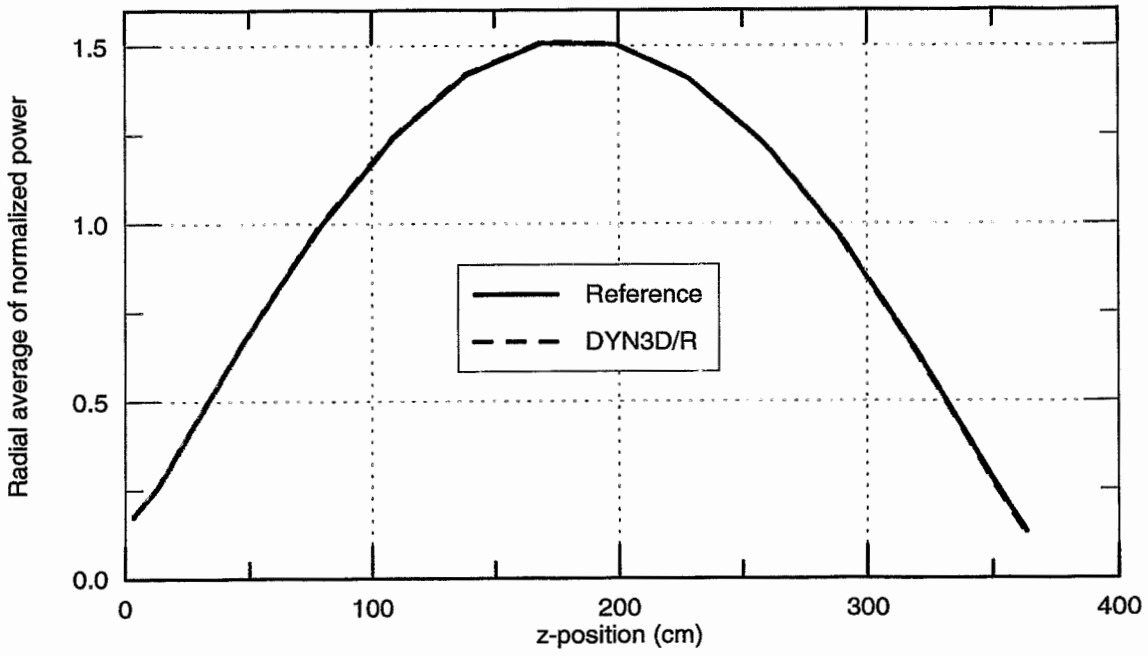

Fig. 4.3.1: Radially averaged axial power distribution (result B2)

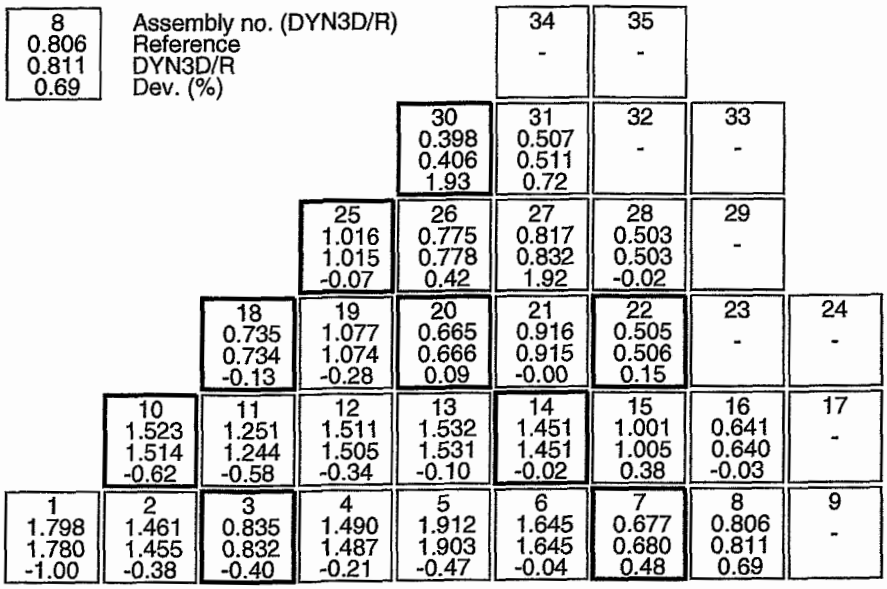

Fig. 4.3.2: Axially averaged radial power distribution (result B3)

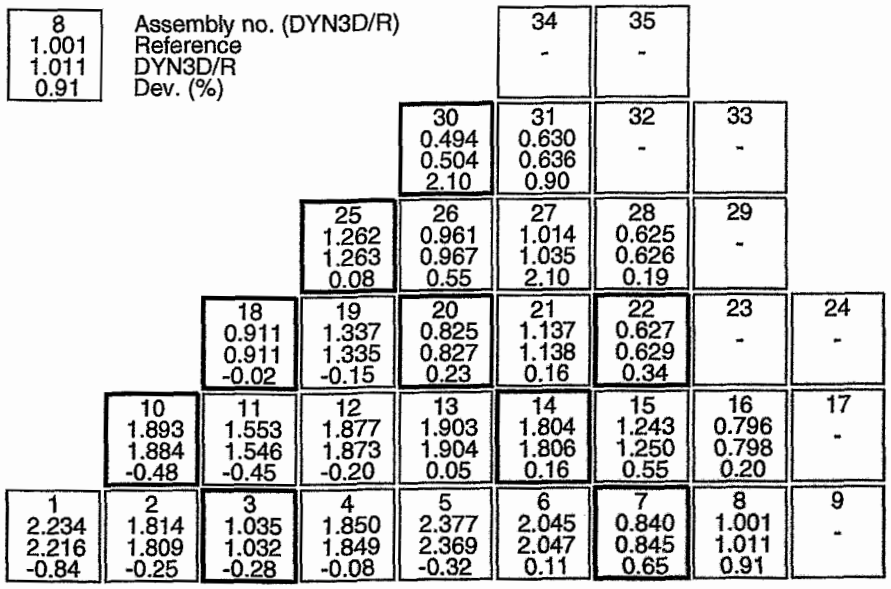

Fig. 4.3.3: Radial power distribution at axial layer number 6 (result B4)

8 0.525 0.526 0.28	Assembly no. (DYN3D/R) Reference DYN3D/R Dev. (%)				34 -	35 -		
				30 0.259 0.263 1.55	31 0.330 0.331 0.33	32 -	33 -	
			25 0.661 0.658 -0.43	26 0.504 0.504 0.03	27 0.532 0.540 1.52	28 0.328 0.326 -0.41	29 -	
		18 0.477 0.475 -0.52	19 0.701 0.696 -0.65	20 0.432 0.431 -0.29	21 0.596 0.593 -0.39	22 0.328 0.328 -0.24	23 -	24 -
	10 0.992 0.982 -1.02	11 0.814 0.806 -0.95	12 0.984 0.977 -0.71	13 0.997 0.992 -0.48	14 0.945 0.941 -0.40	15 0.651 0.651 -0.04	16 0.417 0.415 -0.42	17 -
1 1.171 1.154 -1.40	2 0.951 0.943 -0.80	3 0.543 0.538 -0.78	4 0.970 0.964 -0.58	5 1.245 1.235 -0.85	6 1.071 1.066 -0.44	7 0.440 0.440 0.07	8 0.525 0.526 0.28	9 -

Fig. 4.3.4: Radial power distribution at axial layer number 13 (result B5)

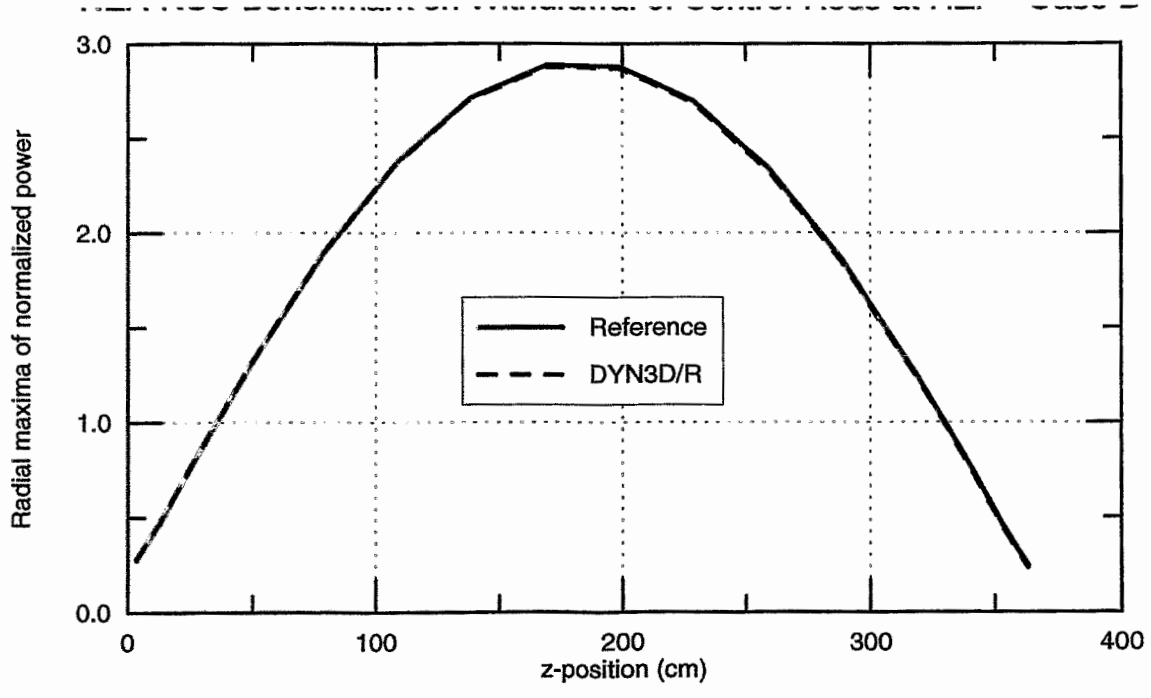

Fig. 4.3.5: Envelope axial power distribution Fq(z) (result B6)

4.3.2 Transient Core Averaged Results

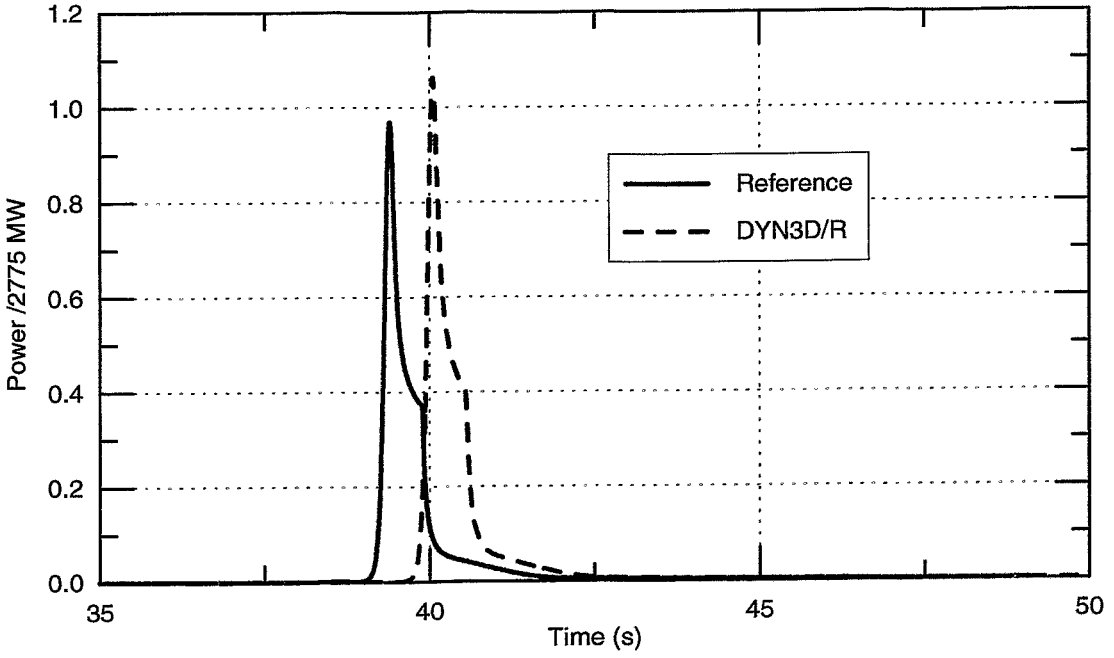

Fig. 4.3.6: Fission power to nominal value (result C1)

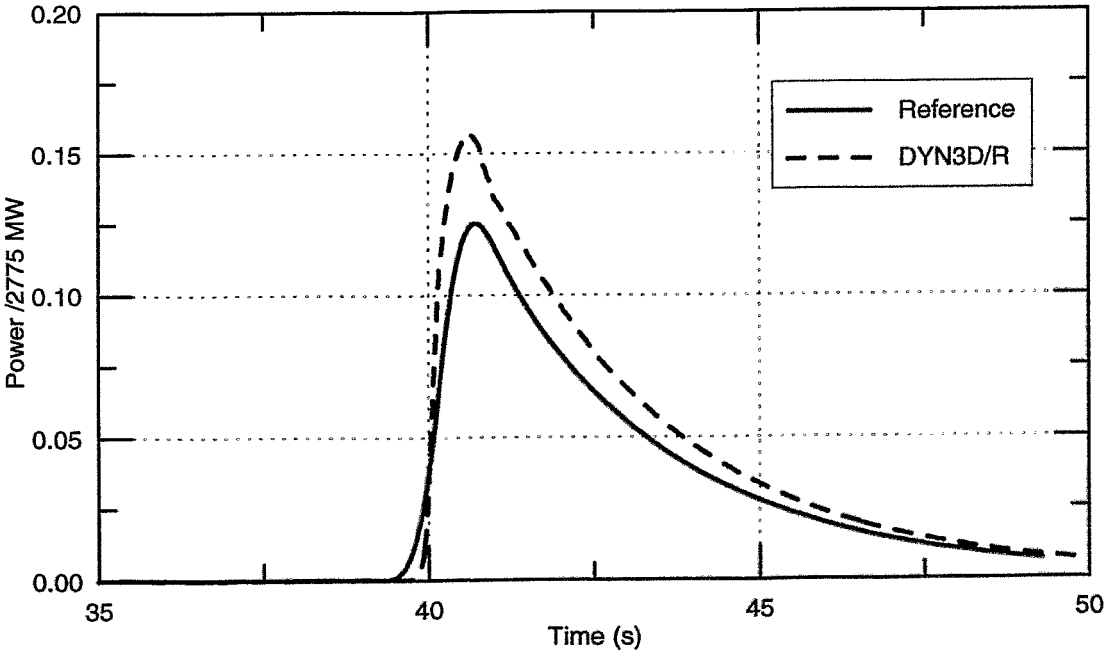

Fig. 4.3.7: Coolant heating to nominal value (result C2)

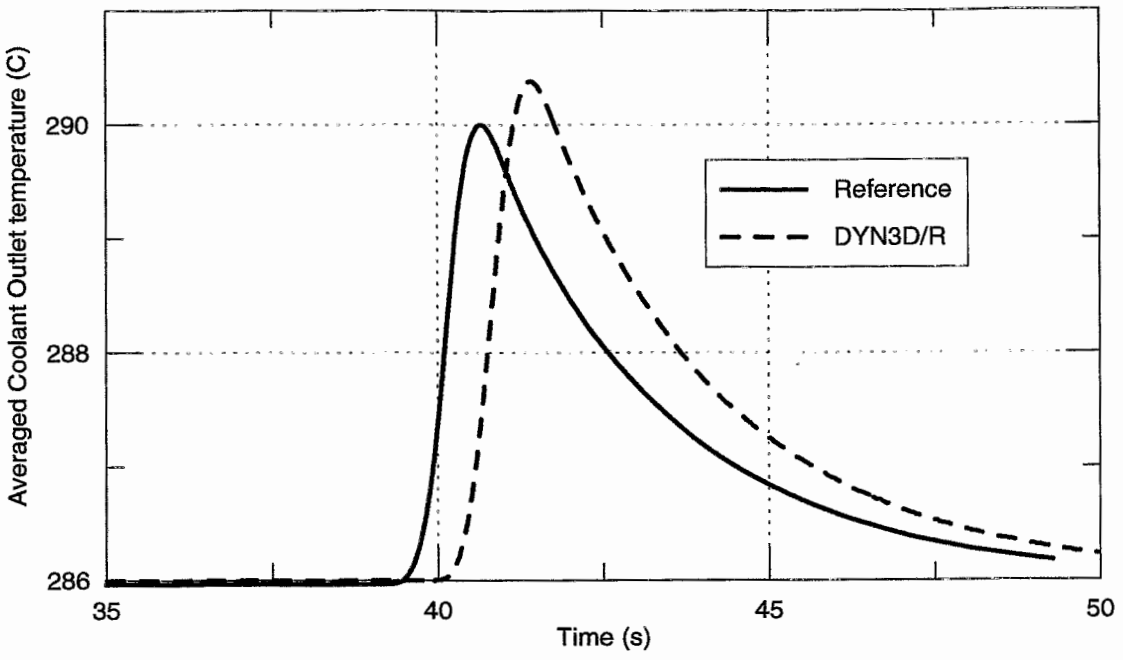

Fig. 4.3.8: Coolant outlet temperature (result C3)

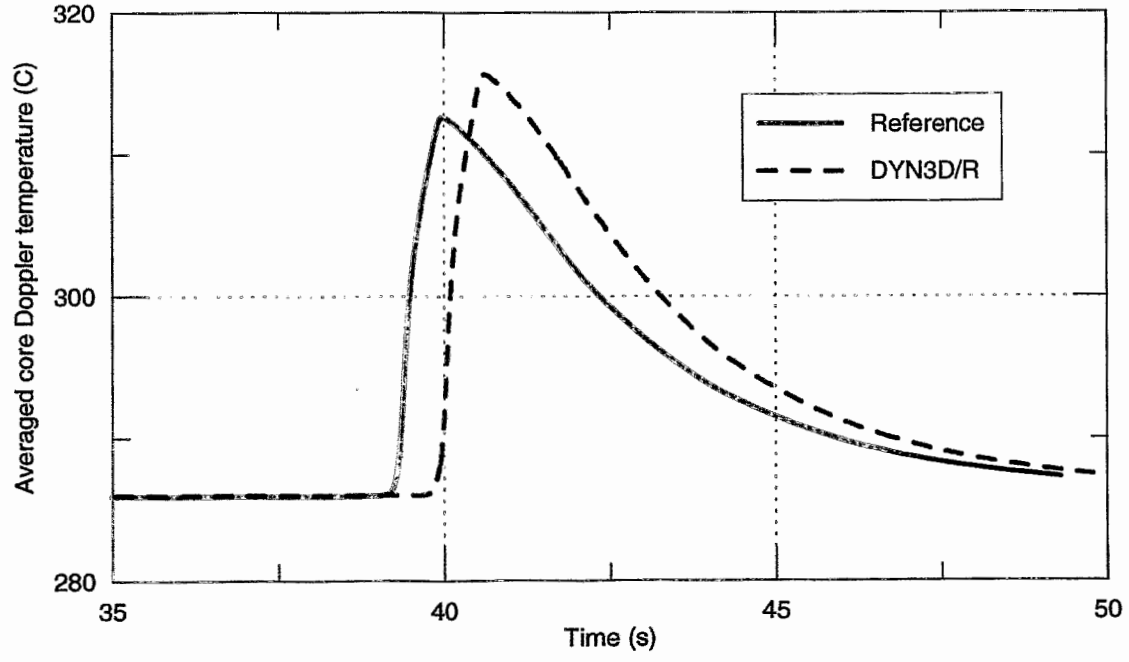

Fig. 4.3.9: Fuel Doppler temperature (result C4)

4.3.3 Transient Hot Pellet Results

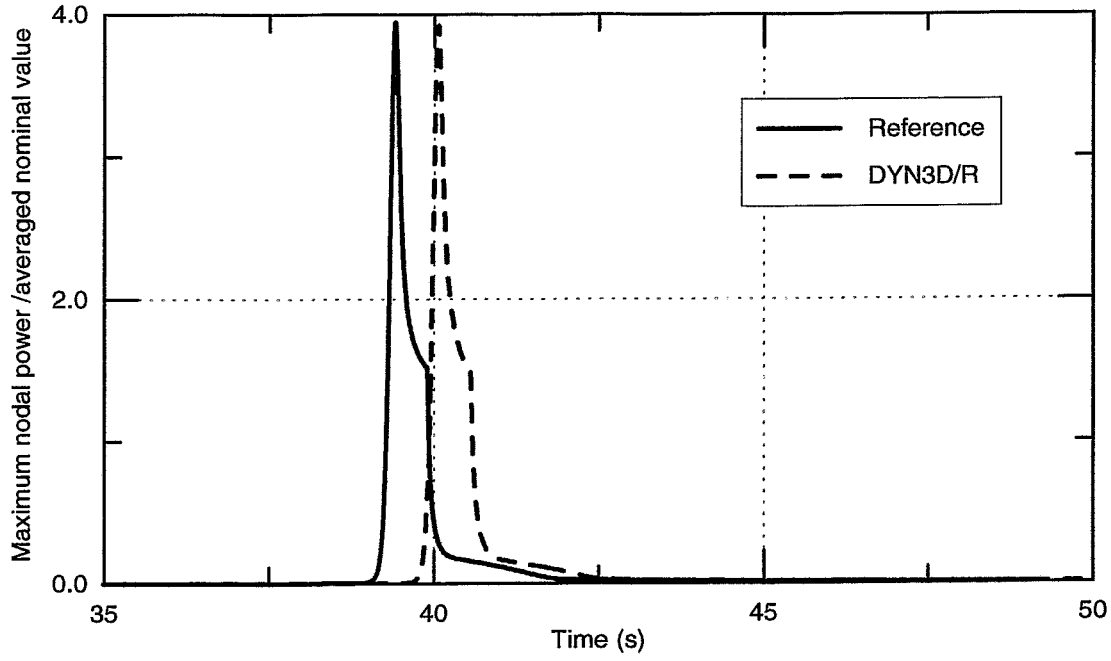

Fig. 4.3.10: Fission power of hot pellet to nominal average value (result D1)

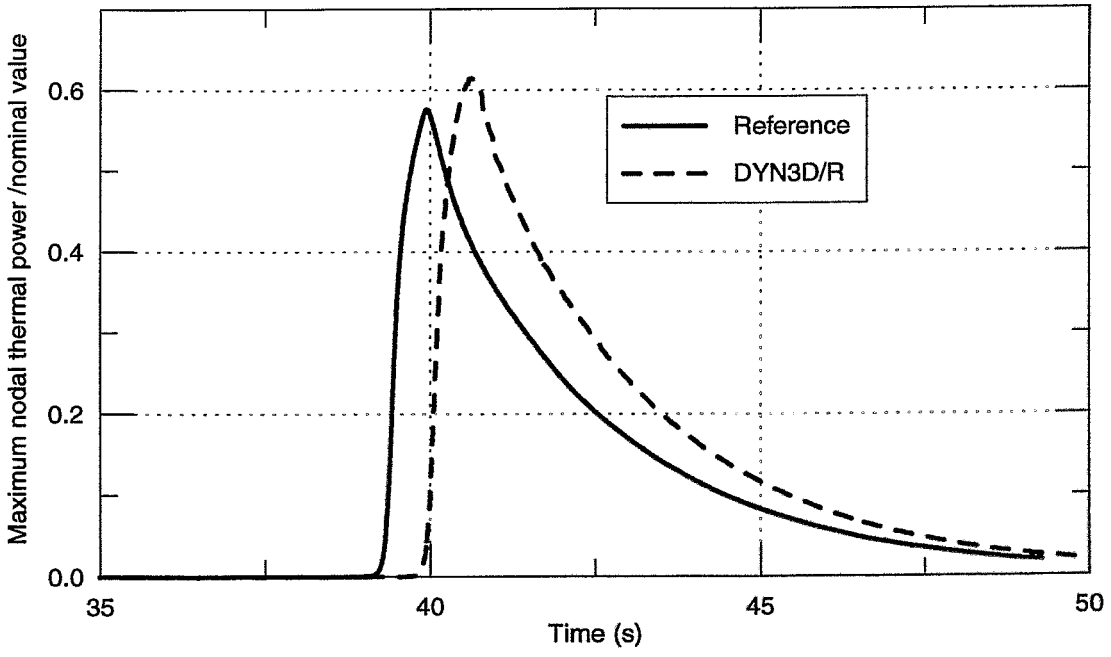

Fig. 4.3.11: Coolant heating of hot pellet to nominal average value (result D2)

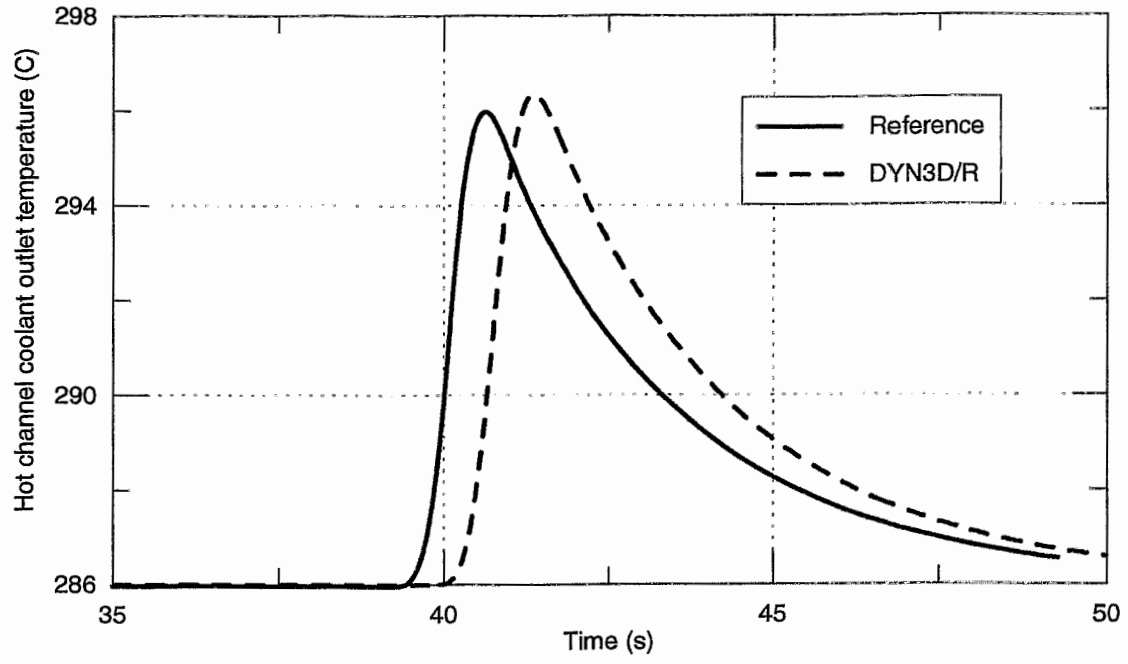

Fig. 4.3.12: Coolant temperature at the outlet of the hot channel (result D3)

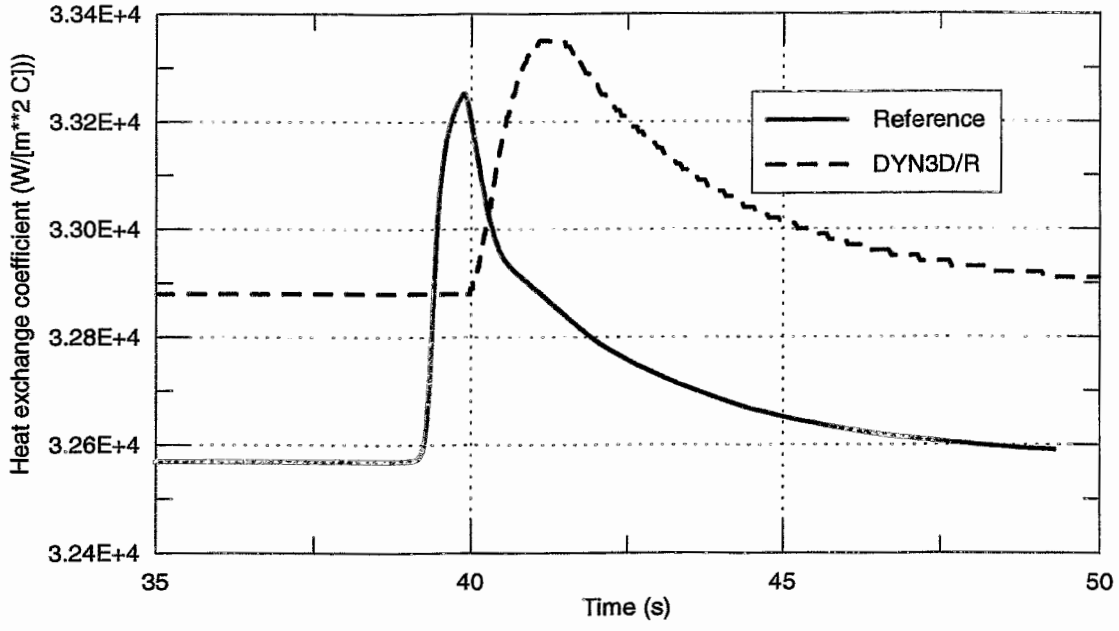

Fig. 4.3.13: Heat exchange coefficient between cladding and coolant of the hot pellet (result D4)

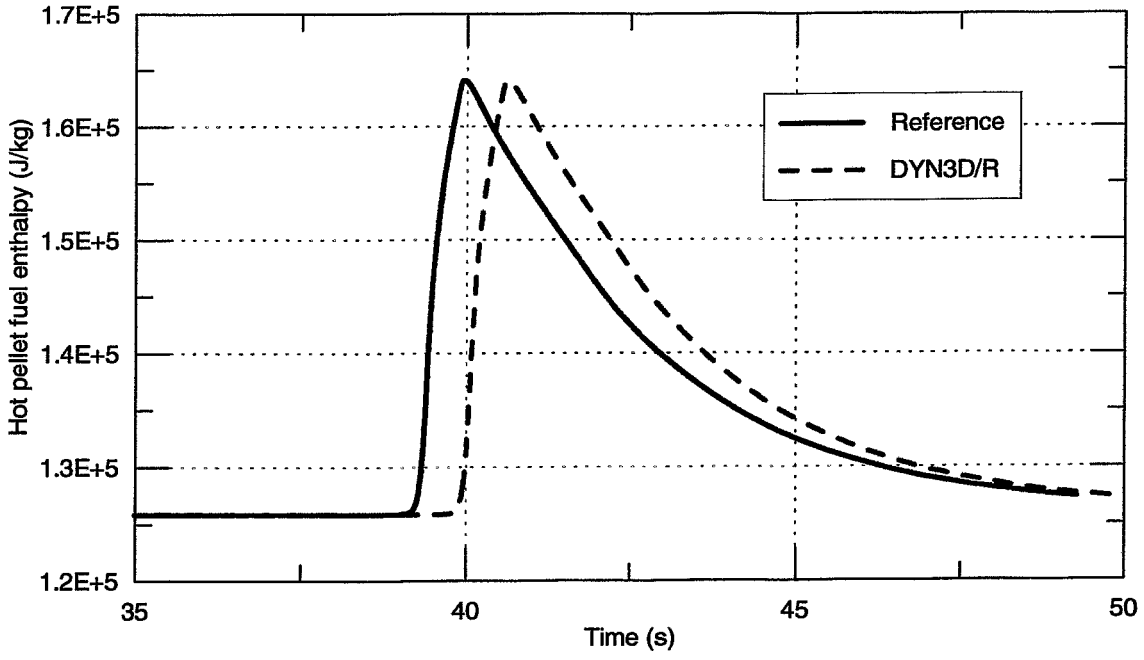

Fig. 4.3.14: Fuel enthalpy of the hot pellet (result D5)

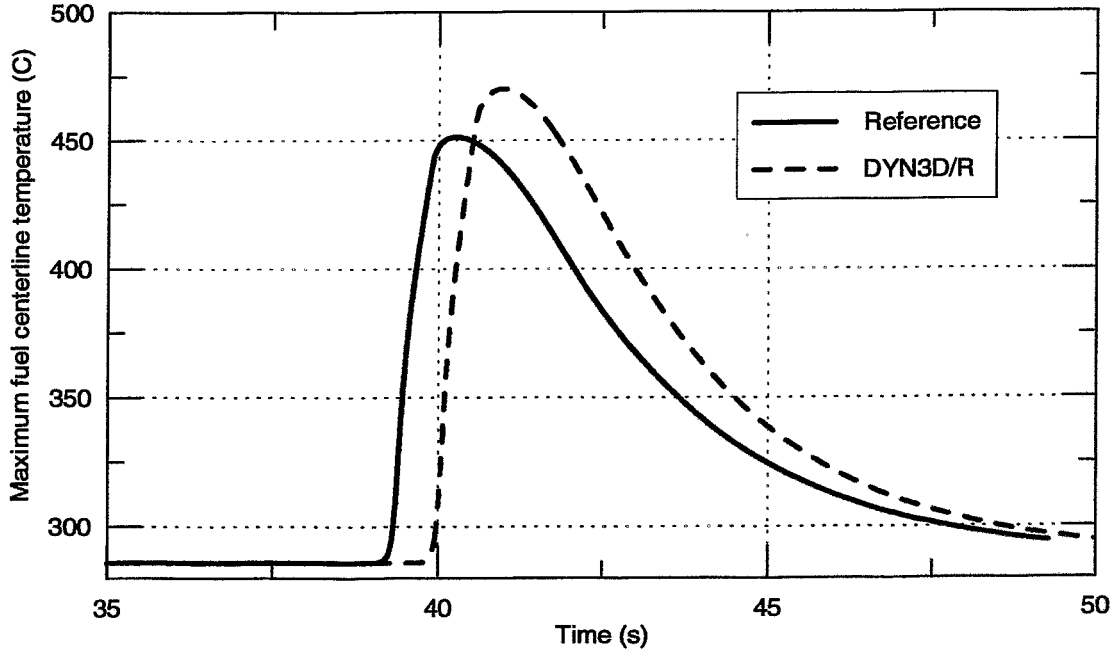

Fig. 4.3.15: Fuel temperature at the hot pellet centerline (result D6)

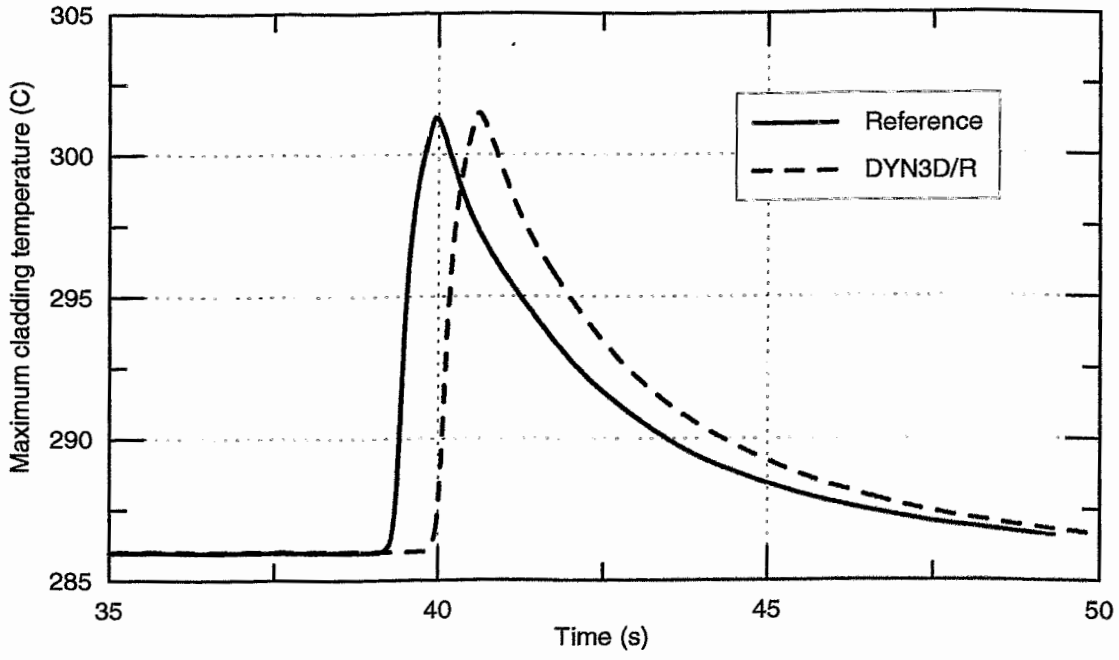

Fig. 4.3.16: Cladding outer surface temperature at the hot pellet (result D7)

4.2.4 Snapshots at Time of Power Maximum

The power maximum calculated by DYN3D/R is at the time t_{max} = 40.06 s. The vlaue of fission power relativ to the nominal power is 1.0608 (result E1). The deviation to the reference value 0.9685 is 0.0923.

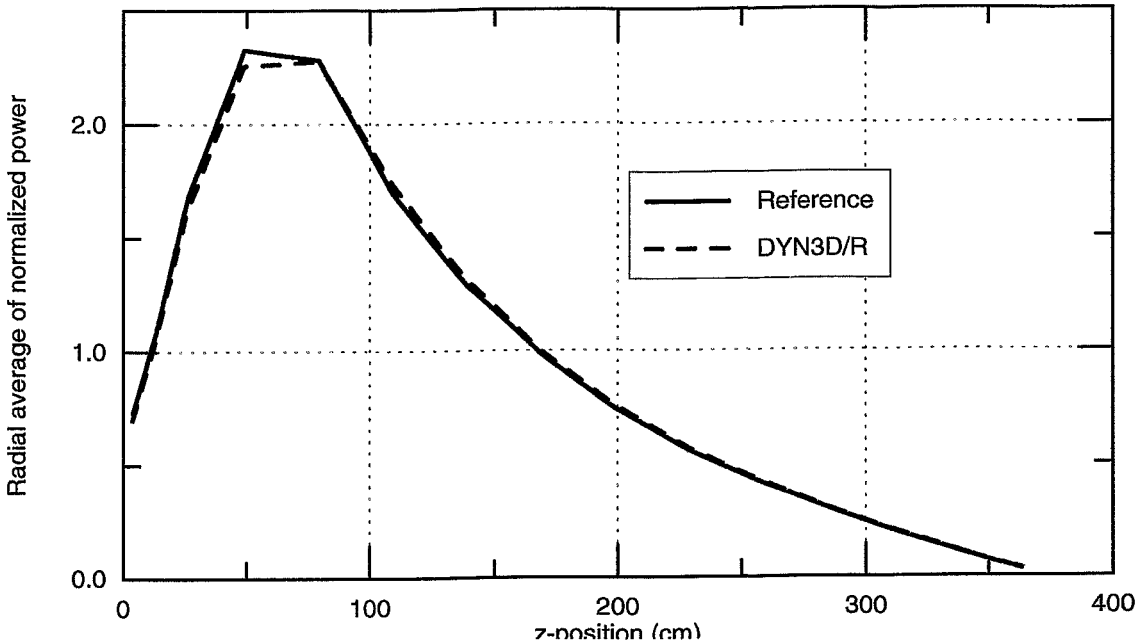

Fig. 4.3.17: Radially averaged axial power distribution (result E2)

8 0.781 0.787 0.85	Assembly no. (DYN3D/R) Reference DYN3D/R Dev. (%)				34 -	35 -		
				30 0.445 0.452 1.54	31 0.570 0.571 0.15	32 -	33 -	
			25 1.077 1.075 -0.26	26 0.903 0.903 0.03	27 0.973 0.987 1.41	28 0.651 0.648 -0.47	29 -	
		18 0.636 0.635 -0.05	19 1.076 1.073 -0.28	20 0.963 0.955 -0.84	21 1.101 1.101 0.05	22 0.810 0.806 -0.50	23 -	24 -
	10 1.108 1.104 -0.34	11 0.991 0.988 -0.35	12 1.334 1.331 -0.23	13 1.482 1.483 0.03	14 1.451 1.452 0.01	15 1.057 1.063 0.60	16 0.648 0.649 0.07	17 -
1 1.246 1.238 -0.64	2 1.038 1.038 -0.04	3 0.649 0.648 -0.12	4 1.270 1.269 -0.05	5 1.715 1.710 -0.28	6 1.539 1.541 0.09	7 0.660 0.664 0.68	8 0.781 0.787 0.85	9 -

Fig. 4.3.18: Axially averaged radial power distribution (result E3)

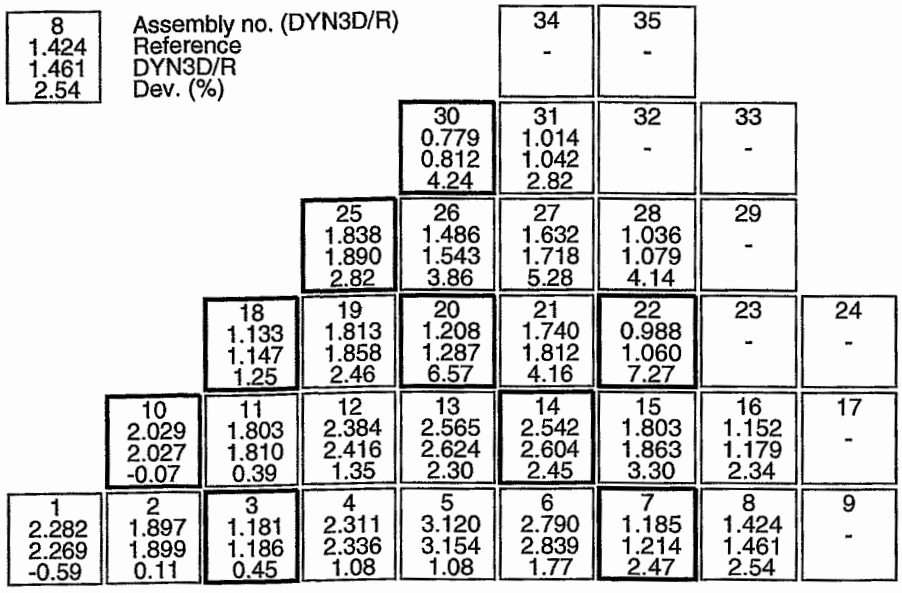

Fig. 4.3.19: Radial power distribution at axial layer number 6 (result E4)

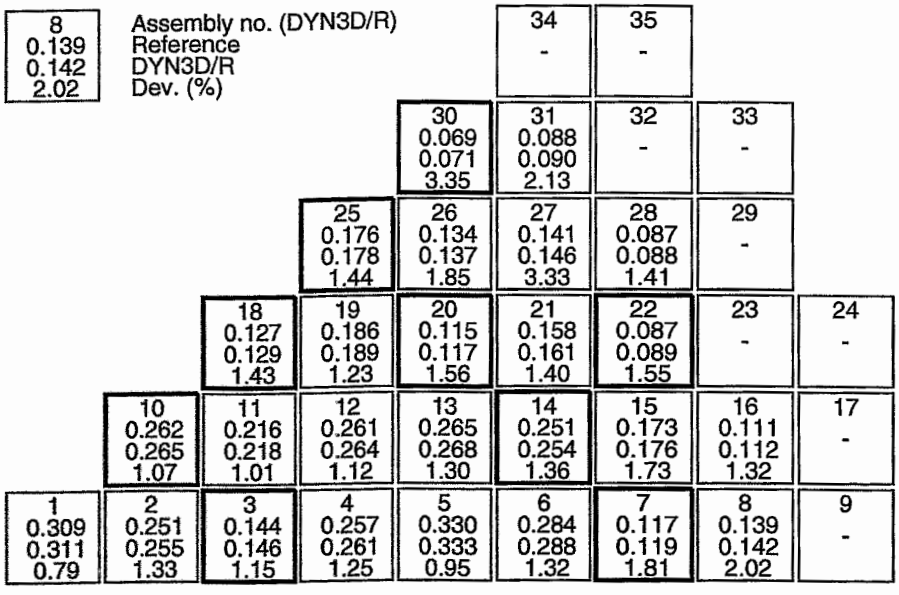

Fig. 4.3.20: Radial power distribution at axial layer number 13 (result E5)

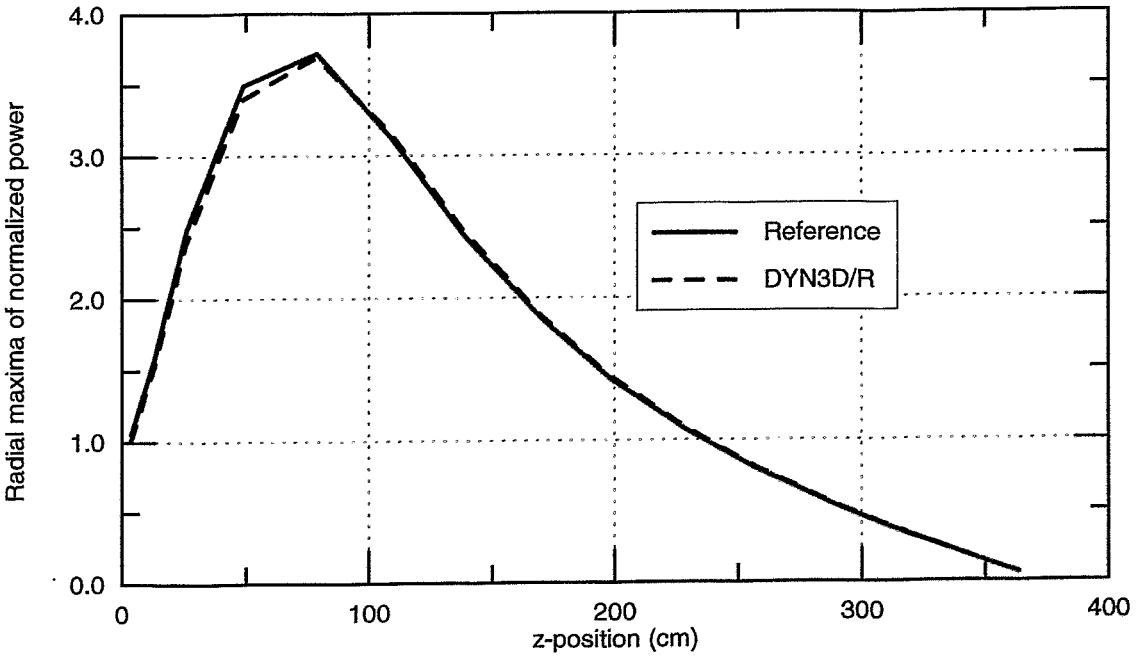

Fig. 4.3.21: Envelope axial power distribution Fq(z) (result E6)

4.3.5 Calculation with Different Axial Nodalization

Like fig. 4.2.7 of case B we see at fig. 4.3.6 a similar shift of power peak calculated by DYN3D/R in comparison to the peak of reference. In case D also a DYN3D/R calculations with 20 axial nodes was carried out. The same axial layers as in chapter 4.2.5 were used, because the situation of case D is similar to case B.

Fig. 4.3.22 shows the curves of the fission power for the reference and the results of the two different DYN3D/R calculations. The position of power peak of the calculation with 20 axial nodes is close to the reference. The situation is similar for the other results being demonstrated by some examples. Fig. 4.3.23 shows the comparisons for the hot pellet fuel enthalpy. It can be seen that the curve obtained with 20 axial layers is nearly identical with the reference. We see on A better agreement with reference solutions can be observed in fig 4.3.24 - 4.3.26 than in fig. 4.3.18 - 4.3.20 which show the radial power distributions in the moment of power maximum.

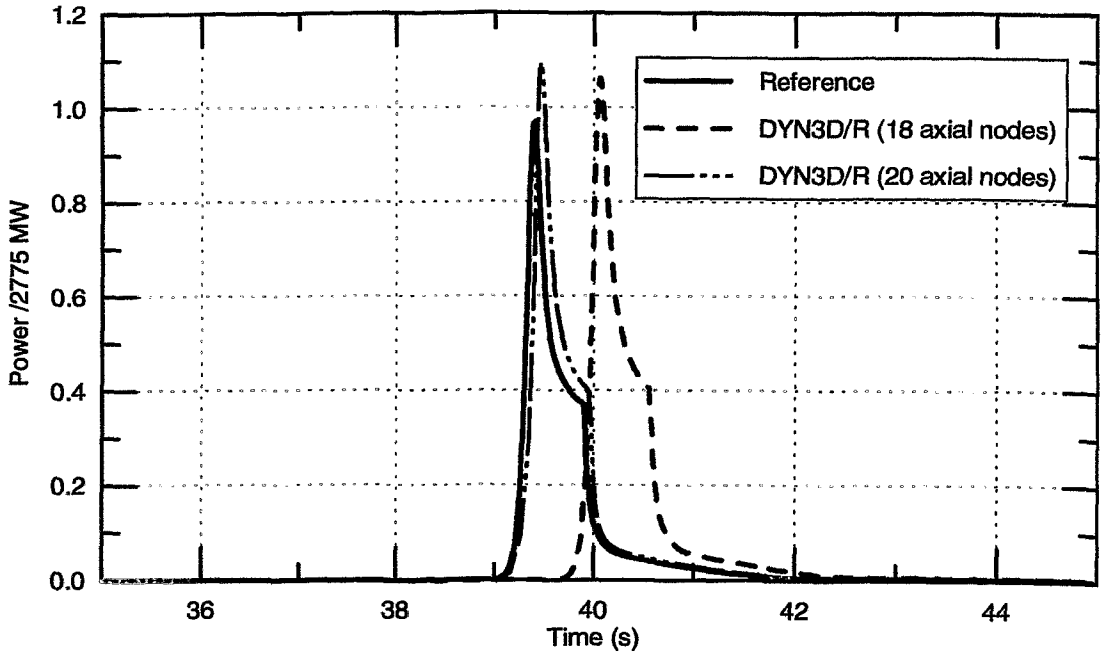

Fig. 4.3.22: Fission power to nominal value (result C1). Comparison of different DYN3D/R calculations with the reference.

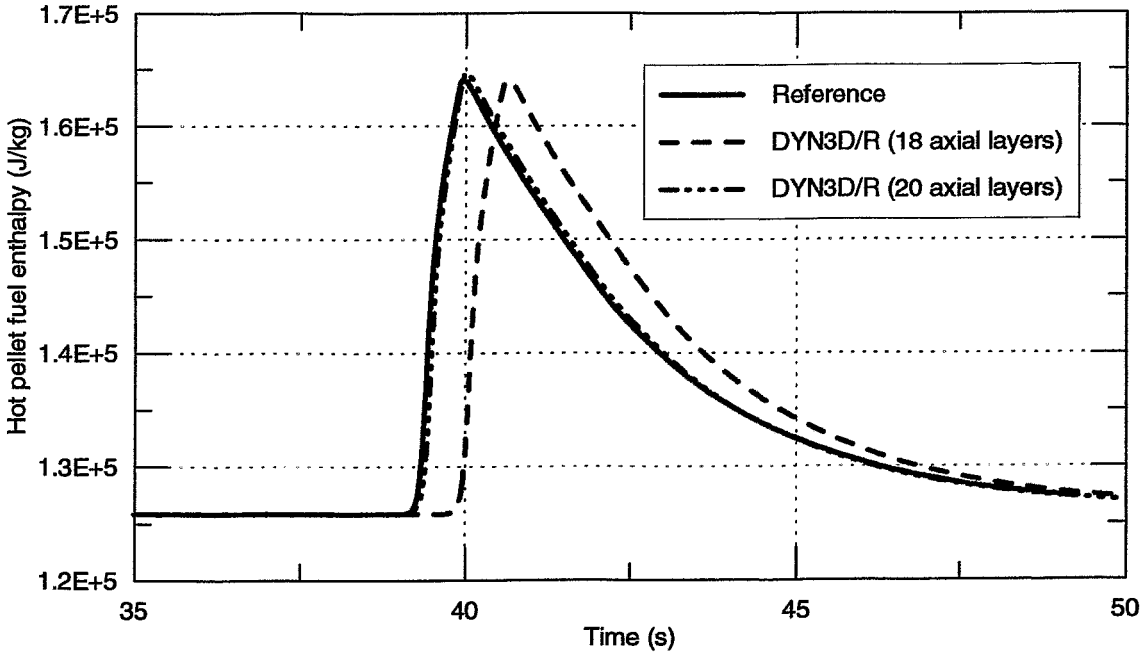

Fig. 4.3.23: Fuel enthalpy of the hot pellet (result D5). Comparison of different DYN3D/R calculations with the reference.

8 0.781 0.786 0.69	Assembly no. (DYN3D/R) Reference DYN3D/R Dev. (%)				34 -	35 -		
				30 0.445 0.452 1.68	31 0.570 0.571 0.25	32 -	33 -	
			25 1.077 1.076 -0.18	26 0.903 0.905 0.24	27 0.973 0.989 1.61	28 0.651 0.650 -0.17	29 -	
		18 0.636 0.634 -0.22	19 1.076 1.073 -0.26	20 0.963 0.960 -0.25	21 1.101 1.104 0.28	22 0.810 0.811 0.12	23 -	24 -
	10 1.108 1.099 -0.75	11 0.991 0.985 -0.66	12 1.334 1.328 -0.42	13 1.482 1.482 -0.04	14 1.451 1.451 -0.05	15 1.057 1.064 0.61	16 0.648 0.648 -0.01	17 -
1 1.246 1.232 -1.12	2 1.038 1.033 -0.48	3 0.649 0.646 -0.44	4 1.270 1.266 -0.30	5 1.715 1.706 -0.49	6 1.539 1.538 -0.08	7 0.660 0.663 0.57	8 0.781 0.786 0.69	9 -

Fig. 4.3.24: Axial averaged radial power distribution (result E3). Comparison of DYN3D/R calculation using 20 axial nodes with the reference values.

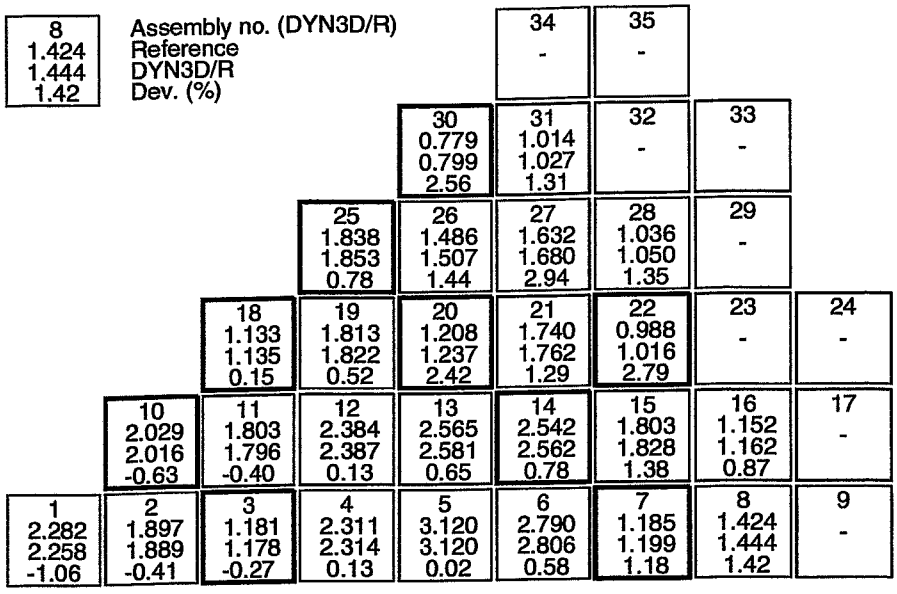

Fig. 4.3.25: Radial power distribution at axial layer number 6 (result E4). Comparison of DYN3D/R calculation using 20 axial nodes with the reference values.

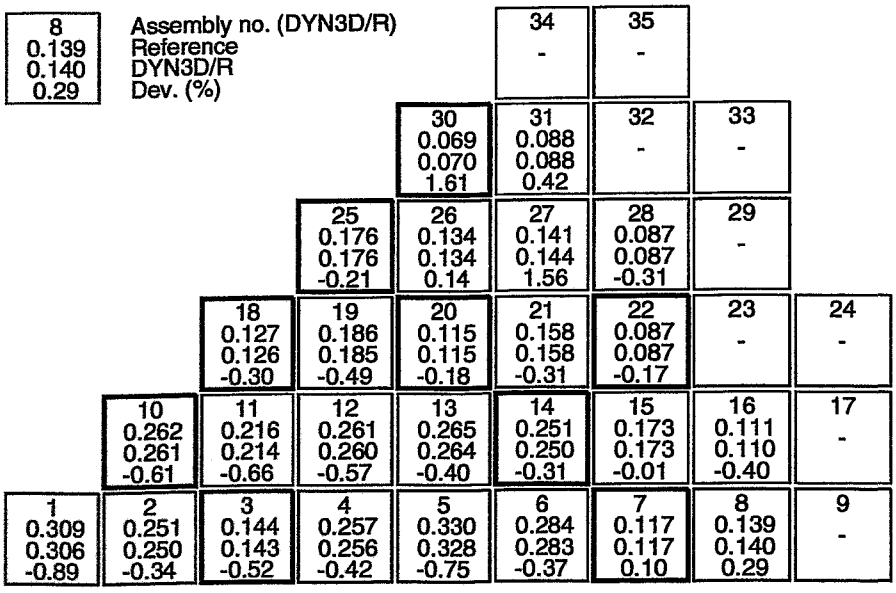

Fig. 4.3.26: Radial power distribution at axial layer number 13 (result E4). Comparison of DYN3D/R calculation using 20 axial nodes with the reference values.

5. Conclusions

The 3D core model DYN3D/R, a version of DYN3D for Cartesian geometry, was verified with the help of benchmark problems. Concerning the transient benchmarks on control rod ejections and withdrawal of control rods the considered problems are the only ones which have been available so far for PWR's. The neutron physical data and the thermophysical properties of fuel and clad were given in the definitions of the benchmarks. Small adaptations were made in DYN3D/R to implement these formulas. The heat transfer from cladding to water and the properties of water were not given and own correlations have to be used. Considering the investigated benchmark problems the DYN3D/R solutions by using the standard mesh show a good agreement with the reference results.

Concerning the withdrawal of control rods it was shown that the small deviations to the reference solution, as the time shift of power maximum, can be reduced by choosing a finer mesh in space. If the standard axial mesh is used and the lower end of control rods is moved through a node, the applied method for damping the cusping effects influences the time behaviour of reactivity. Especially, if the reactivity is near to prompt critical small differences of reactivity have an impact on the time of the power increase. The power peak determined by the reactivity insertion and the negative Doppler effect can be influenced also. A finer axial mesh reduces the differences of the reactivity gain.

Considering the presented results of comparisons it can be stated that DYN3D/R is capable of analyzing reactivity transients in a PWR with quadratic fuel assemblies.

References

1. U. GRUNDMANN, U. ROHDE, "DYN3D/M2 a Code for Calculation of Reactivity Transients in Cores with Hexagonal Geometry",
   Rep. FZR 114, Research Center Rossendorf (1993), Reprint of Rep. ZfK - 690, Central Institute for Nuclear Research (1989)

2. U. GRUNDMANN, "The Code DYN3DR for Steady-State and Transient Analyses of Light Water reactor Cores with Cartesian Geometry", Rep. FZR 114, Research Center Rossendorf (1995)

3. "Argonne Code Center: Benchmark Problem Book", Rep. ANL-7416, Suppl. 2, Argonne National Laboratory, (1977)

4. H. FINNEMANN, A. GALATI; "NEACRP 3-D LWR Core Transient Benchmark" Report NEACRP-L-335, Rome, 1992

5. H. FINNEMANN, H. BAUER, A. GALATI, R. MARTINELLI; "Results of LWR Core Transient Benchmarks",
   Report NEA/NSC/DOC(93) 25, OECD NEA, 1993

6. R. FRAIKIN and H. FINNEMANN, "NEA-NSC 3-D/1-D PWR Core Transient Benchmark Uncontrolled Withdrawal of Control Rods at Zero Power", Rep. NEA/NSC/(93) 9, Paris, (1993)

7. E. SARTORI, NEA Document "ZZ-3DLWRCT - 2 NEA 1398/03", Paris (1997)

8. R. FRAIKIN,"Review of a NEA-NSC Benchmark on Uncontrolled Withdrawal of Control Rods at Zero Power", *Proceedings of the Int. Conf. on the Physics of Reactors PHYSOR96*, pp. J-99 - J-108, Mito, Japan (1996).